AD-A090 171 SINGER CO FAIRFIELD NJ KEARFOTT DIV F/G 14/2
ANGULAR RATE SENSOR DEVELOPMENT.(U)
DEC 78 R E WEBER DNA001-78-C-0126
UNCLASSIFIED Y256A934 DNA-4866F NL

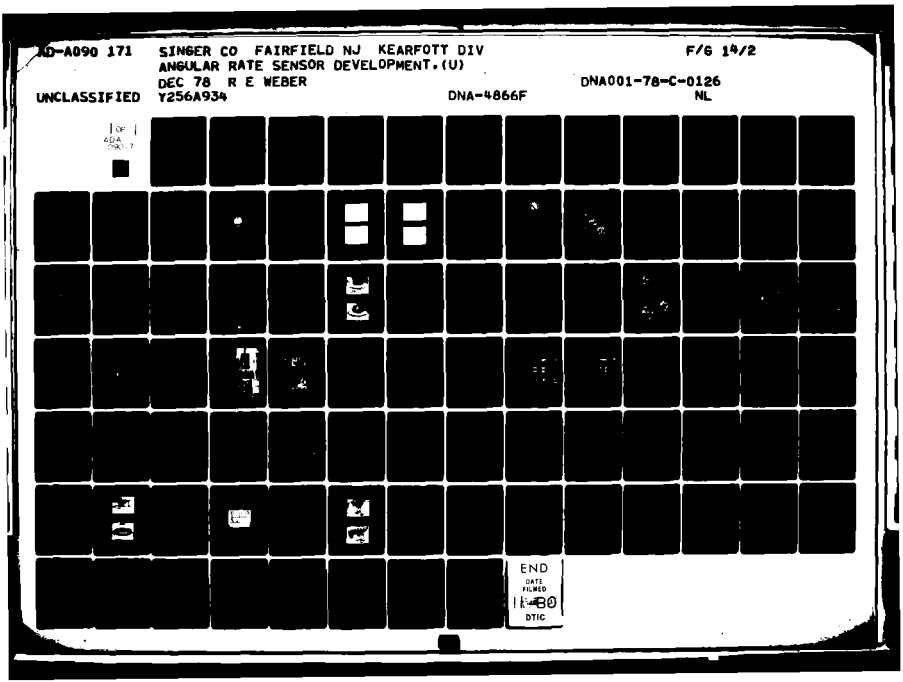

DNA 4866F

ANGULAR RATE SENSOR DEVELOPMENT

R. E. Weber
The Singer Company
Kearfott Division
90 New Dutch Lane
Fairfield, New Jersey 07006

30 December 1978

Final Report for Period 20 February 1978—30 December 1978

CONTRACT No. DNA 001-78-C-0126

THIS WORK SPONSORED BY THE DEFENSE NUCLEAR AGENCY
UNDER RDT&E RMSS CODE B344078462 H11CAXSX35280 H2590D.

Prepared for

Director
DEFENSE NUCLEAR AGENCY
Washington, D. C. 20305

Destroy this report when it is no longer needed. Do not return to sender.

PLEASE NOTIFY THE DEFENSE NUCLEAR AGENCY, ATTN: STTI, WASHINGTON, D.C. 20305, IF YOUR ADDRESS IS INCORRECT, IF YOU WISH TO BE DELETED FROM THE DISTRIBUTION LIST, OR IF THE ADDRESSEE IS NO LONGER EMPLOYED BY YOUR ORGANIZATION.

UNCLASSIFIED

SECURITY CLASSIFICATION OF THIS PAGE *(When Data Entered)*

REPORT DOCUMENTATION PAGE

READ INSTRUCTIONS BEFORE COMPLETING FORM

1. REPORT NUMBER: DNA 4866F	2. GOVT ACCESSION NO.: AD-A090171
3. RECIPIENT'S CATALOG NUMBER:	
4. TITLE (and Subtitle): ANGULAR RATE SENSOR DEVELOPMENT .	5. TYPE OF REPORT & PERIOD COVERED: Final Report. 20 Feb [illegible]—30 Dec 78
	6. PERFORMING ORG. REPORT NUMBER: Y256A934
7. AUTHOR(s): R. E. Weber	8. CONTRACT OR GRANT NUMBER(s): DNA 001-78-C-0126
9. PERFORMING ORGANIZATION NAME AND ADDRESS: The Singer Company, Kearfott Division, 90 New Dutch Lane, Fairfield, New Jersey 07006	10. PROGRAM ELEMENT, PROJECT, TASK AREA & WORK UNIT NUMBERS: Subtask H11CAXSX352-80
11. CONTROLLING OFFICE NAME AND ADDRESS: Director, Defense Nuclear Agency, Washington, D.C. 20305	12. REPORT DATE: 30 December 1978 13. NUMBER OF PAGES: 92
14. MONITORING AGENCY NAME & ADDRESS *(if different from Controlling Office)*: X352 90	15. SECURITY CLASS *(of this report)*: UNCLASSIFIED 15a. DECLASSIFICATION DOWNGRADING SCHEDULE

16. DISTRIBUTION STATEMENT *(of this Report)*

Approved for public release; distribution unlimited.

17. DISTRIBUTION STATEMENT *(of the abstract entered in Block 20, if different from Report)*

18. SUPPLEMENTARY NOTES

This work sponsored by the Defense Nuclear Agency under RDT&E RMSS Code B344078462 H11CAXSX35280 H2590D.

19. KEY WORDS *(Continue on reverse side if necessary and identify by block number)*

Angular Rate Sensor
High Rates
High Shock Environment
Low Power
Wide Dynamic Range

20. ABSTRACT *(Continue on reverse side if necessary and identify by block number)*

This document is the final report on an effort whose objective was to deliver two prototype versions of the Kearfott Angular Rate Sensor (KARS). The KARS is basically a damped angular accelerometer. It comprises a conductive liquid annulus (Mercury) positioned in the gap of a permanent magnet. Upon application of an angular input to the case, the liquid annulus initially remains immobile. The relative motion of the liquid to the case is sensed by measurement of the potential generated in the liquid as it cuts the lines of force of

DD FORM 1 JAN 73 1473 EDITION OF 1 NOV 65 IS OBSOLETE

UNCLASSIFIED

SECURITY CLASSIFICATION OF THIS PAGE *(When Data Entered)*

410165

20. ABSTRACT (Continued)

the permanent magnet. The potential is measured on two electrodes submerged in the Mercury. As a result of this effort, two working prototype units were constructed, tested and delivered.

PREFACE

This work was sponsored by the Defense Nuclear Agency under Government Contract Number DNA001-78-C-0126. The Contracting Officers Representative for work was T. E. Kennedy of Shock Physics Directorate, Headquarters, DNA Washington, D.C. 20305. The authorization for this work was DNA 001-78-C-0126, Task H11CAXSX352.

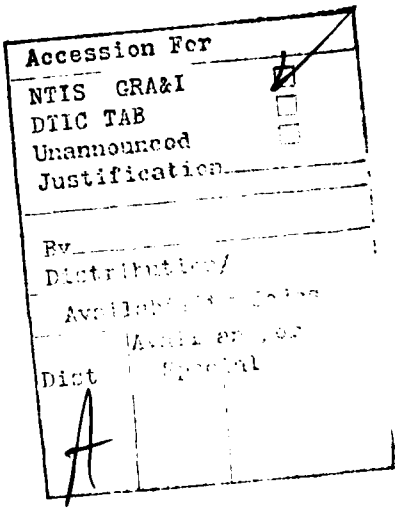

Conversion factors for U.S. customary to metric (SI) units of measurement.

To Convert From	To	Multiply By
angstrom	meters (m)	1.000 000 X E -10
atmosphere (normal)	kilo pascal (kPa)	1.013 25 X E +2
bar	kilo pascal (kPa)	1.000 000 X E +2
barn	meter^2 (m^2)	1.000 000 X E -28
British thermal unit (thermochemical)	joule (J)	1.054 350 X E +3
calorie (thermochemical)	joule (J)	4.184 000
cal (thermochemical)/cm^2	mega joule/m^2 (MJ/m^2)	4.184 000 X E -2
curie	giga becquerel (GBq)*	3.700 000 X E +1
degree (angle)	radian (rad)	1.745 329 X E -2
degree Fahrenheit	degree kelvin (K)	$t_k = (t° f + 459.67)/1.8$
electron volt	joule (J)	1.602 19 X E -19
erg	joule (J)	1.000 000 X E -7
erg/second	watt (W)	1.000 000 X E -7
foot	meter (m)	3.048 000 X E -1
foot-pound-force	joule (J)	1.355 818
gallon (U.S. liquid)	meter^3 (m^3)	3.785 412 X E -3
inch	meter (m)	2.540 000 X E -2
jerk	joule (J)	1.000 000 X E +9
joule/kilogram (J/kg) (radiation dose absorbed)	Gray (Gy)**	1.000 000
kilotons	terajoules	4.183
kip (1000 lbf)	newton (N)	4.448 222 X E +3
kip/$inch^2$ (ksi)	kilo pascal (kPa)	6.894 757 X E +3
ktap	newton-second/m^2 ($N-s/m^2$)	1.000 000 X E +2
micron	meter (m)	1.000 000 X E -6
mil	meter (m)	2.540 000 X E -5
mile (international)	meter (m)	1.609 344 X E +3
ounce	kilogram (kg)	2.834 952 X E -2
pound-force (lbf avoirdupois)	newton (N)	4.448 222
pound-force inch	newton-meter (N·m)	1.129 848 X E -1
pound-force/inch	newton/meter (N/m)	1.751 268 X E +2
pound-force/$foot^2$	kilo pascal (kPa)	4.788 026 X E -2
pound-force/$inch^2$ (psi)	kilo pascal (kPa)	6.894 757
pound-mass (lbm avoirdupois)	kilogram (kg)	4.535 924 X E -1
pound-mass-$foot^2$ (moment of inertia)	kilogram-$meter^2$ ($kg·m^2$)	4.214 011 X E -2
pound-mass/$foot^3$	kilogram/$meter^3$ (kg/m^3)	1.601 846 X E +1
rad (radiation dose absorbed)	Gray (Gy)**	1.000 000 X E -2
roentgen	coulomb/kilogram (C/kg)	2.579 760 X E -4
shake	second (s)	1.000 000 X E -8
slug	kilogram (kg)	1.459 390 X E +1
torr (mm Hg, 0° C)	kilo pascal (kPa)	1.333 22 X E -1

*The becquerel (Bq) is the SI unit of radioactivity; 1 Bq = 1 event/s.
**The Gray (Gy) is the SI unit of absorbed radiation.

A more complete listing of conversions may be found in "Metric Practice Guide E 380-74," American Society for Testing and Materials.

TABLE OF CONTENTS

LIST OF ILLUSTRATIONS

LIST OF ILLUSTRATIONS (cont'd)

LIST OF ILLUSTRATIONS (cont'd)

LIST OF TABLES

SECTION I

INTRODUCTION

1. DESCRIPTION OF REPORT

This report is the final report on a contract whose objective was to deliver two prototype production versions of the Kearfott Angular Rate Sensor (KARS); the tasks considered in the performance of this contract were:

1. Design, build and test two brassboard angular rate sensors. Compare results to KARS Product Specification and modify design as required and document results.

2. Based on the above results/modifications design, build, test and deliver two prototype production versions of the angular rate sensor.

In the following sections of the report, each of the two tasks above will be addressed. The product specification referred to in Task 1 is a released Singer Kearfott Division (SKD) document and is included as an appendix to this report.

2. BACKGROUND

The unit is basically a damped angular accelerometer and is shown pictorially in Figure 1. It comprises a conductive liquid annulus (mercury) positioned in the gap of a permanent magnet. Upon application of an angular input to the case, the liquid annulus initially remains immobile. The relative motion of the liquid to the case is sensed by measurement of the potential generated in the liquid as it cuts the lines of force of the permanent magnet. The potential is measured on the two electrodes (not shown) submerged in the mercury. For a complete description of the KARS the reader is referenced to the Final Report of a previous contract with DNA entitled Angular Rate Sensor Program Contract No. DNA001-77-C-0140 Report No. DNA4529F. Its purpose was to evaluate the technology associated with the KARS and to verify that it was at a level of development such that a production version could be designed. The successful completion of that contract resulted in the present contract.

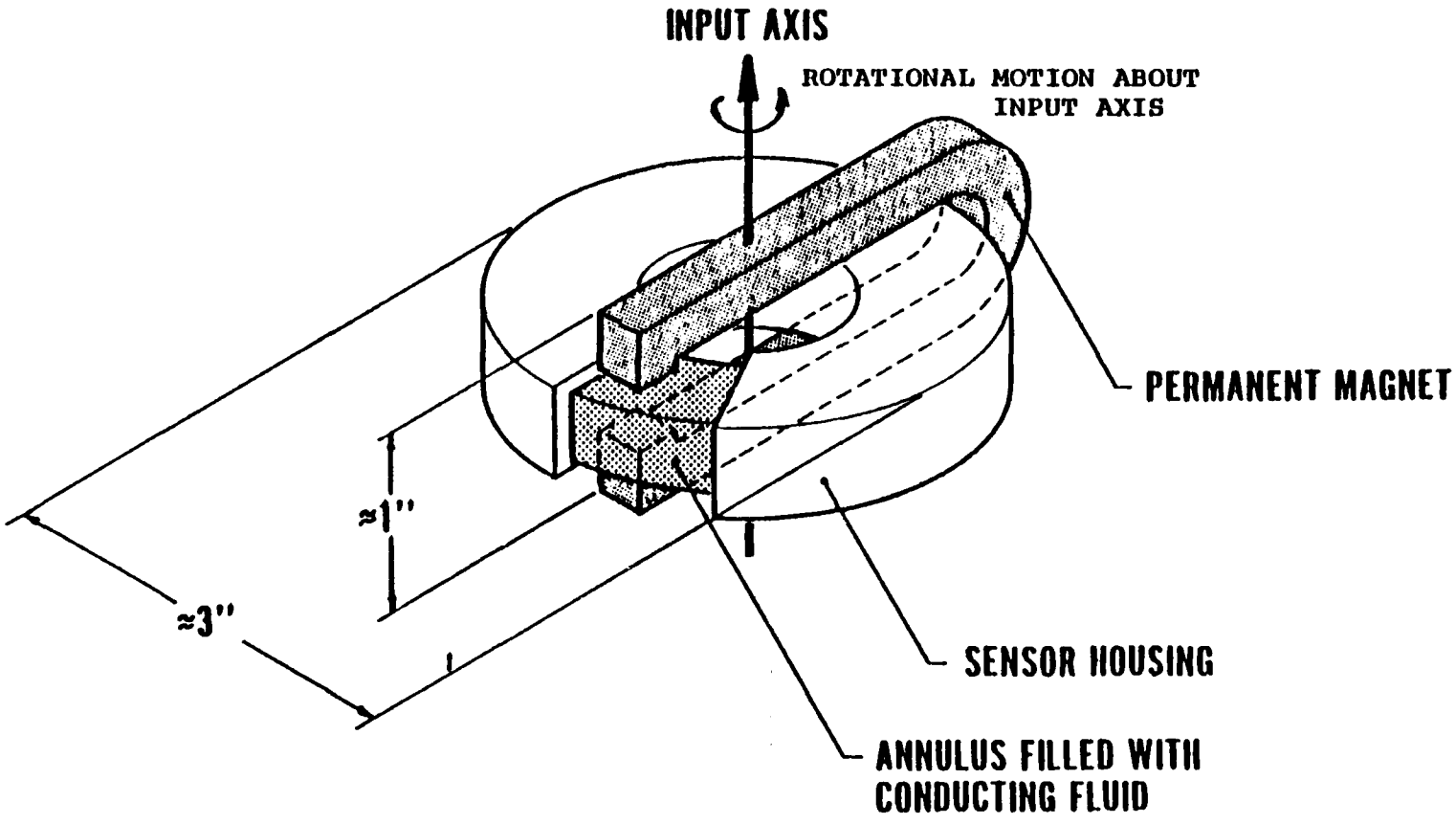

Figure 1. Kearfott Angular Rate Sensor

3. OPERATING PRINCIPLE

The conductive liquid ring used in the KARS assembly acts as a lumped inertia element viscously linked to the instrument housing. The differential equation describing the motion of such system has been written and solved. The reader is referenced to the previously mentioned Report No. DNA4529F for complete details and only the solution is shown below as Equation 1.

$$e_o = K\dot{\theta}_c(s) \qquad s > jW_o \qquad (1)$$

Where : e_o = output voltage (v)

K = Magnetic generator constant (V/s/rad)

θ_c = Angular input to the instrument case (rad)

W_o = Sensor lower corner frequency (rad/s)

SECTION II

BRASSBOARD SENSOR

4. DESIGN

The KARS has the capability to measure a wide range of input rates and is only limited by the saturation characteristics of the electronic processing circuit connected to it. For this particular application three distinct regimes were chosen and are listed below in Table 1.

Table 1

Regime	Max Input Rate °/sec	Bandwidth Hz
1	10	500
2	3,000	2,000
3	30,000	5,000

A full scale output of 5 VDC for each regime, 2% (of full scale) resolution and a low frequency corner of one hertz or less is required. In addition to the field temperature range (-35°C to 71°C) a severe shock environment (10,000 g's) will be seen by the unit. Results of the first contract indicated that these requirements could be met and a brassboard version of the sensor was designed. Its purpose was to evaluate the sensor performance with respect to its requirements and the environmental influences. The sensor can be broken up into two major areas one being mechanical and the other being electrical and are discussed separately in the following sections of the report.

4.1 Mechanical

Results of the previous contract showed that to meet noise criteria it was more beneficaal to increase gain by using multiple pickoffs than by simply increasing the gain in the electronic circuit. Based on this, a sensor incorporating eight (8) pickoff sets was made by modifying some hardware from the first contract and using a thin circular disc magnet covering the bottom and top surfaces. Figure 2 shows a picture of this sensor. All the possible combinations from one (1) to eight (8) pickoffs were tested and in general good agreement with the results of the first contract was obtained. However, the gain started to fall off as the pickoff number was increased from six (6) thru eight (8). At eight the increase in gain had dropped from 8/1 to 6/5/1 as a result of

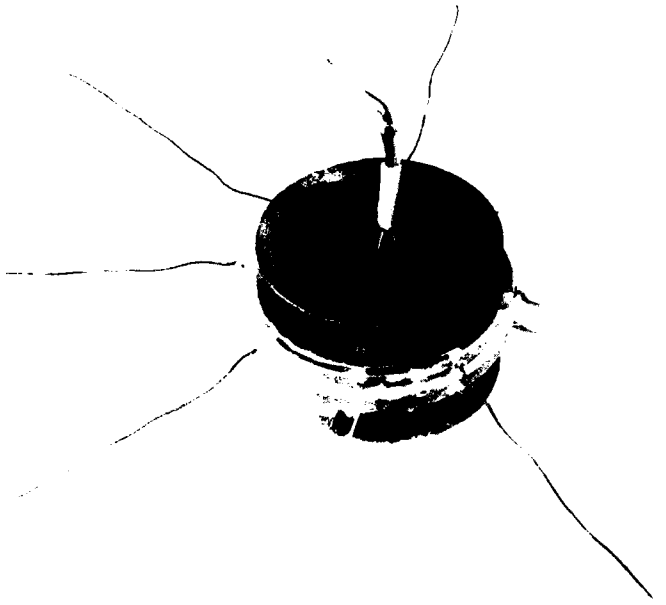

Figure 2. 8 Pickoff Version KARS

of the magnetic field around the mean circumference. This potential problem, the mating of surface problem (flatness sensor/magnet) and the multiple pickoff electrode seal problem resulted in another look at the multiple pickoff configuration versus electrical gain tradeoff which required a closer look at the noise sources and the electrical components used in the previous tests. This problem will be discussed in the electrical design section.

A return path was another possibility that would increase the scale factor in the current design. When the air gaps required to prevent shorting the magnetic paths and the increase in complexity in parts and mating surfaces that are required are considered this approach was rejected. Structural considerations during the shock load became the main consideration.

An increase in scale factor is possible if a reduction in the magnetic gap can be achieved. The present aspect ratio of the mercury annulus was chosen arbitrarily, but with the idea of obtaining the maximum moment of inertia about the input axis with no basis for the minimum required. A version of the sensor with an annulus whose thickness was equal to 1/2 of the original design (0.125 inches new/0.250 inches old) was designed and built. This unit incorporates a dual pickoff configuration feeding a voltage adding circuit, the resulting scale factor was 10 mV°/sec with a low frequency corner of belwo 0.1 Hz. Comparison testing of the 1/2 thickness and full thickness KARS shows no difference in low frequency corner response with respect to this application. The fidelity of the wave shapes at 5 to 10°/sec at frequencies of 10 and 20 Hz as compared to the input are the same. Figures 3 and 4 shows typical response wave forms at stated inputs and scale sensitivity. Based on these observations the 1/2 thickness unit was selected as the baseline design.

To evaluate the O-Ring as the thermal expansion compensation mechanism, the original test fixture for this purpose was used. A modification to the face seal was made and is shown as Figure 5.

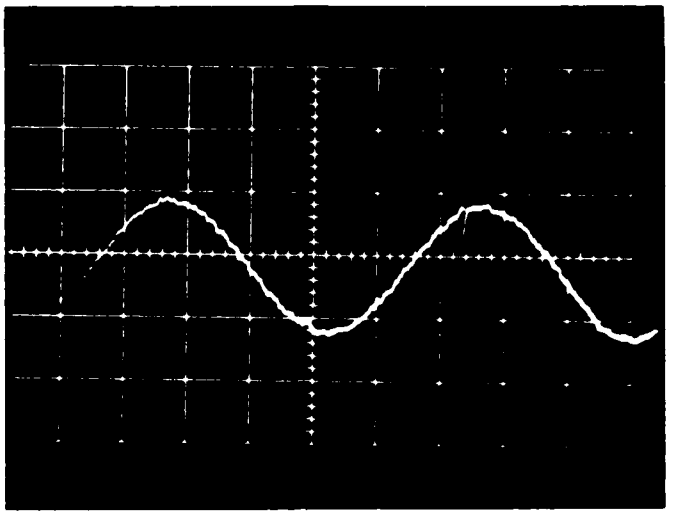

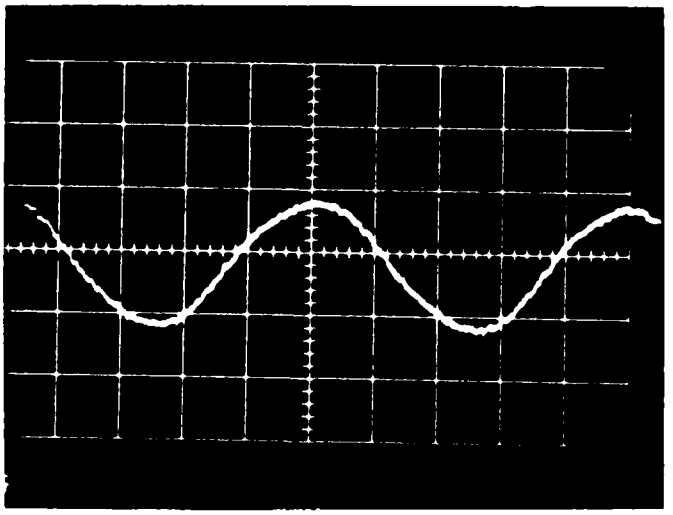

Figure 3. Output Wave Forms Full Model

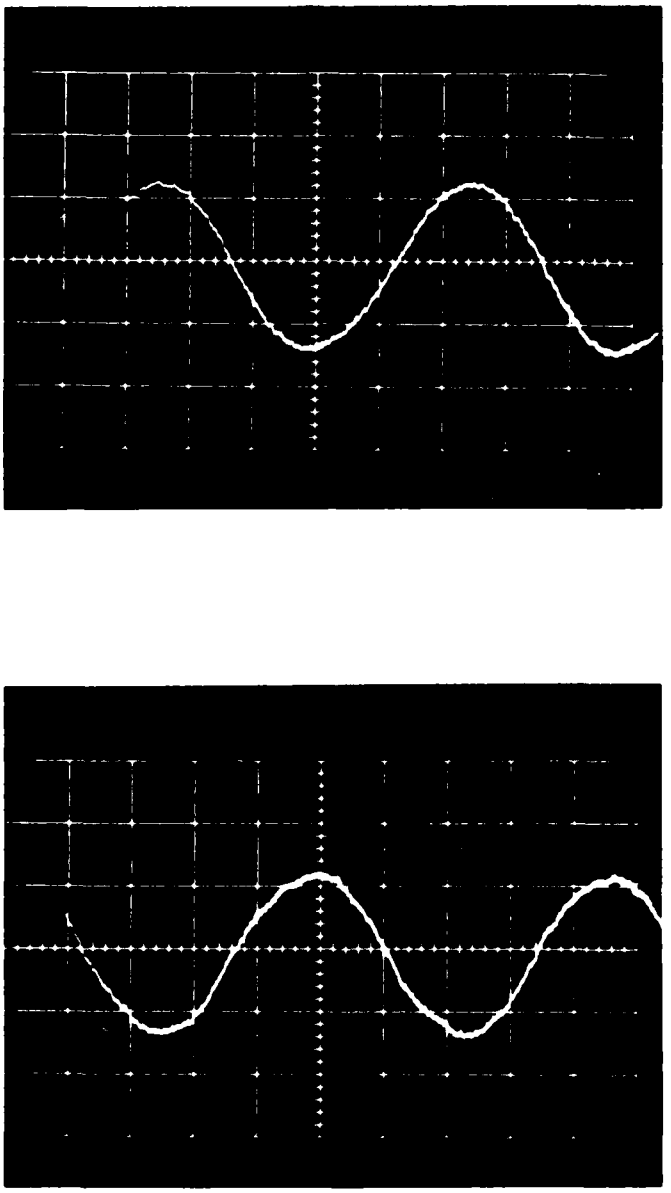

Figure 4. Output Wave Forms 1/2 Model

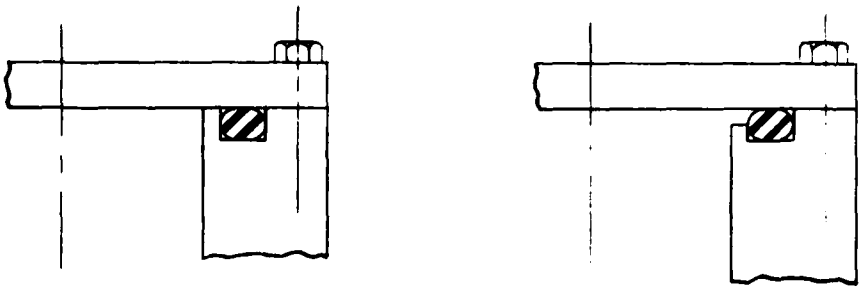

Figure 5

Thermal Expansion Compensation Mechanism

This modification allows more surface area of the O-Ring to be exposed to the mercury. Tests show that when subjected to the upper temperature limit of 71°C the maximum pressure measured was 165 psig. This test was repeated four times with good correlation. Figure 6 is a picture of the test fixture. The pressure transducer used to measure the pressure rise can be seen in the top center of the fixture. A further modification to eliminate the lip completely, to simplify fabrication, was made and tested showing similar results.

Engineering drawings were made based on the 1/2 thickness mercury ring, two pickoffs and incorporating an O-Ring as the compliant member but not for sealing. Sealing was obtained by first coating the mating surfaces with a commercial solvent for Plexiglas, the sensor non-conductive body material, and then the pieces pressed together to form a uniform bond/seal. In the assembly to prove out the O-Ring compliant member a poor seal was obtained which resulted in a large void in the mercury and prevented any testing. This could be a potential problem using this method of sealing and cannot be easily corrected as the pieces are bonded together. To eliminate this problem the sensor was sealed with O-Rings and screws for evaluation work. The use of the O-Ring as seal and compliant member turned out to be the best solution and was incorporated into the baseline design. Figure 7 is a picture of the brassboard O-Ring/screw sensor design.

The design of the sensor support structure to support the sensor has been completed and was analyzed by a finite element stress/strain computer program to determine its response to

Figure 6. Test Fixture - Thermal Expansion Mechanism

Figure 7. Brassboard Sensor

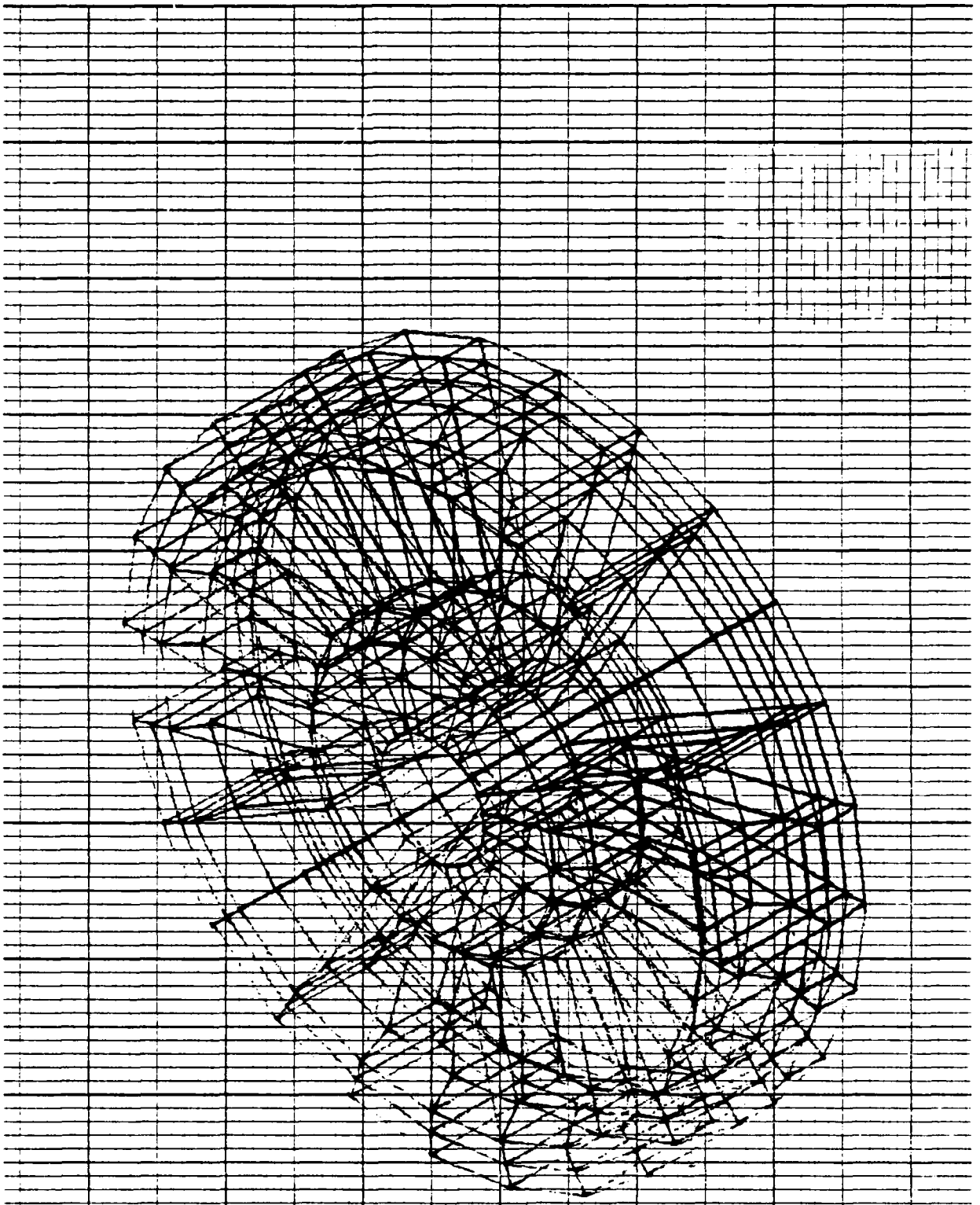

Figure 8. Geometry Plot Finite Element Program

STRESS ANALYSIS.KAROS RIND

the 10,000 g shock. Figure 8 is a geometry plot of the complete structure showing how the structure was broken up for the program. After some initial trimming the combined stresses are within acceptable limits. A conventional strength of material stress analysis was also performed by hand calculation. There were differences in values, but the same conclusion of a safe design was arrived at. Ultimate tensile strength of 130K psi was used in both approaches as a titanium alloy (6 AL 4VA) had been selected for support structure. The basis of this selection was light weight, strength and the lack of iron in the composition.

Initial plans were to build and test this structure but the combination of test facilities (10,000 g, 3.2 millisec duration) and time a decision was made to trust the stress analysis and only build the final design.

Initially it was planned to fill the KARS through tubes that would be pinched off forming a crushed defusion bonded seal. Two were to be used, one to pull a vacuum and the other to back fill with mercury. Seal problems developed between the tubes and the sensor which did not yield to a easy solution so a new design was incorporated. This design is similar to seal on a medical ampule bottle. A rubber seal is held in place by a hollow set screw and the seal is punctured with a hypodermic needle to gain access thru the seal. Figure 9 is a sketch of this type seal showing the hypodermic neelde in place. After the fill has been completed the hollow set screw is replaced by a solid one and the void above filled with an epoxy sealer.

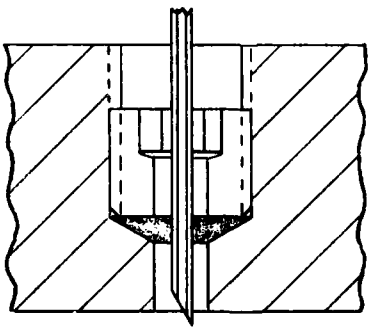

Figure 9

Mercury Fill Evacuation Port

This type of seal has been used in other sensors made by Singer Kearfott Division (SKD) and proved to be extremely reliable on the KARS. Simple electrode seals were obtained by using a close fitting feed thru hole and sealed with an epoxy compound.

4.2 Electrical

The electrical design proved to be more of a problem than was expected due to the high gain required in the 10°/sec regime to deliver 5 volts full scale, a 2% resolution and be stable. Table 2 is a restatement of some data from the first contract final report DNA 4529F Table 3 with an addition of a column for the noise to signal ratio at 10%/sec.

Table 2

Number Of Pickoffs	Scale Factor MV/°/Sec	Noise MV	Noise/Signal 10°/Sec %
1	1.83	0.8	4.37
2	3.86	1	2.59
3	5.57	1	1.79
4	7.10	0.8	1.13

As original planned a large number of pickoffs were to be used between parallel magnets and from the above trend there would be no problem with the resolution specification. However, when the multiple seal problem, the non-uniformity of the magnetic flux, as detailed in the mechanical design section and the noise/signal deterioriation as the signal was amplified to 5V full scale showed the resolution to be a problem. The solution was a detailed look into low noise op amps and the design of high gain stable circuits. Resulting from this investigation was a design that is shown in schematic form as Figure 10.

As can be seen from Figure 10 the outputs are AC coupled so not to have DC bias shifts in the circuit effecting the output. This type of coupling is possible as the sensor cannot follow

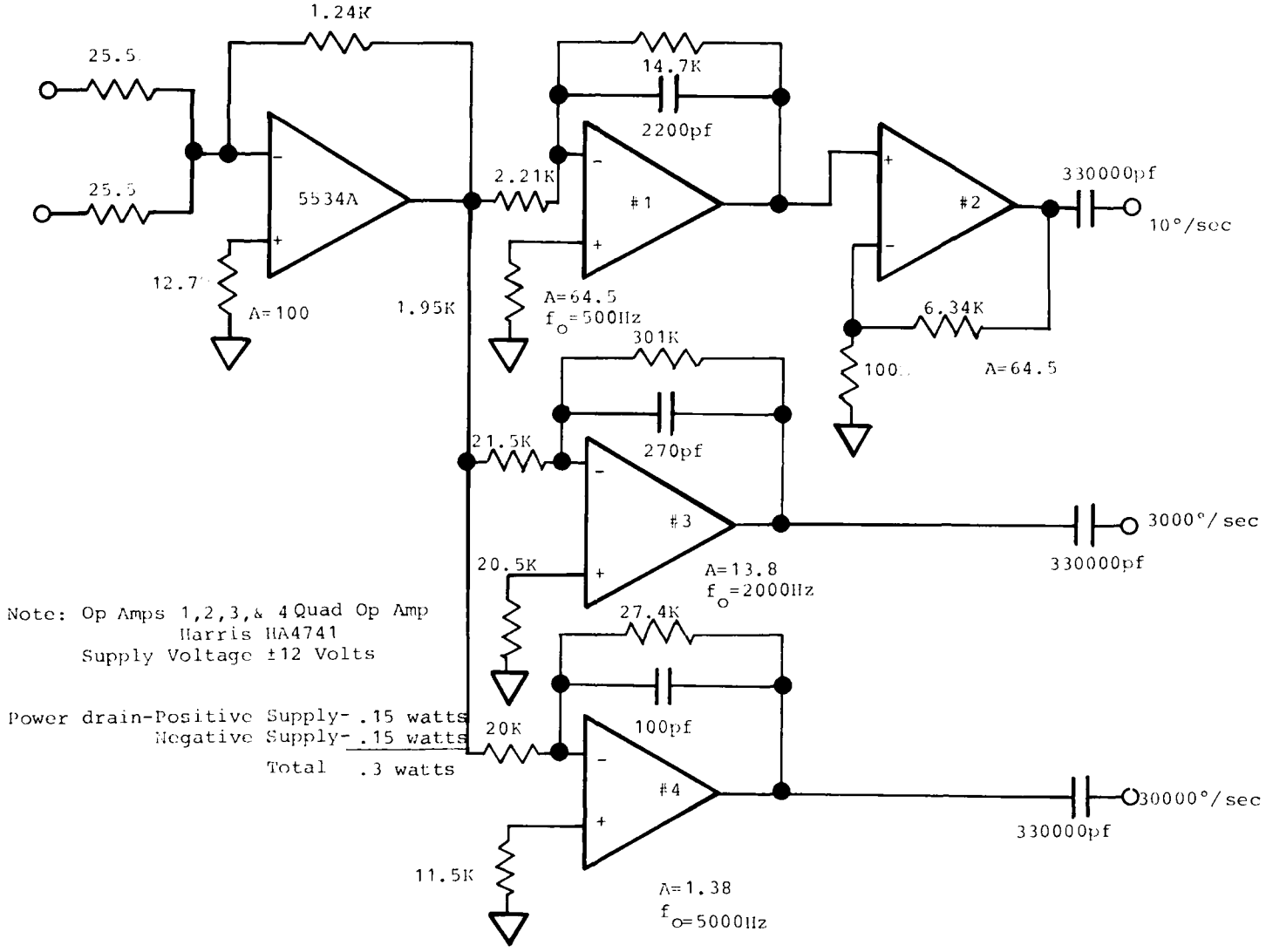

Figure 10. Brassboard Electrical Schematic

DC and, therefore, no need to pass DC voltages is required. The required bandwidths are obtained by using single pole filters in the feedback loop of an op amp in each regime. Interconnections between amplifiers are phased as to give a positive output as defined by the right band rule. (Counter clockwise viewed from top of the KARS).

Electrical components that have been selected are a Signetics op amp SE 5534 AT for the first stage, a Harris HA-1-4741-2 Quad op amp for the remaining stages. A National LM 126 dual polarity tracking voltage regulator delivers ±12 volts to the circuit from a ±15 volt supply voltage. A voltage regulator was incorporated to eliminate any sensor output change due to power line variation.

Brassboard electronic circuits were constructed by using phenolic vector boards wiring and sockets for integrated circuits. All components selected are Military qualified and should not be a problem over the temperature or vibration environmental range. Figure 11 shows a typical brassboard circuit configuration.

The output will consist of four wires, three color coded outputs and one common low or ground.

Input requirements will be ±15 volts DC supplied by three wires two hot and one return. Input power requirements should be less than 1/2 watt.

5. TEST RESULTS

KARS testing was performed using a rate table operating in a sinusoidal mode. Scale factor and low frequency corner testing were amplified on this table. Figure 12 shows a typical result for the three output circuits. Good correlation was obtained with theoretical and actual outputs and shows linear response at the higher rates. This testing was performed at a frequency of 5 Hz; however, testing at a variety of frequencies shows no appreciable change in performance.

Some data at higher input rates has been obtained. At a frequency of 2 Hz, two data points were obtained at 175 and 338°/sec with good correlation between sensor and table

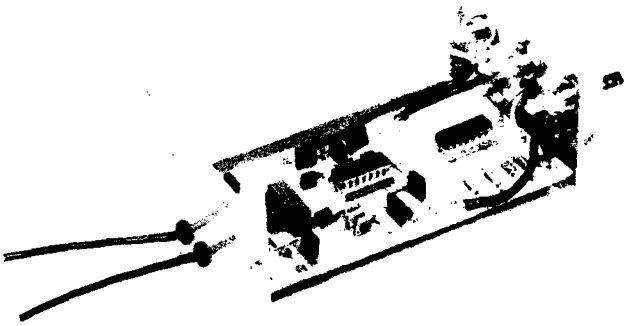

Figure 11. Brassboard Circuit

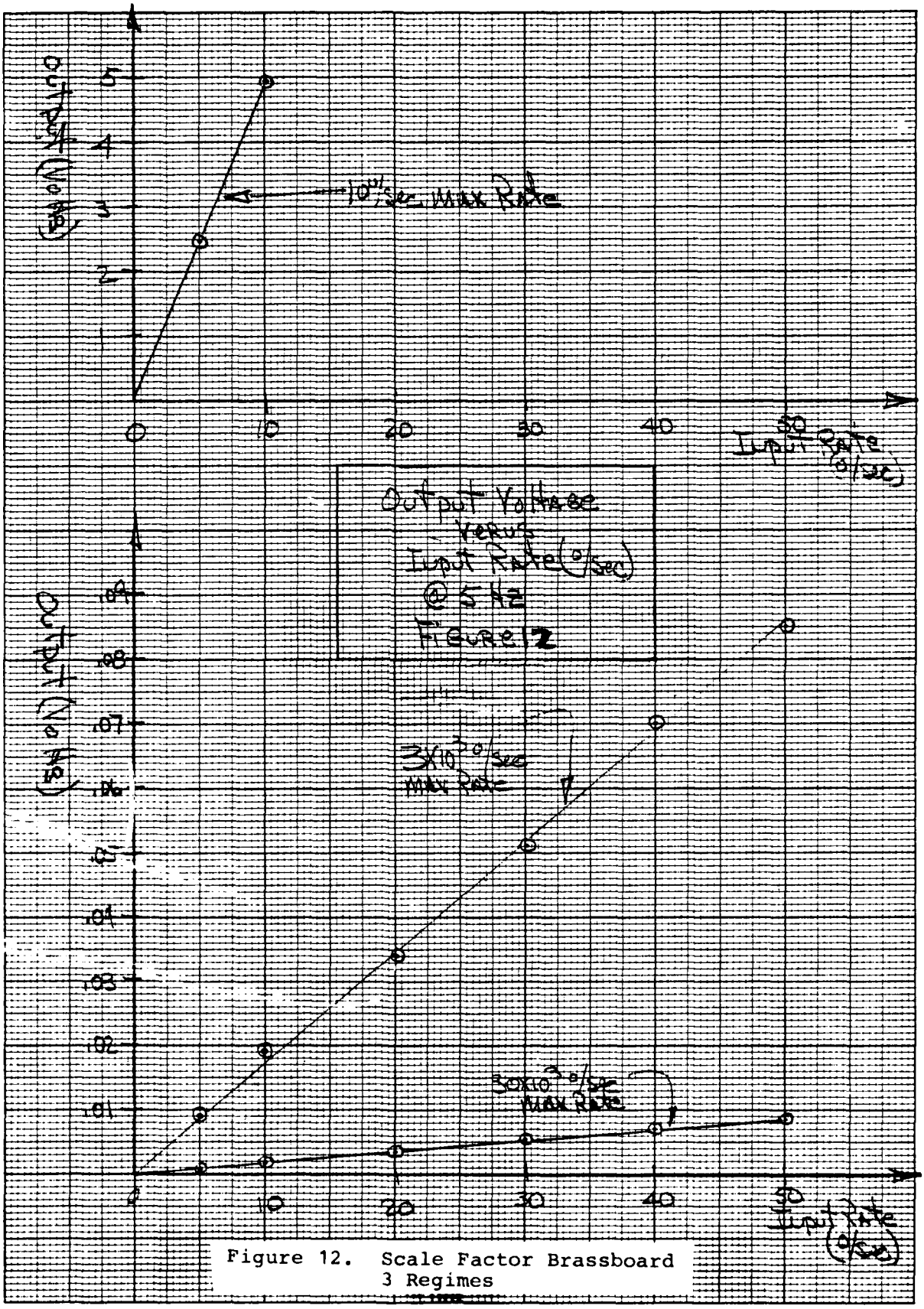

Figure 12. Scale Factor Brassboard
3 Regimes

indicated rates. These table rates are beyond limits stated for the machine but, discussions with the manufacturer (Genisco) showed that it was possible to get to the full torque limit of the rate table and do no damage.

By reducing the table inertia it was possible to approach 1000°/sec as an input rate in the oscillatory mode. Some trimming of the servo control loop was required based on information supplied by the manufacturer. Additionally a low inertia table top was fabricated and assembled on the table. Comparison of the sensor output with the table input, with the conventional table top, showed good correlation and both show the switch from sinusoidal wave form to triangular when the drive torque starts to limit.

Noise measurements have been made in the outputs and are 0.042, 0.0023 and 0.00045 Volts RMS for the 10, 3000 and 30,000°/sec circuits respectively. These measurements were made with a true RMS voltmeter with an integrating time constand of 10 sec.

To evaluate the effectiveness of the filter corners and to get an understanding of the frequency noise spectrum, the sensor with its complete electronics was connected to a real time spectral analyzer with a digital plotting capability. Figure 13 is a typical plot and is for the 10°/sec regime. The lower curve shows the circuit as described by Figure 10 and the 39 X 10^{-3} VRMS is an good agreement with the noise level previously stated and shows the single pole filter break to be at apprxoimately 500 Hz. The upper curve is the same circuit with the 2200 of capacitor removed showing unfiltered response to 5 kHz. Vertical scales are in db while the horizontal is log frequency starting at 12.5 Hz and extending to 5 kHz, the SV 100 means that 100 samples were processed for the average wave form displayed. High frequency corners for the 3000 and 30,000°/sec regimes were measured to be 2000 and 5700 Hz respectively. The low frequency corners were all below 1 Hz at 0.55 Hz.

This circuit was mounted in a standard electrical Bud box, potted and subjected to the temperature extremes (-35°C; 71°C). Evaluation of the circuit showed no change in the performance after exposure to these temperatures. In addition, the circuit was operated with a function generator as the signal source over the operational temperature range (-29°C to 71°C) and functioned successfully with less than

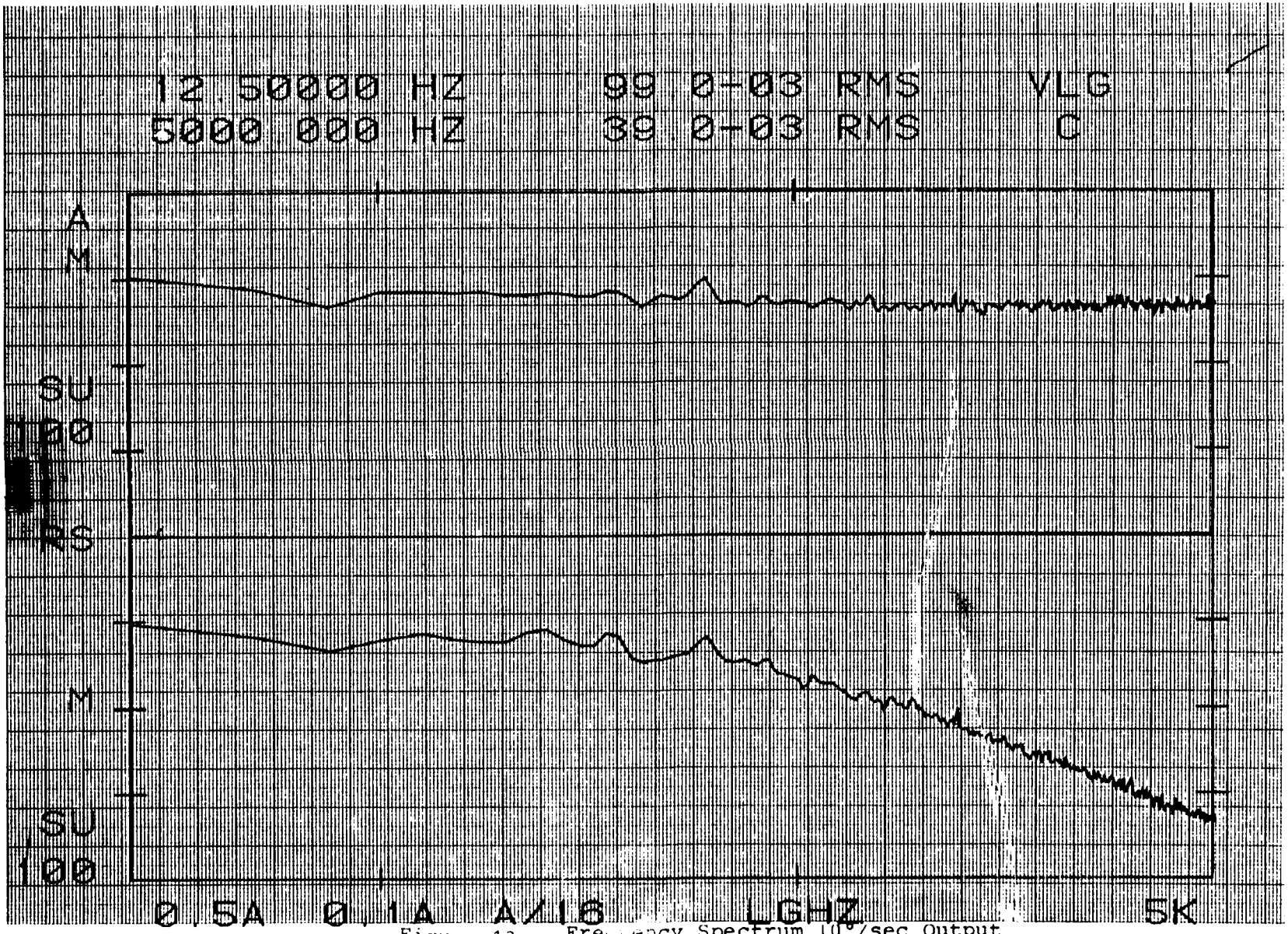

Figure 13. Frequency Spectrum 10°/sec Output Brassboard Sensor

a 1% change in the individual bandwidths for the three regimes. To demonstrate operation the three regimes were individually functioned at full scale outputs.

This potted circuit was subjected to the transportation vibration specification for this system. Figure 14 shows the circuit mounted on vibration in the two orientations tested. Figure 15 shows the shape of input acceleration frequency profile for a typical run. Scale factor check after these tests showed no change.

To reduce the part count the bias resistors were eliminated from circuit. To prevent bias shifts in the high gain regime #1 circuit an additional high pass filter was required. Figure 16 shows the new circuit. No change in scale factor in regime #1 was observable as predicted, however, the low frequency corner slipped up to 1.2 Hz and required the changing of AC coupled output capacitor from 0.33 uf to 1 uf which dropped the low frequency corner below 1 Hz. This circuit is the choice for the baseline design.

6. MODIFICATIONS

The concept of using a brassboard to checkout the design proved to be very useful in this program. The following are the problems uncovered and the action taken and are tested in Table 3.

Table 3

Modifications Brassboard Design

Problem	Modification
● Fill Problem Pinch Tube	Rubber Compression Seal
● Sensor Seal	O-Ring For Seal & Thermal Compensation Mechanism
● Resolution Full Scale Output Regime #1	Change Pickoff Design From 8 to 2 and Design Low Noise, High Gain, Stable Electronic Circuit.
● Regime #1 Low Frequency Corner Above 1 Hz	Modify AC Coupled Output Capacity From 0.33 uf to 1 uf.

These changes/modifications have been implemented successfully and have been included in the baseline configuration of the KARS.

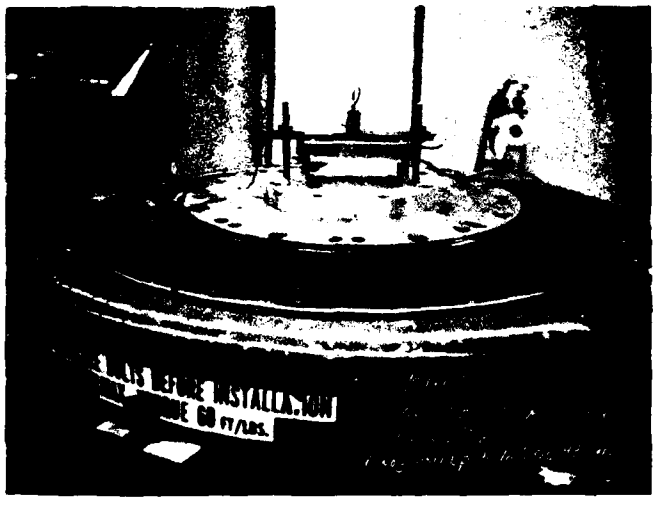

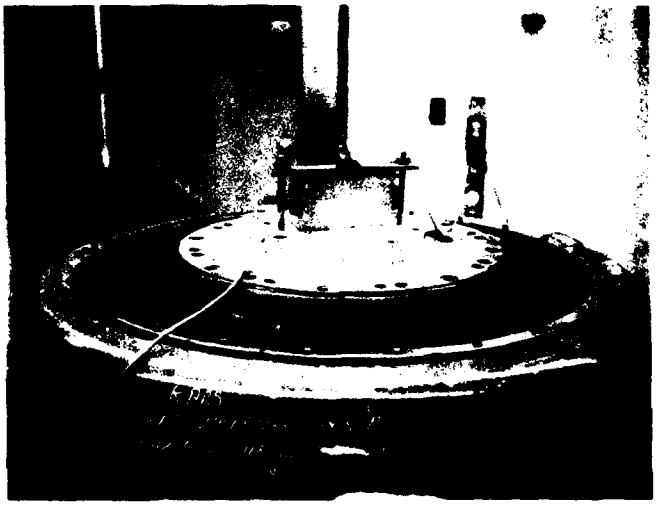

Figure 14. Brassboard Electrical Circuit Vibration Test

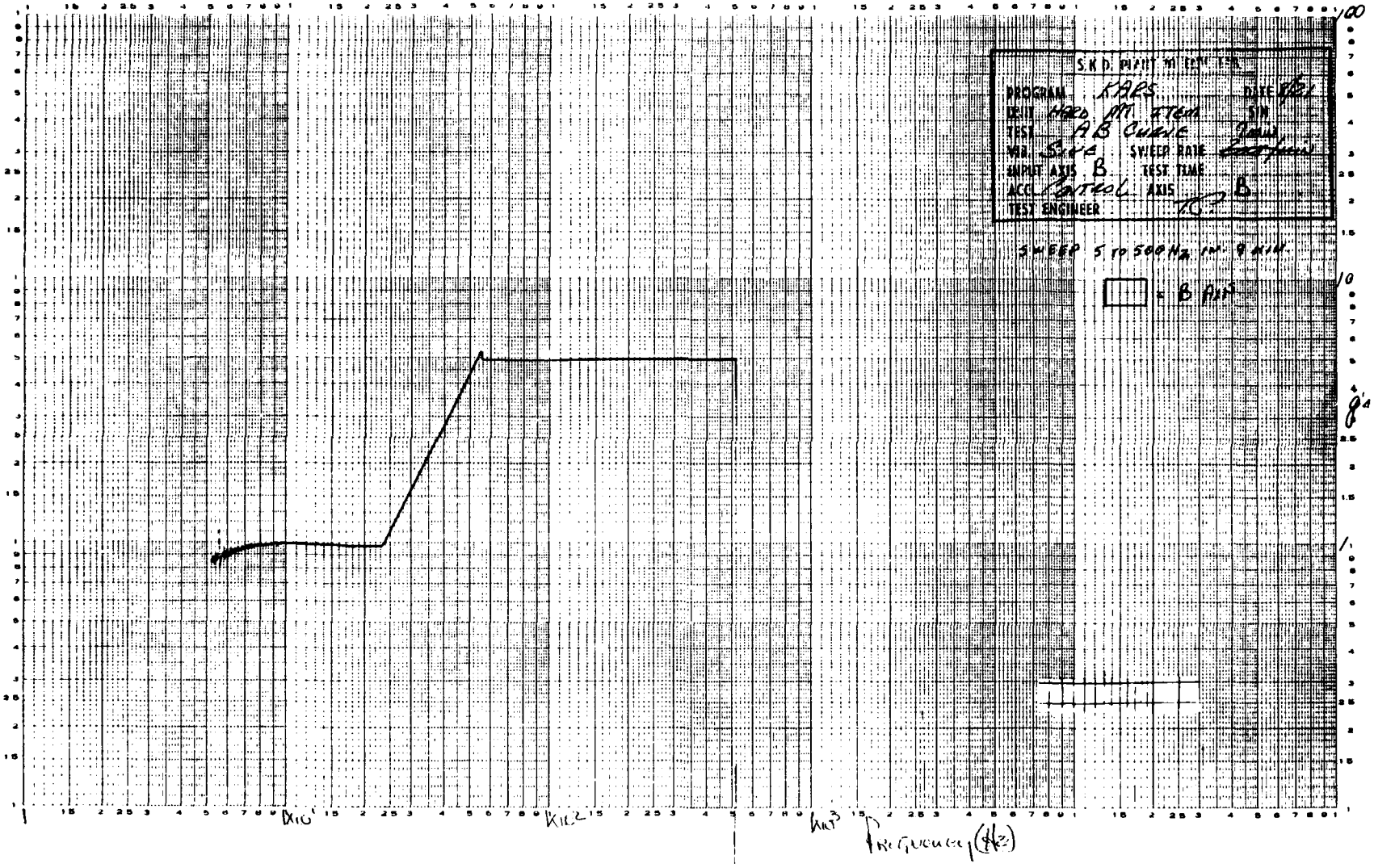

Figure 15. Vibration Spectrum Brassboard Circuit

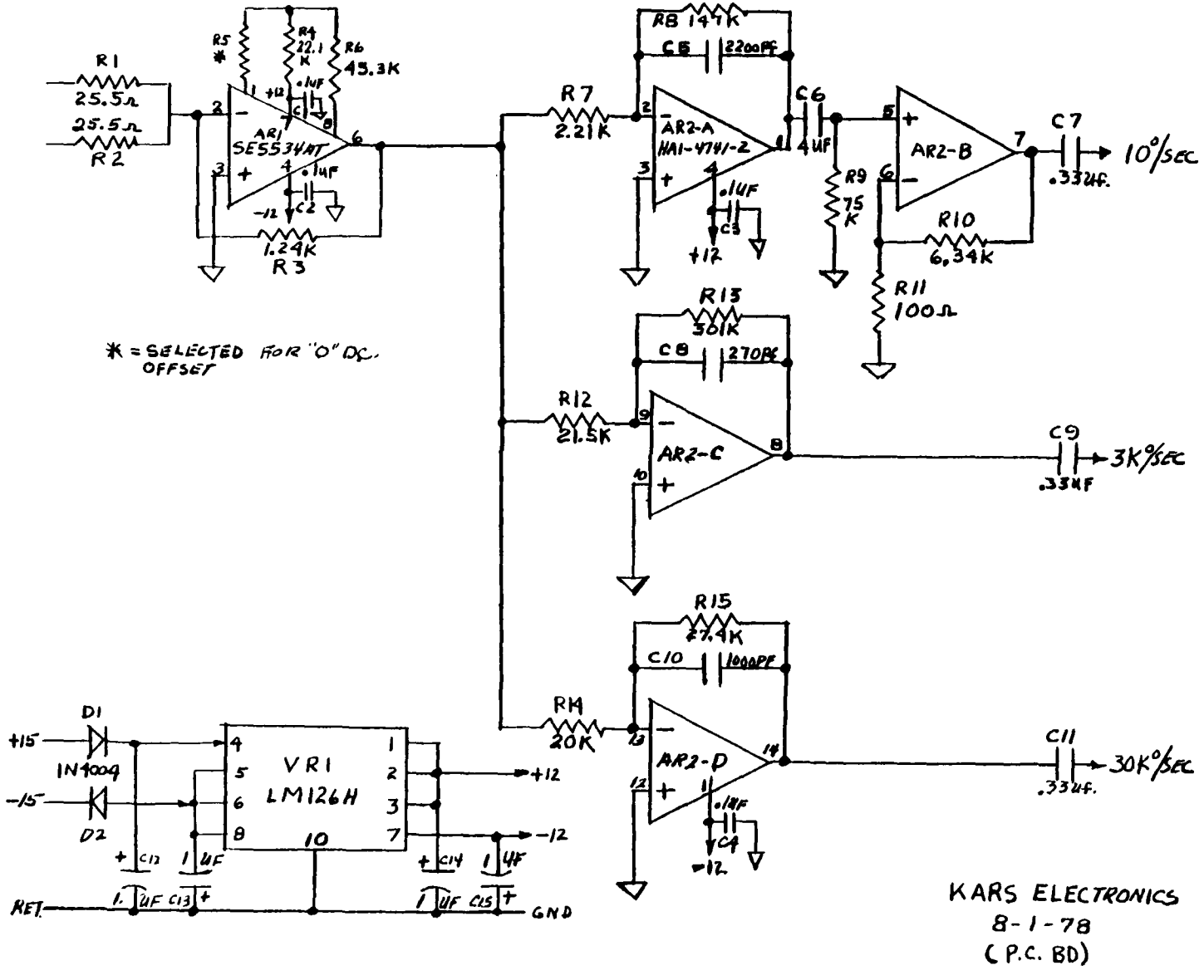

Figure 16. Mod 2 Brassboard Electrical Circuit

SECTION III

PROTOTYPE PRODUCTION SENSOR

7. DESIGN

The prototype production version of the KARS is the baseline developed using the brassboard proven concepts. This design is a two pickoff version using a plastic sensor housing surrounded by a metal structure for strength. O-Ring's are used as both the primary mercury seal and the thermal compensation mechanism. Pure gain is provided as required to bring the output level to 5 VDC at maximum inputs in the three operating regimes of the sensor. Bandwidth is proved by single pole filters in the feedback loop of the gain amplifiers and capacitive coupling is used to eliminate any bias shifts.

7.1 Hardware Description

The KARS outline is defined by SKD drawing #K130A062 which is shown in this report as Figure 17. It is basically cyclindrical in shape with a centerline and flange provisions for mounting. The sensor is sensitive to rates about the centerline producing a positive output for a counter clockwise motion of the case when viewed from the top. Three ranges (10, 3000 & 30,000°/sec maximum input rate) provide a 5VDC full scale output and all three ranges work independently and can be monitored simultaneously. Power requirement is 0.3 watts ±15 VDC and is supplied through the cable harness. Outputs are monitored via three wire shielded cable in the cable harness. The KARS consists of a sensor with its electronics surrounded by and supported by a outer housing set. Figure 18 shows a major part breakdown consisting of upper, lower housing, cover sensor and electronic P/C board. In this early picture of the parts the sensor was not filled with Mercury, however, the Samarium Cobalt magnets are in place. In addition, the O-Rings were not installed. Upper and lower housings and cover are made of a 6-aluminum 4-vanadium titanium alloy while the sensor housings are made of Rohm & Hass Plexiglas 55, an aircraft quality acrylic thermoplastic. The sealing/thermal compensation is obtained by using two Nitrile O-Rings and Parker Company Compound #N674-70. All of the wires have teflon insulation and were etched prior to potting with Dow Corning Sylguard 186. A commercial thread locking compound, Glyptal, was used on the 2-56 screws securing the cover to the upper support housing. Due to the cement/water environment in actual use the screws to hold the KARS together and

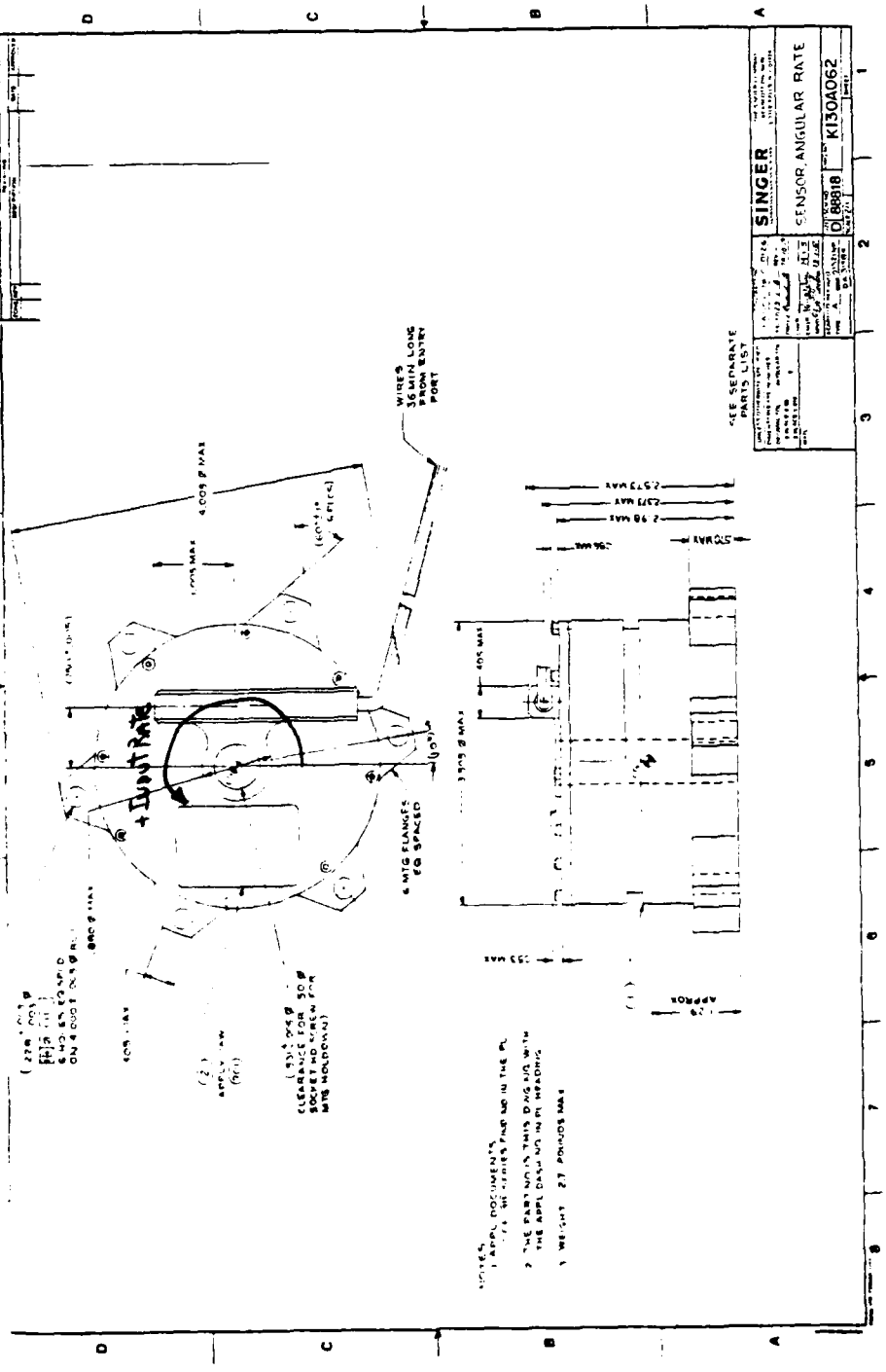

Figure 17. KARS Outline Drawing SKD #K130A062

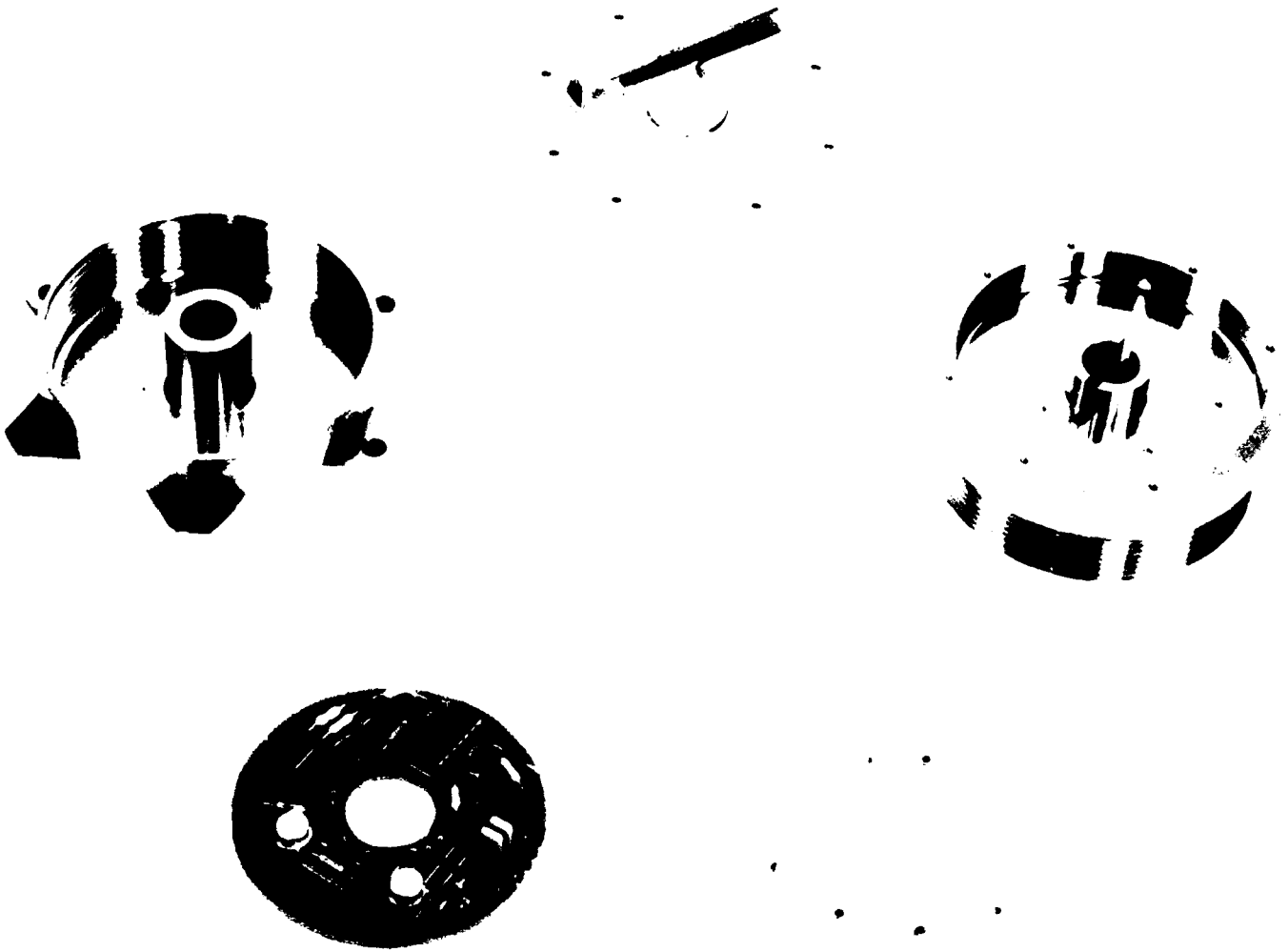

SINGER | PHOTO NO 43895 Figure 18. KARS Major Part Breakdown

the ones to mount to the test location are made of the same titanium alloy, 6-aluminum 4-vanadium. By using the same material cathodic protection can be obtained. Figure 19 shows the KARS assembled with cover removed to show the electronic P/C board and how its mounted in the upper support housing.

A close up view of the P/C board is shown in Figure 20. The first stage SE5534AT can be identified in lower left hand corner, while the National LM126H is in the lower right hand corner. At the top center is the Harris Quad 4741-2 amplifier, the gold rivets at 3 and 9 o'clock are the input connections from the dual pickoffs. SKD drawing #K130A062 appearing as Figure 17 defines the KARS outline and mounting interface information. Appearing as Figure 21 is the electrical schematic for the sensor and defines the input power and output level connections. These two drawings define the installation of the KARS and its hook up. Figure 22 is a picture of the assembled unit.

7.2 Test Methods

All of the rate testing on this program was performed using a Genisco Model 1100-5 Rate Table. Typically the Genisco system consists of a direct drive rate table assembly including drive spindle mounted torque motor, precision tachometer generator and electrical slip rings; an all transistorized high power servo amplifier and a power supply; and a high precision voltage reference and divider network. Of special interest to this program is that by use of an external input plug, sinusoidal input signals can be summed to the servo loop producing sinusoidal table motions. The table motion is only limited by table inertia, system bandwidth and torque capabilities.

As supplied by the vendor with a 14 in diameter aluminum table, rates of 140°/sec at a frequency of 3 Hz are possible. The external input has a sensitivity of 1 volt/°/second and the tachometer has an output nominal scale factor of 0.070 V/°/second. Source for the external input was a Interstate Electronics Corporation Model F51A function generator which had a low and high output level connections and a variable cross over adjustment in the sine function which was useful. Output voltage levels were

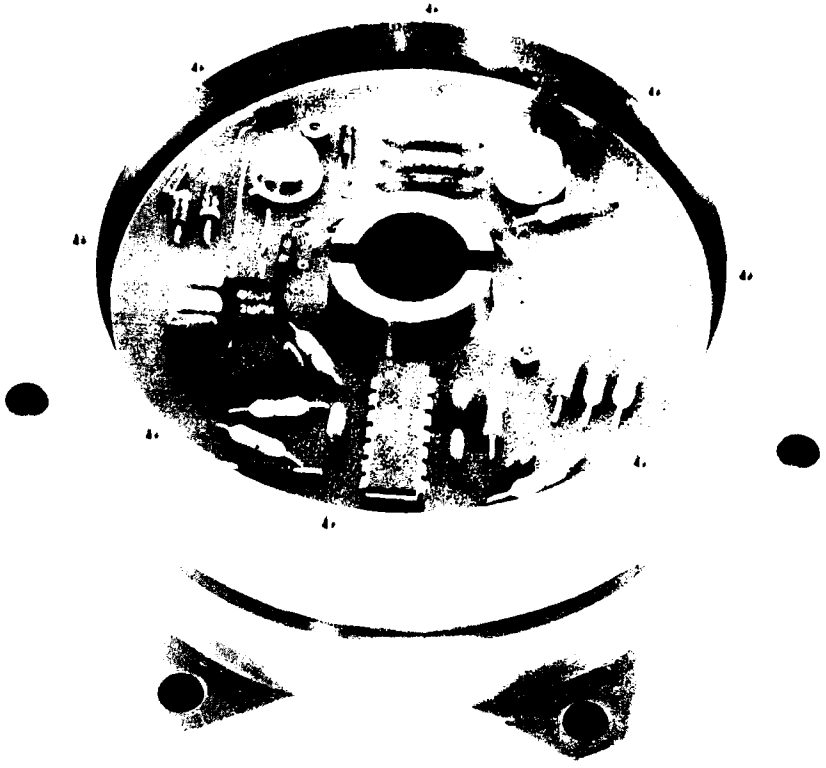

SINGER KEARFOTT DIVISION | PHOTO NO 43893

Figure 19. KARS Partial Assembly View

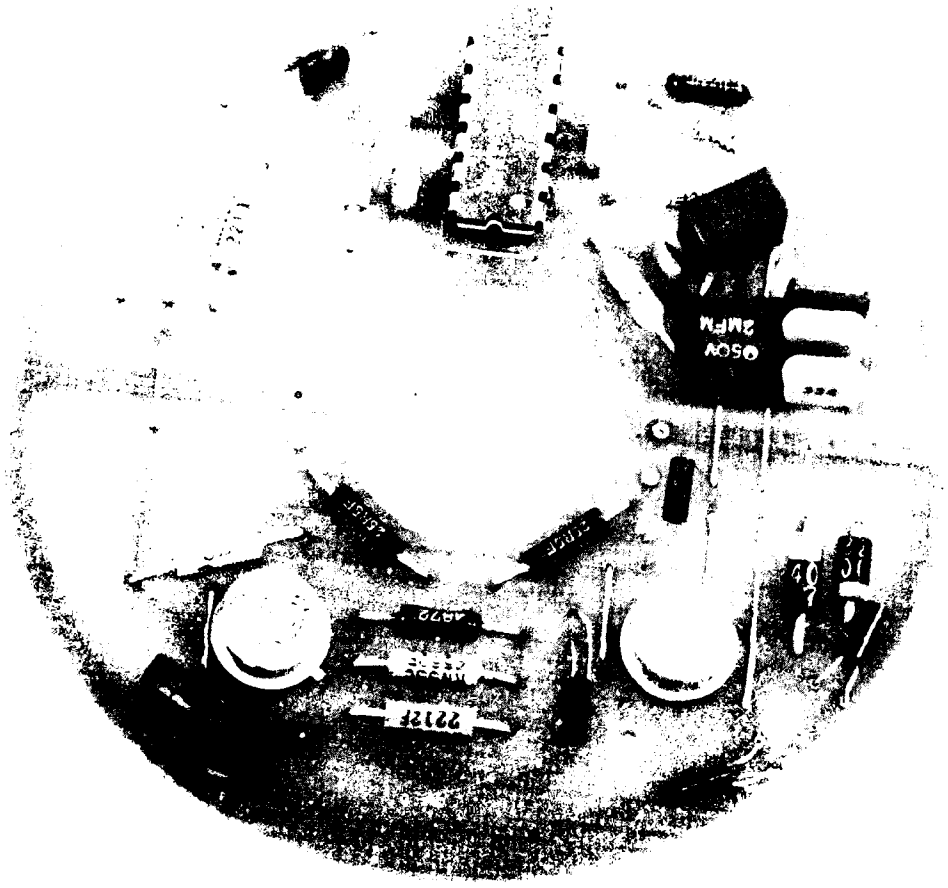

SINGER | PHOTO NO 43894

Figure 20. Closeup View P/C Board

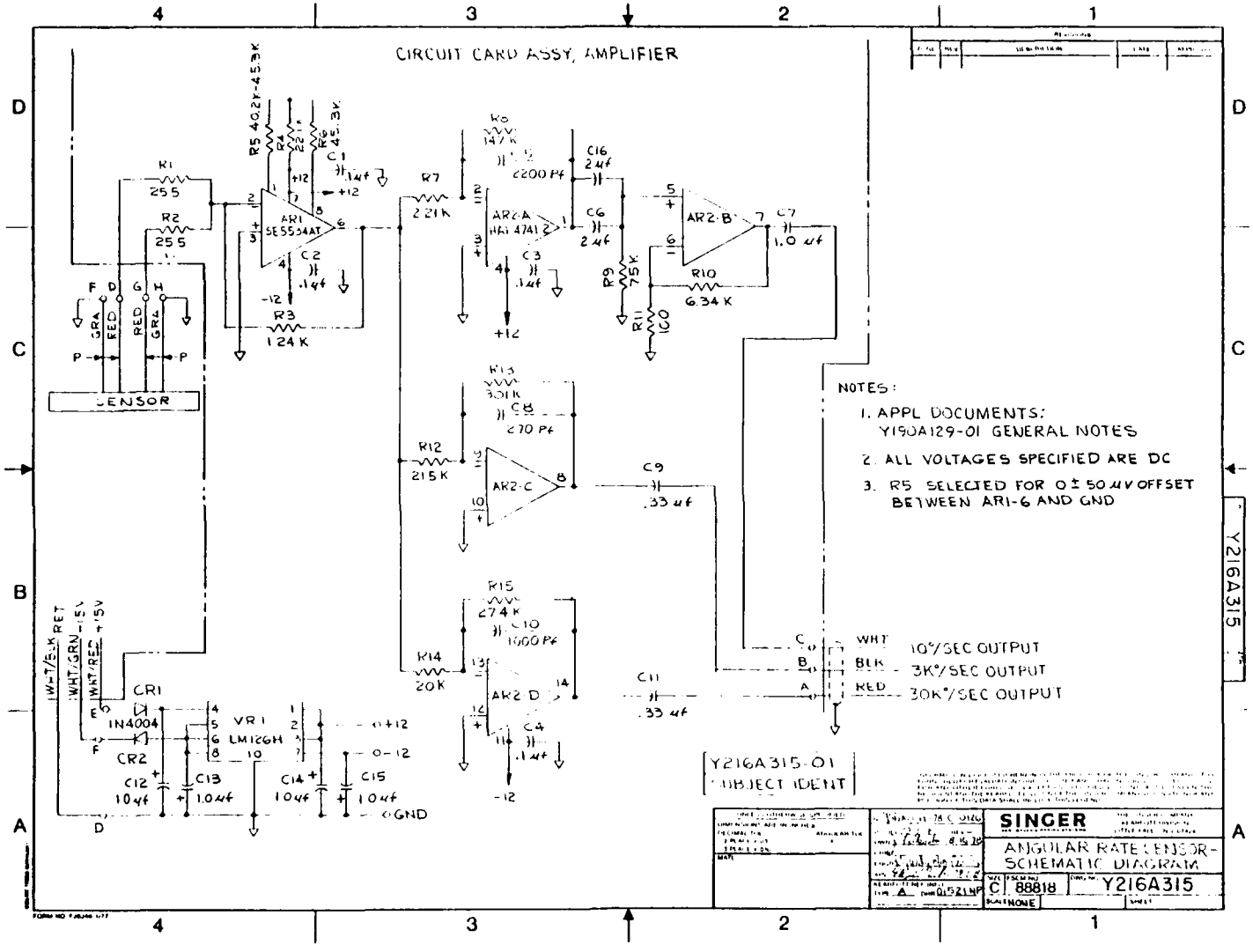

Figure 21. SKD Drawing #Y216A315 Schematic Diagram

SINGER KEARFOTT DIVISION | PHOTO NO 43892 Figure 22. KARS Kearfott Angular Rate Sensor

measured using a Fluke Model 873A which was good down to 5 Hz, below this a Disa Model 55D35 was used which was good to0.1Hz. Signal wave form was displaced on Tektronix Model 545 with a type 1A7A plug-in. This plug has the unique feature of high gain and variable bandwidth filter capability. Low frequency response was measured using Lissajous figures displaced on Hewlett Packard Model 1205B dual channel scope with a A versus B option. All scopes were used in the DC input mode to eliminate any low frequency signal distortion. Sensor power was supplied from a Power Design Model TW5005 dual power supply. Basic 115V AC power was supplied from a single phase source with heavy ground wire terminations to eliminate 60 Hz ground loops.

Figure 23 is a picture of the test stand showing the test equipment. The rate table has the standard 14 inch table head. Shown in the figure on the rate table is a selector switch terminal for convenience testing of the three sensor regimes. For stability the test station was mounted on an inertial quality test pier. Figure 24 shows the low inertial tabletop designed to increase rate capability and the use of the slip ring facility of the rate table. The drive spindle mounted torque motor can be seen under the plexiglas shield. Figure 25 shows another view of the test area, this time with the low inertia test tabletop.

Temperature and vibration testing were performed in the SKD Environmental Test Laboratory using standard test equipment.

Frequency response data were obtained for the electronics by using a Solartron EMR Frequency Response Analyzer Model 1410-01.

The strip chart recorder used for phase checks and sensor response to step input was a Brush Recorder Model 240.

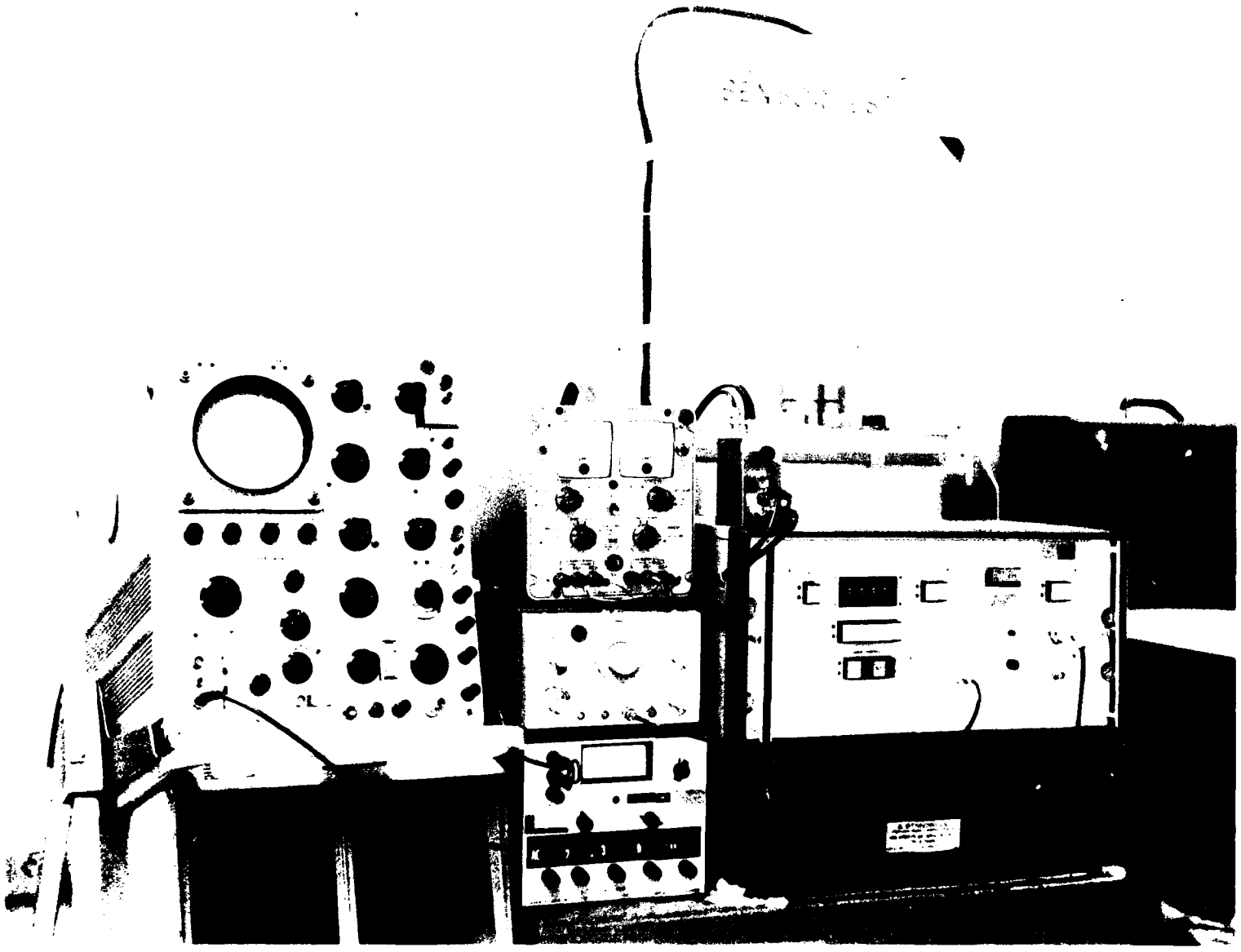

SINGER | PHOTO NO 43899-1

Figure 23. Test Stand

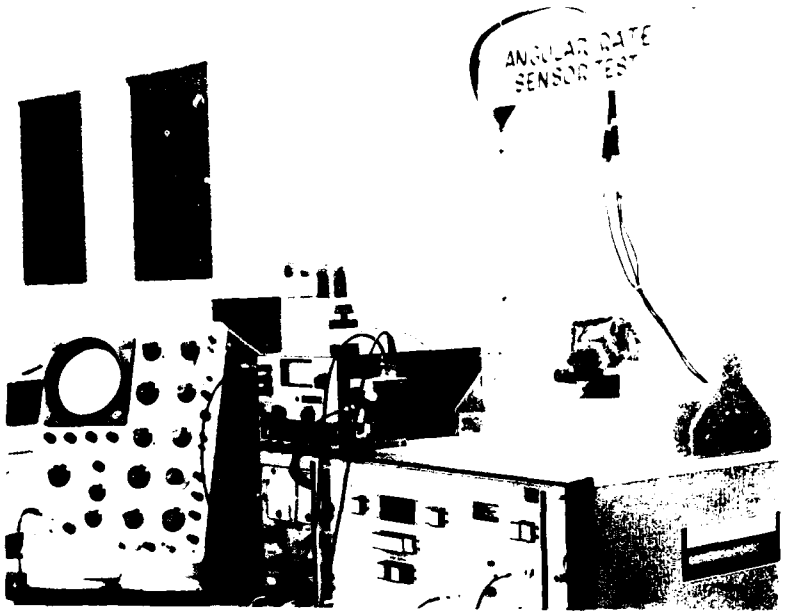

Figure 25. High Rate Test

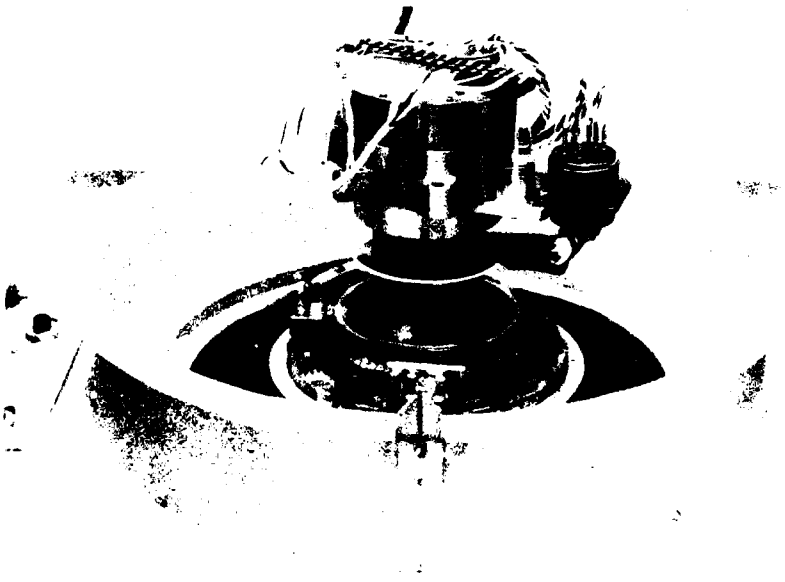

Figure 24. Low Inertia Rate Table Head

8. TEST RESULTS

8.1 Electronics

Separate tests were conducted on the electronics to establish performance and to compare with design requirements. Gain, bandwidth, noise and low frequency response were evaluated. Numerous such measurements were made during design and exist in the program file, only the final design circuit values are included. These represent the circuit boards used in the two deliverable units (S/N 1 & S/N 2) and are shown in Table 4.

Table 4

	Description	S/N 1	S/N 2	Design Goal
Regime #1				
AR1†				
	1st Stage DC Offset	+500 uV	-600 uV	1000 uV
	Gain	90.0	91.7	*
	Frequency	Flat	Flat	Flat
AR2-A/ AR2-B				
	Gain	4202	4082	4160
	High Corner Frequency	512 Hz	480 Hz	500 Hz
	Low Corner Frequency	0.66 Hz	0.63 Hz	0.57 Hz
Regime #2				
AR2-C				
	Gain	13.8	14	13.8
	High Frequency Corner	2000 Hz	2030 Hz	2000 Hz
	Low Frequency Corner	0.72 Hz	0.63 Hz	0.48 Hz
Regime #3				
AR2-D				
	Gain	1.36	1.38	1.38
	High Frequency Corner	5920 Hz	5800 Hz	5809 Hz
	Low Frequency Corner	0.73	0.62 Hz	0.48 Hz

† For description code see Figure 21.

* Trimmed for each sensor scale factor nominal 100.

As can be seen from the table, the design goals were achieved. Included for information and to show the character of the response are Figures 26, 27 and 28 for S/N 1 circuit board. The bandwidths are determined by using the 3db point and the reference point is cited on the individual figures of 0db. Regime #2 and #3 have simple single pole filters for the high and low pass filters used. Regime #1 has simple single pole filter for the low pass filter, but a second order filter for the high pass filter. Figure 29 shows a computer solution to the mathematical model used.

The circuits performance on supply voltage was determined by setting regime #1 at full scale output (10 Vpp) at 50 Hz and the nominal ±15V supply varied from ±13V to ±18V, with no measureable effect. Previous test data on the development units showed this design could operate in the specified environmental; hence, the individual circuit boards were not tested.

As previously noted, resolution had proved to be problem so the noise measurements at max gain utilized in regime #1 (3.78×10^5) were made and proved to be 40 MV_{rms} or 57 MV peak. Specification requirement is for 2% resolution based on full scale output, which then using 5V would be 100 MV peak, which measurements show was met. In regime #2 and #3 the values were 0.42 and 0.14 MV peak respectively. These measurements were made with the input shorted and were taken with a true rms meter set with a 10 sec time constant.

8.2 Assembled Sensor

Performance testing was done with the two prototype deliverable sensors assembled, final wired but unpotted. As stated due to rate table limitations the sensors could not be tested over their full operating range. It was decided to determine the scale factors for the three regimes, response to step inputs, phase check, low frequency corner determination, axis alignment and maximum rate testing. Table 5 summarizes the results for the two units.

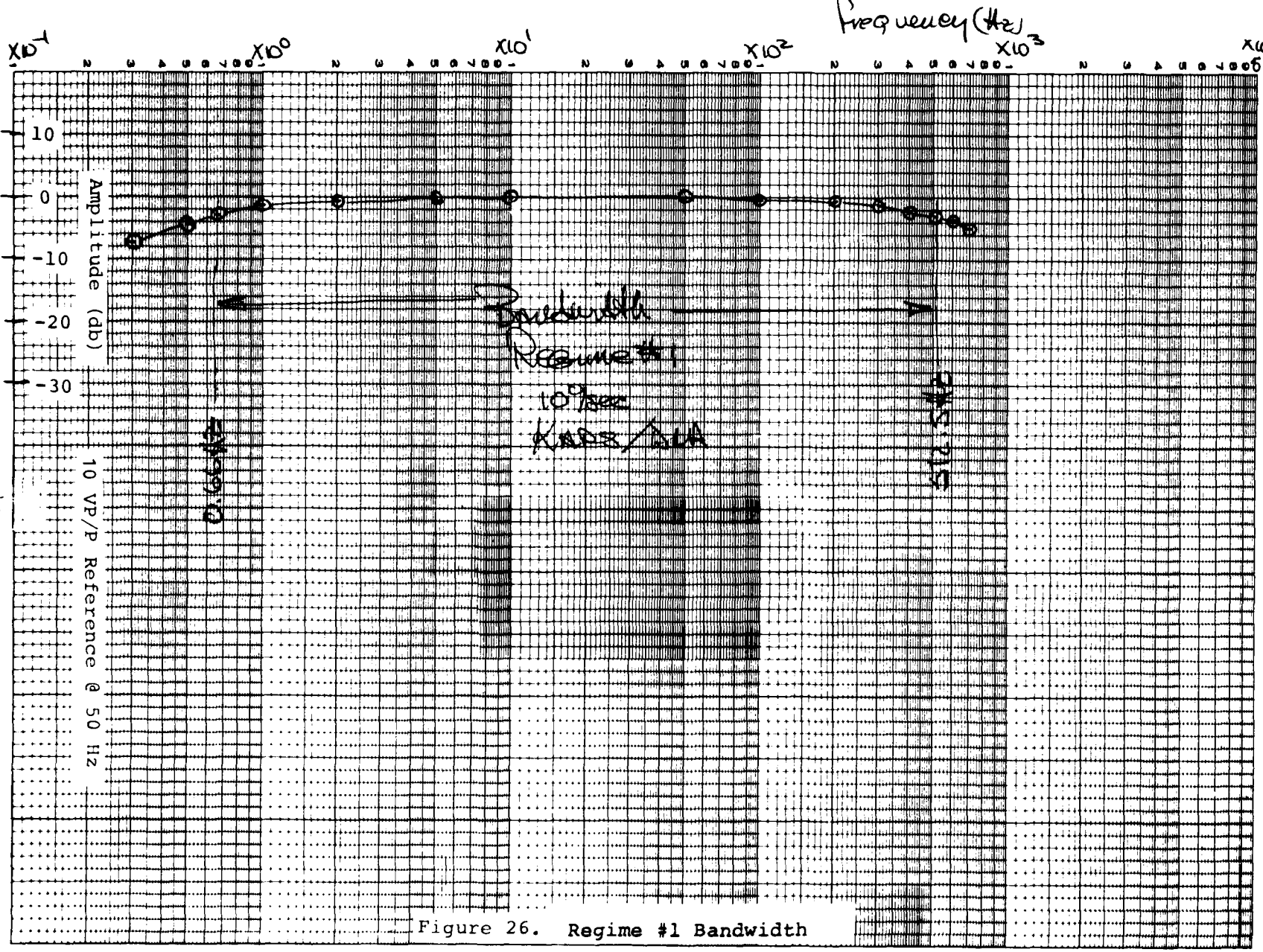

Figure 26. **Regime #1 Bandwidth**

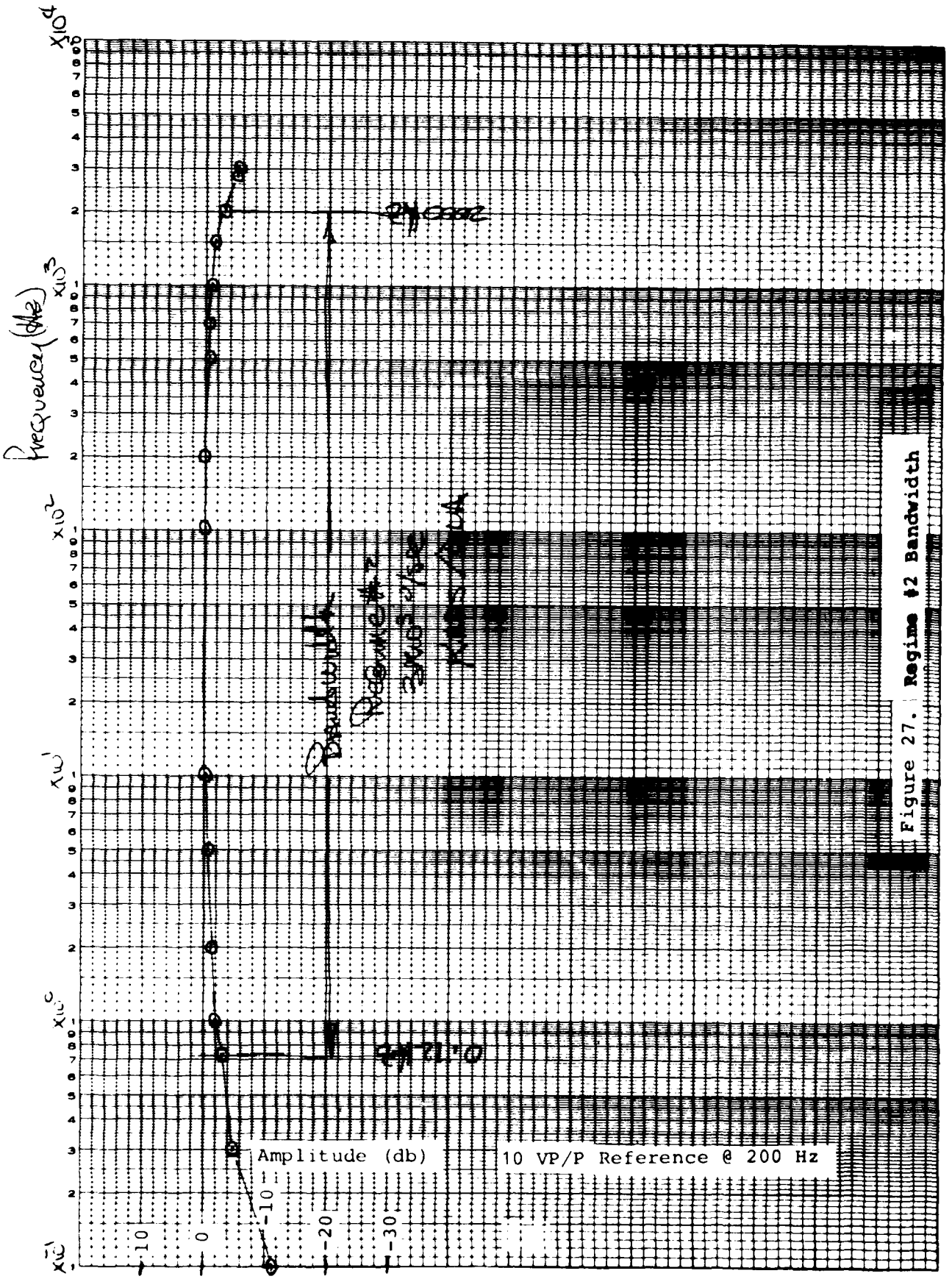

Figure 27. Regime #2 Bandwidth

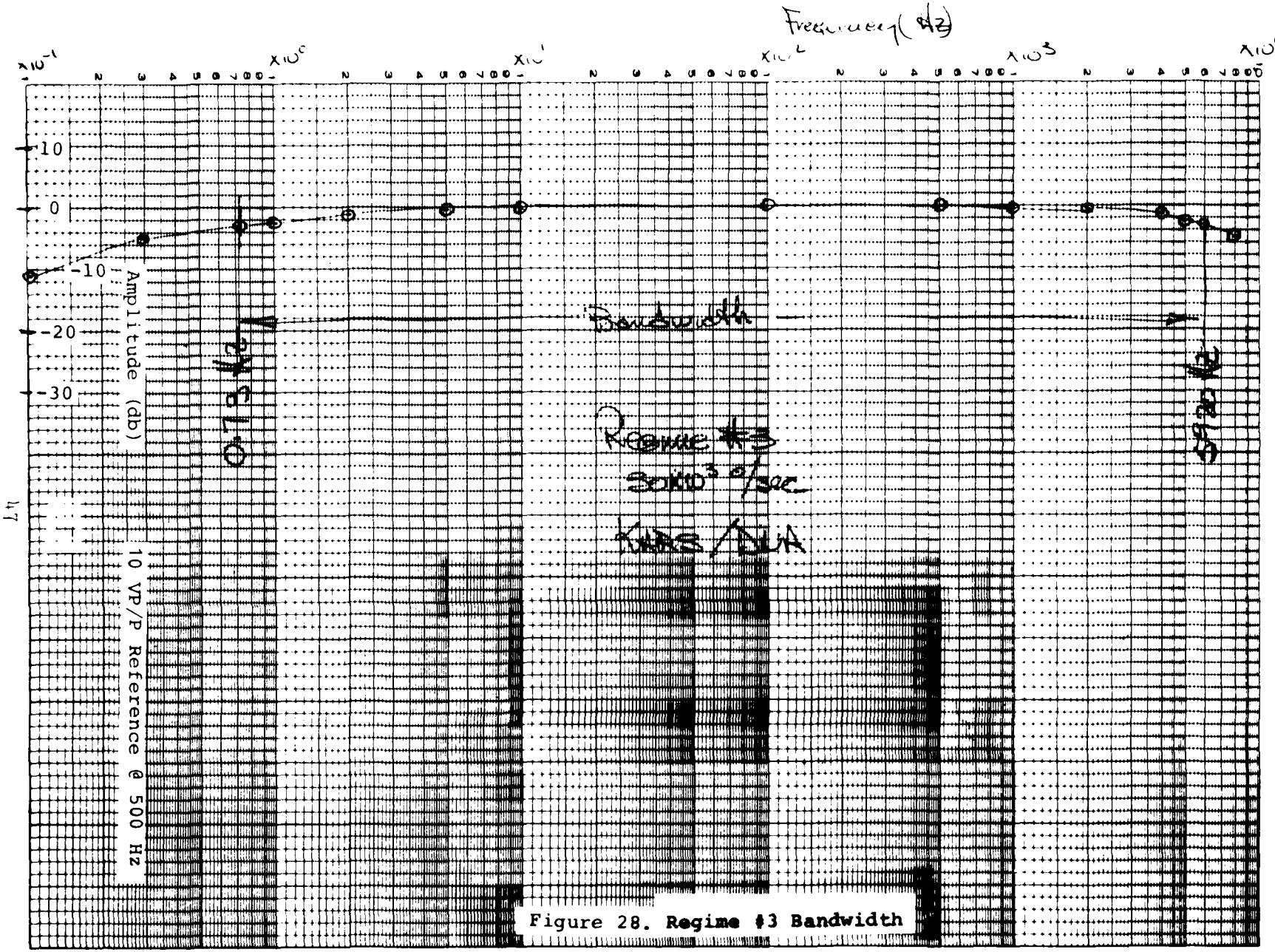

Figure 28. **Regime #3 Bandwidth**

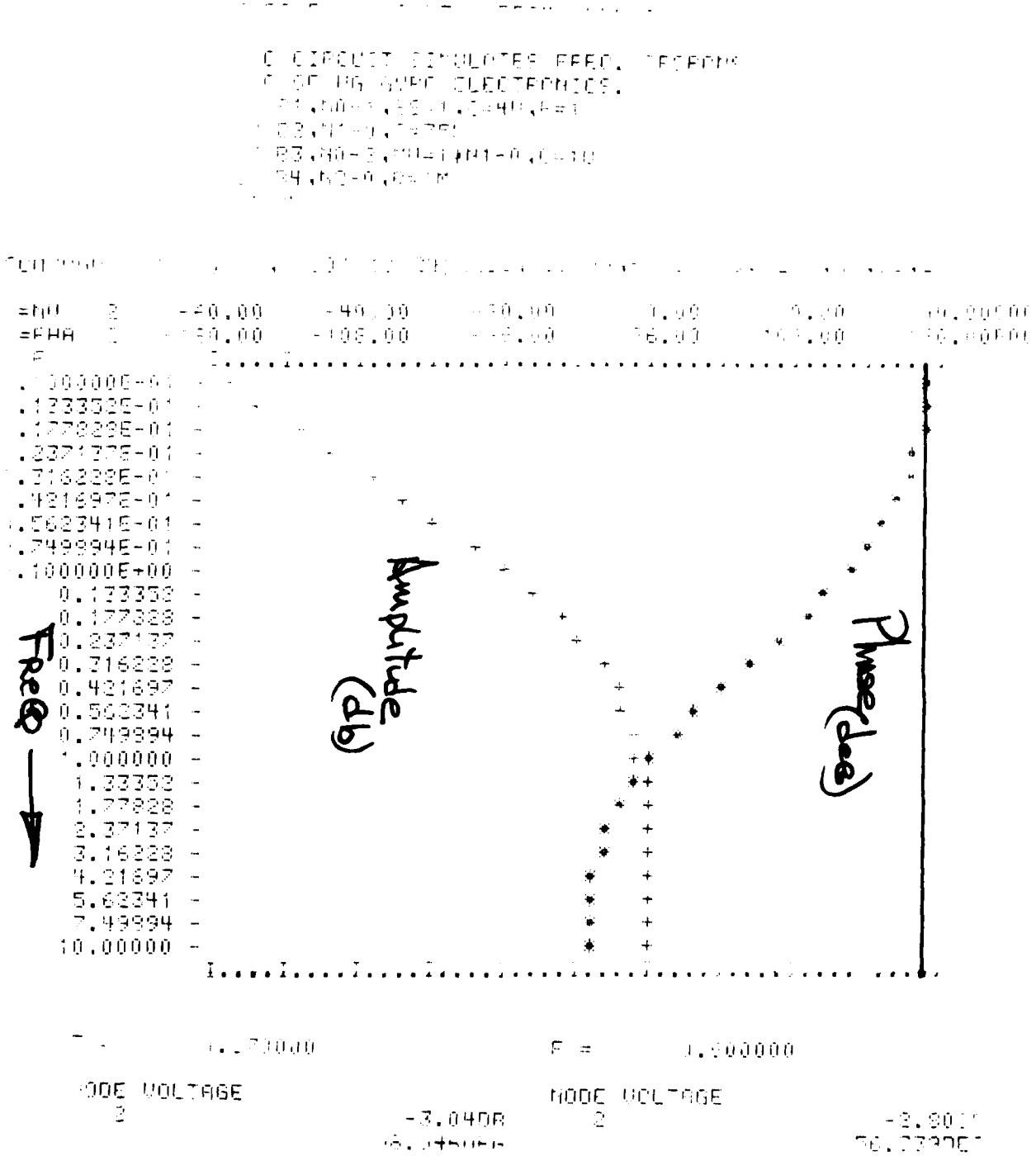

Figure 29. Regime #1 Low Frequency Corner Determination

Table 5

	S/N 1	S/N 2
Scale Factor V/°/sec		
Regime #1	0.48	0.53
Regime #2	0.00154	0.00173
Regime #3	0.000158	0.000168
Low Frequency Corner Hz		
Regime #1	0.7	---
Regime #2	0.65	---
Phase Check	✓	✓

Figures 30, 31 and 32 show a plot of the raw data used to determine the scale factors for S/N 1. Particular note should be taken on Figure 32 which shows the resolution of the 30 X 10^3 regime which shows a threshold at 20°/sec which would be 0.07% spec is 2% (600°/sec). Figure 33 shows the response of the sensor to positive and negative rate inputs and the corresponding signal outputs from the sensor. (Positive output/positive rate, right hand rule).

Figures 34 and 35 show the shape of the low frequency corner response for regimes #1 and #2 respectively. Regime #3 should have the same characteristics as #2 and is so noted on the plot. Figure 36 shows the response to a 3000°/sec step input. As can be seen from the data the step input is really not a step, but a sine ramp to 3000°/sec at approximately 1.4 Hz, based on this and the low frequency response of the system in regime #2 a value of 2400°/sec should be evident. Referring to the trace a value of 2272°/sec was determined which is within 5.3% of the actual value. Considering the method this is good agreement. Figure 37 is a similar response, but with a more compressed time scale showing the complete response of the instrument to a step input of rate.

Figures 38 thru 42 show similar data for S/N 2.

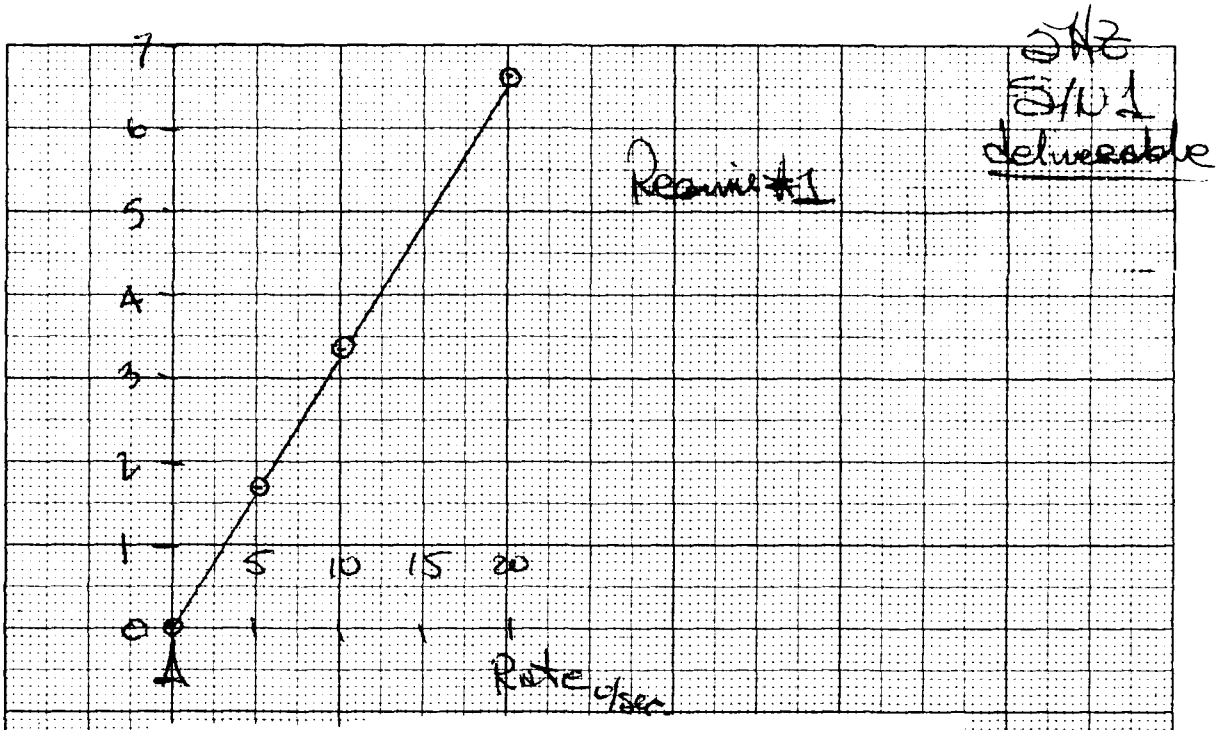

Figure 30. S/N 1 Regime #1 Scale Factor Plot

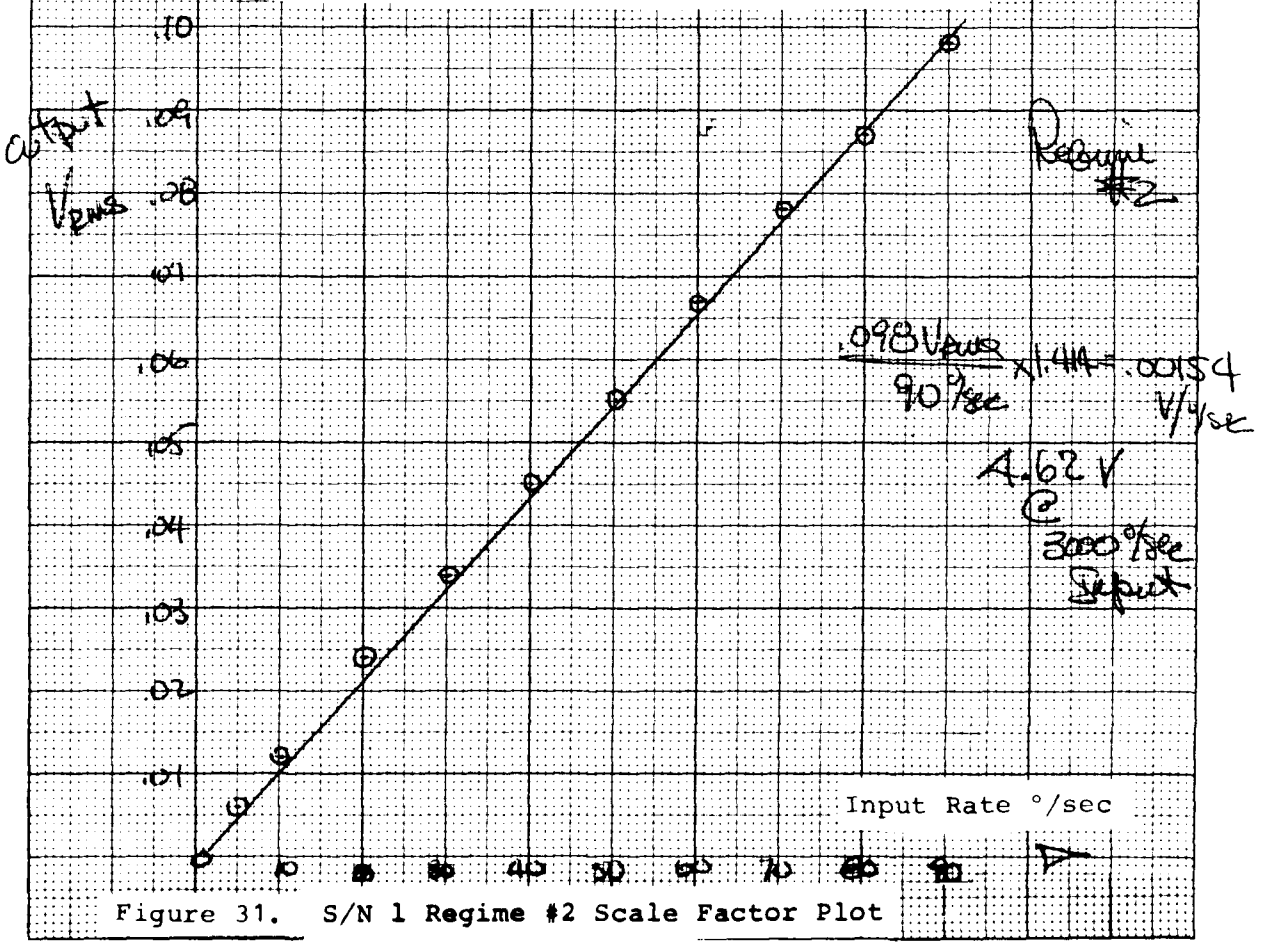

Figure 31. S/N 1 Regime #2 Scale Factor Plot

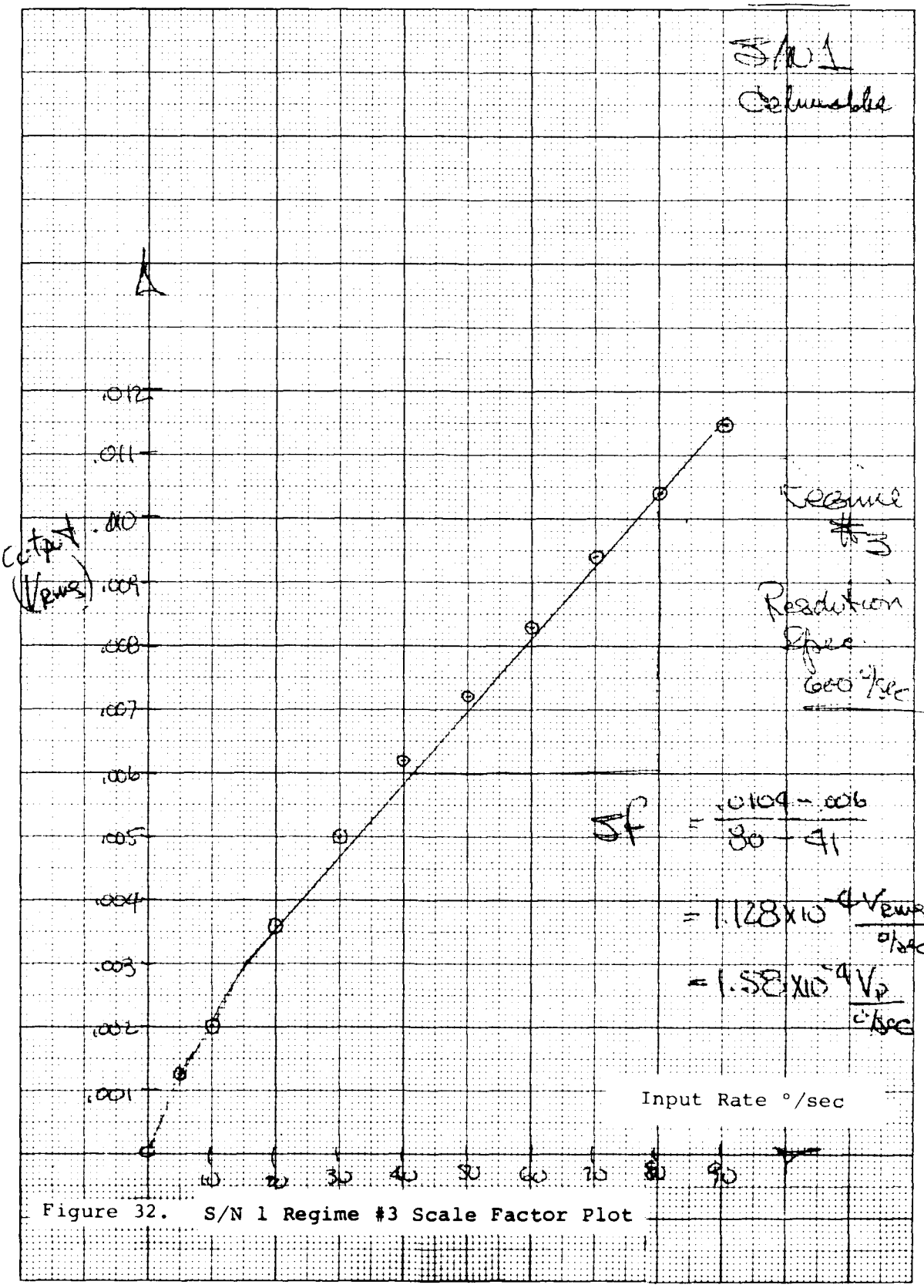

Figure 32. S/N 1 Regime #3 Scale Factor Plot

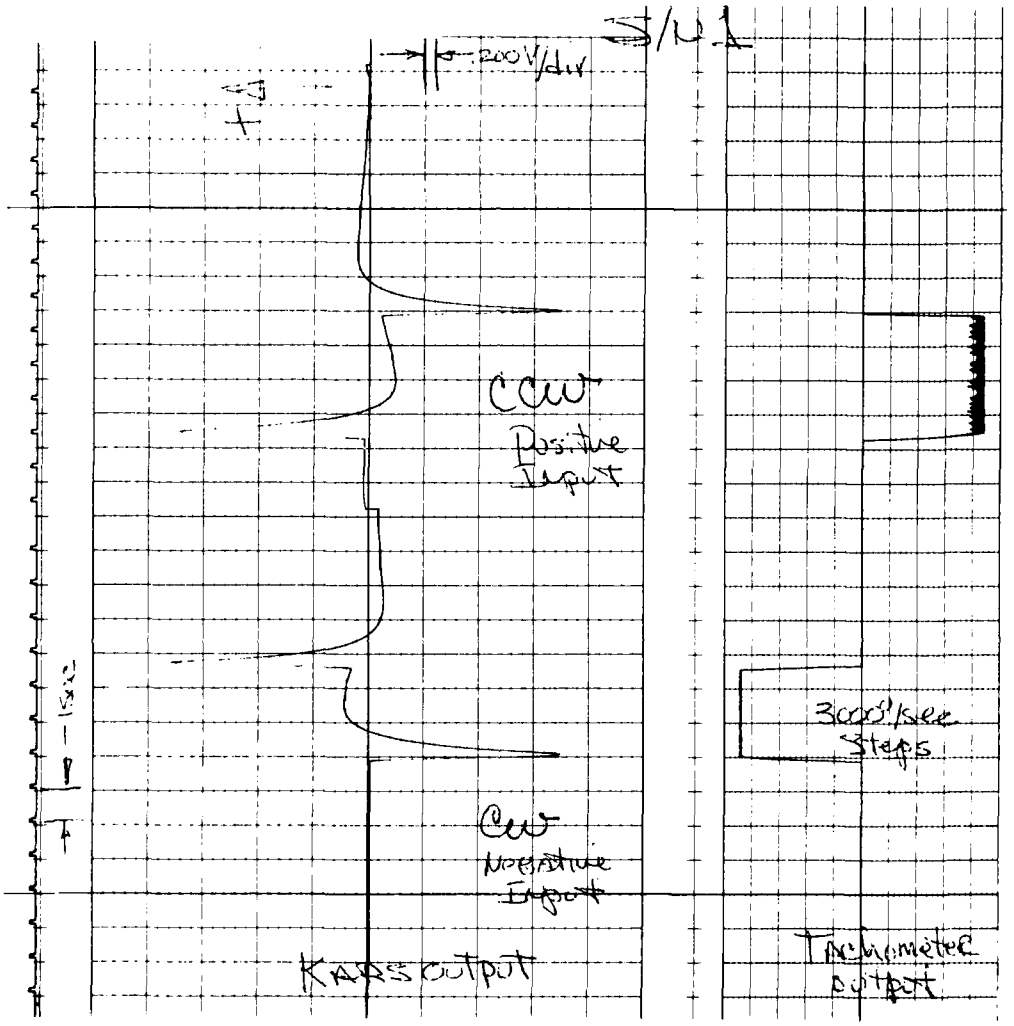

Figure 33. S/N 1 Phase Check Step Input Response

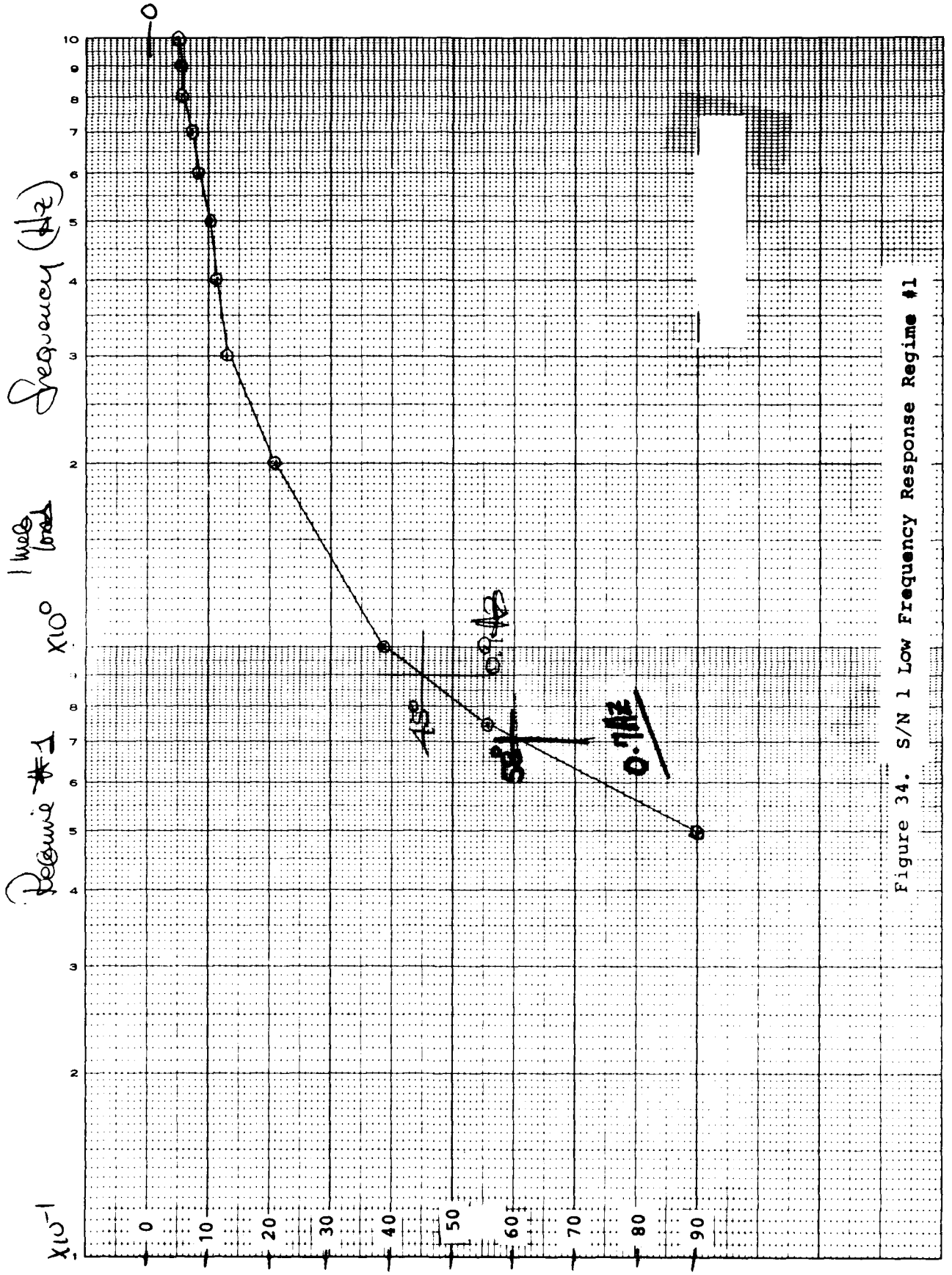

Figure 34. S/N 1 Low Frequency Response Regime #1

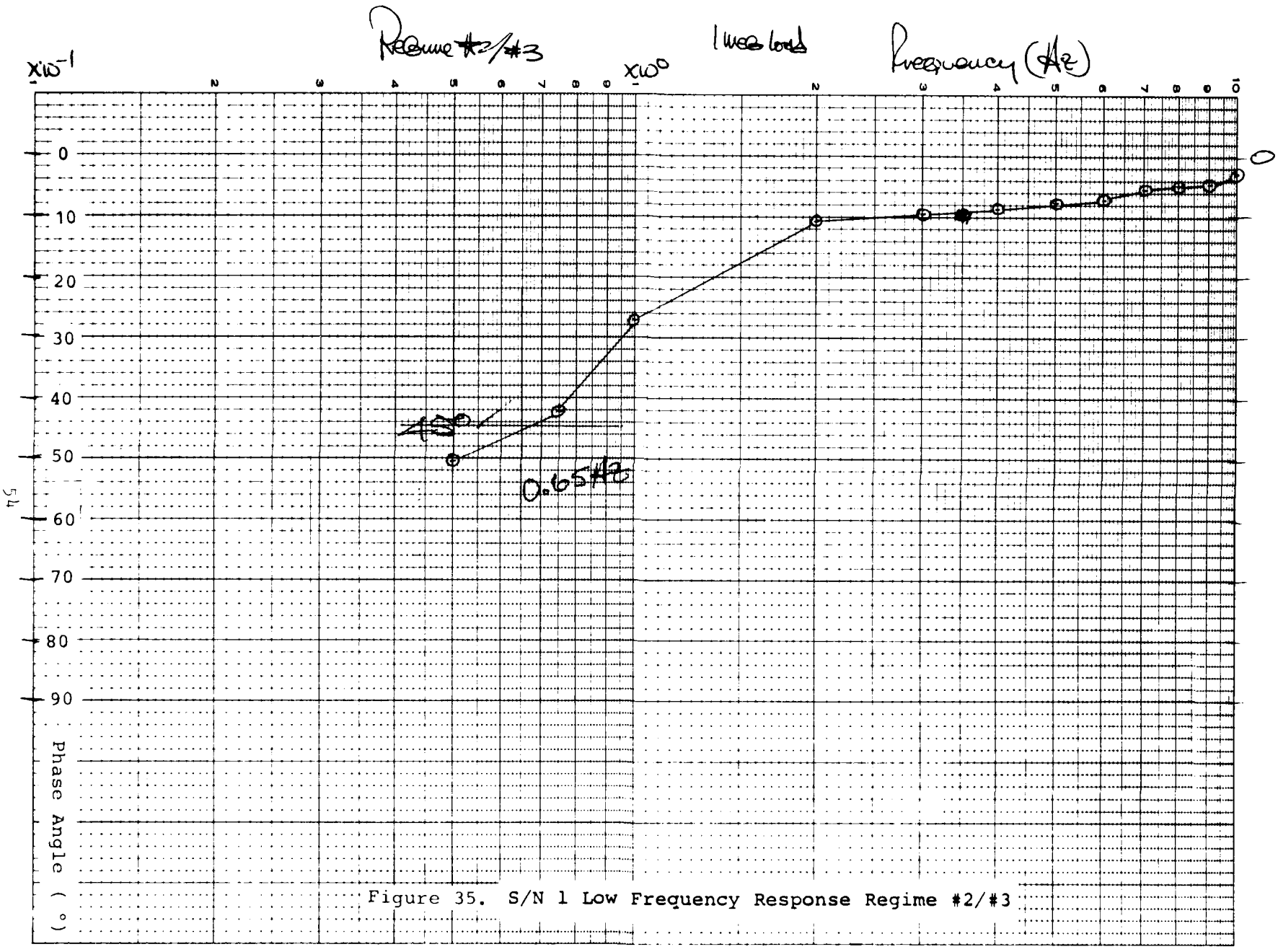

Figure 35. S/N 1 Low Frequency Response Regime #2/#3

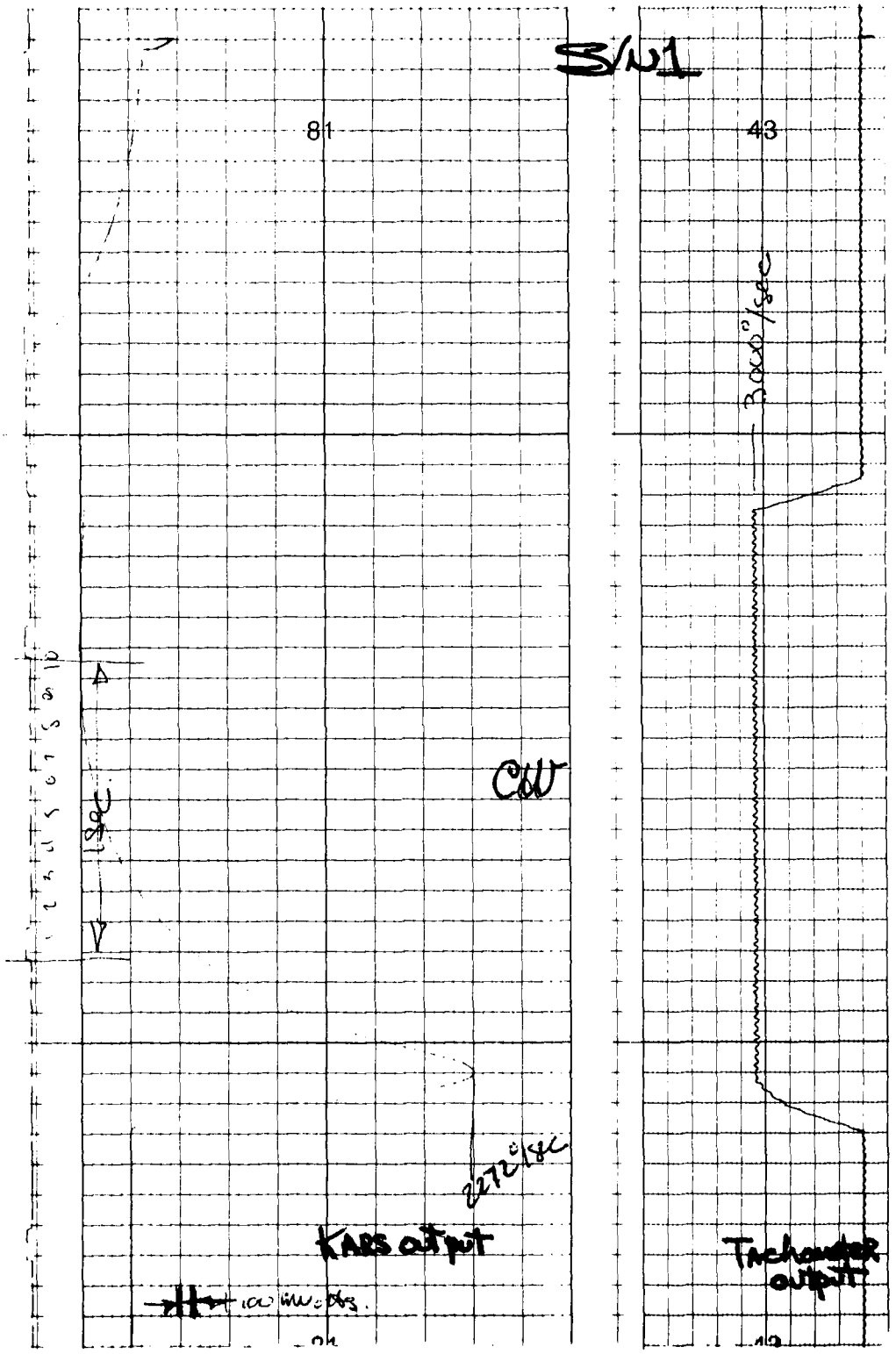

Figure 36. S/N 1 3000°/sec Step Input Response

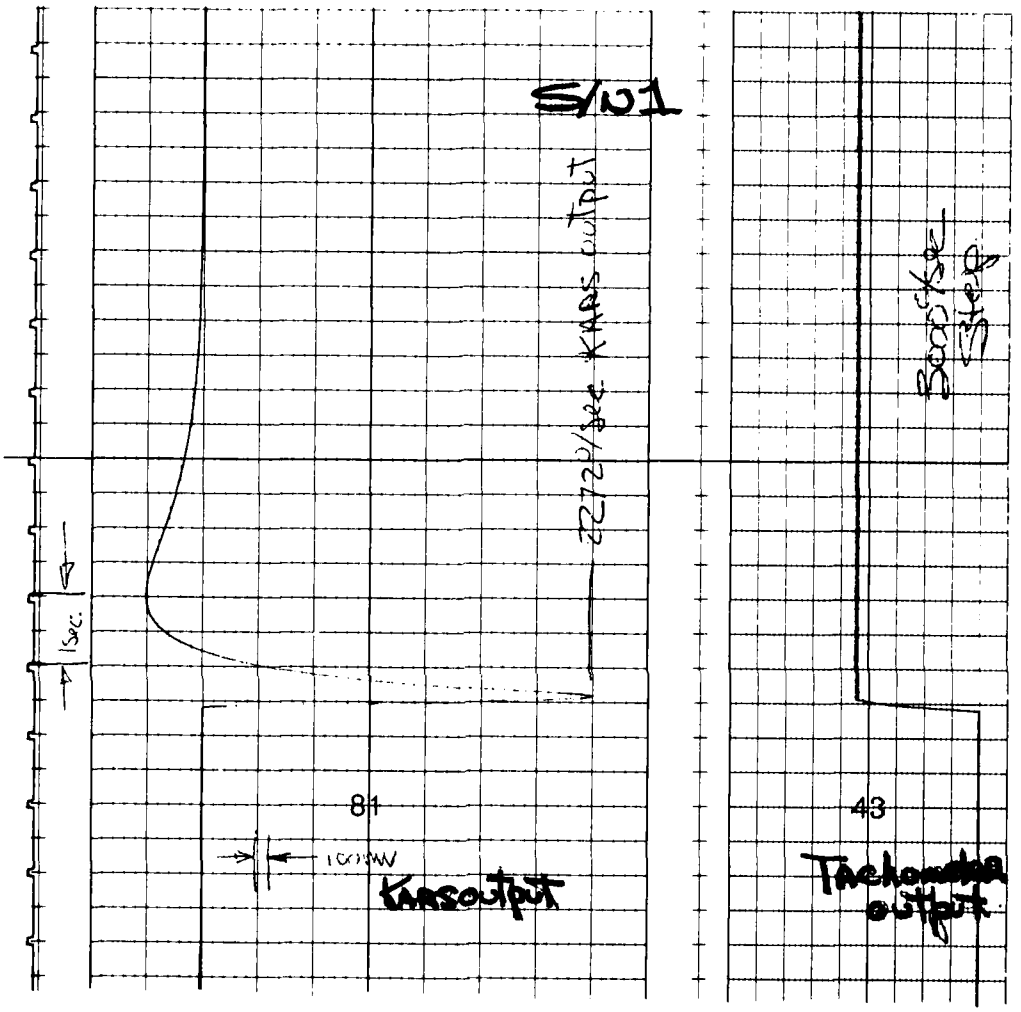

Figure 37. S/N 1 3000°/Sec Step Input
Compressed Time Scale

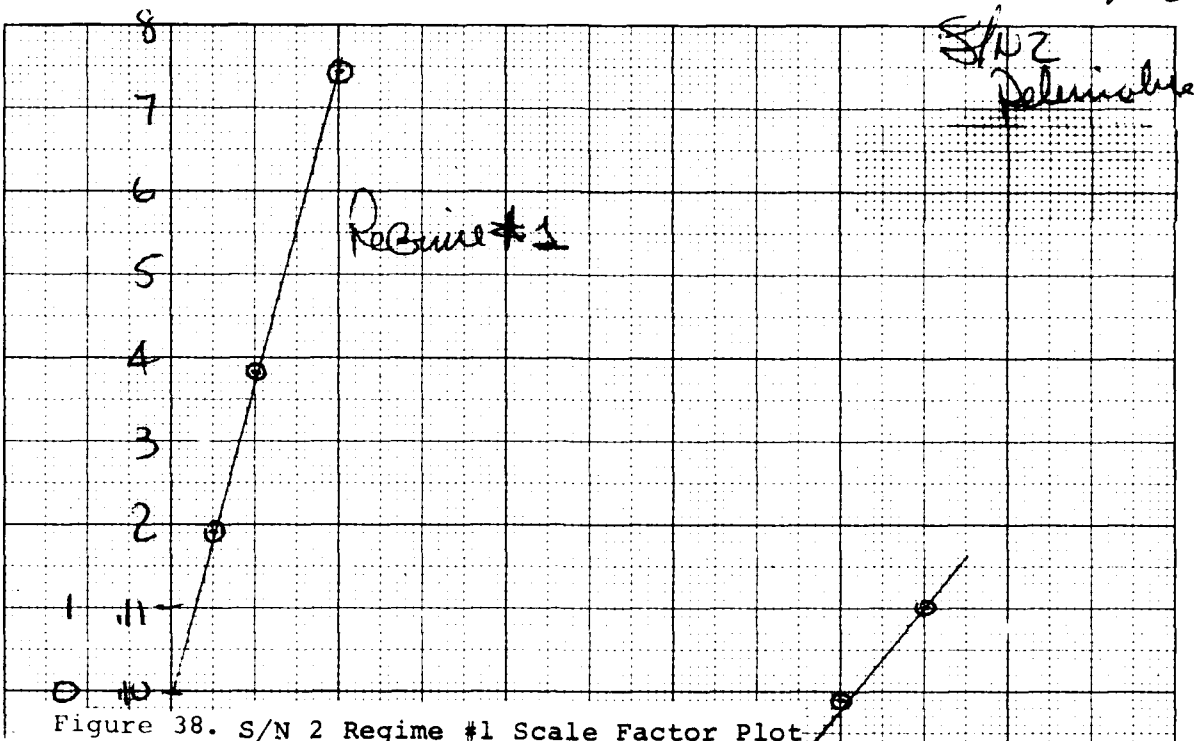

Figure 38. S/N 2 Regime #1 Scale Factor Plot

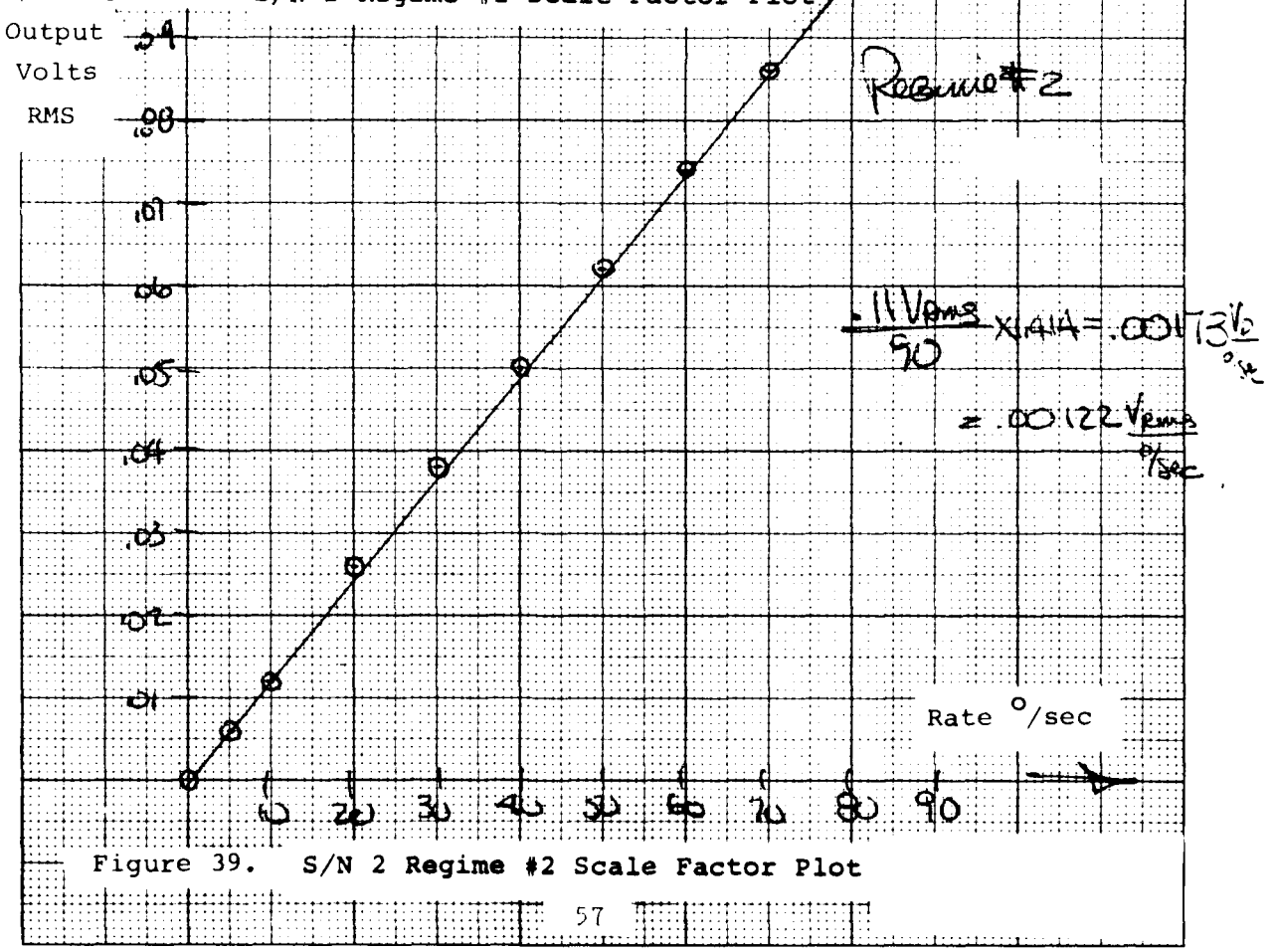

Figure 39. S/N 2 Regime #2 Scale Factor Plot

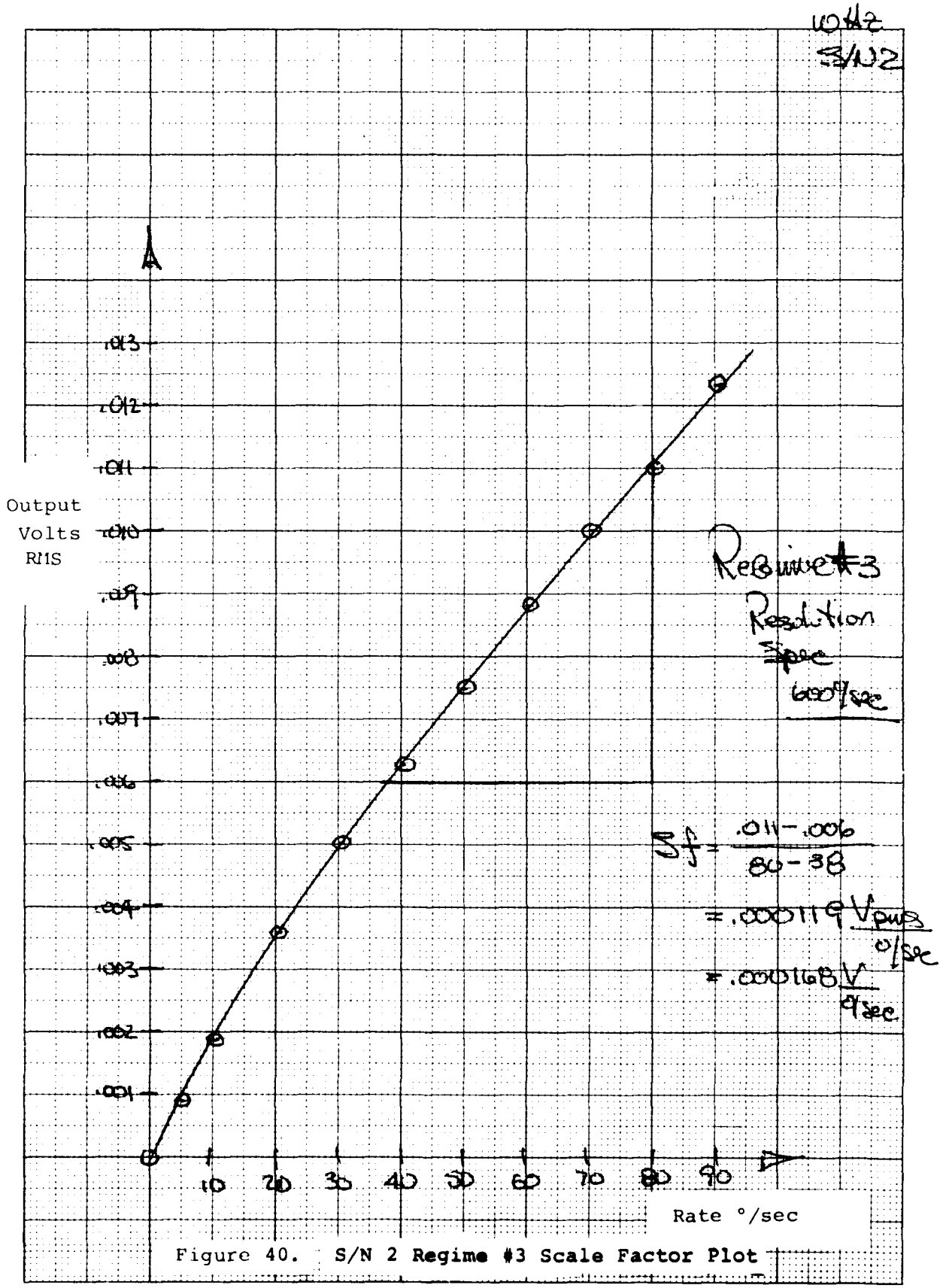

Figure 40. S/N 2 Regime #3 Scale Factor Plot

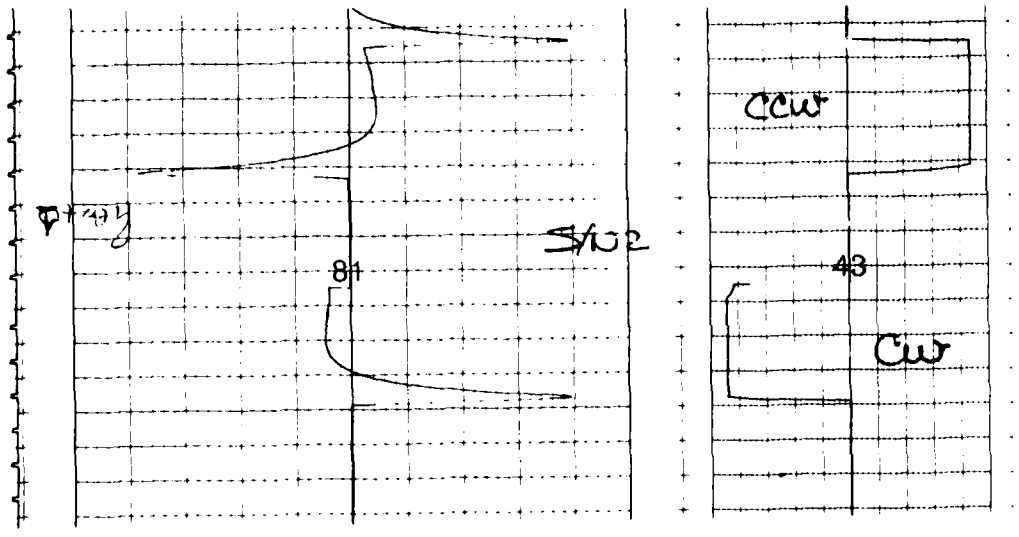

Figure 41. S/N 2 Phase Check Step Input

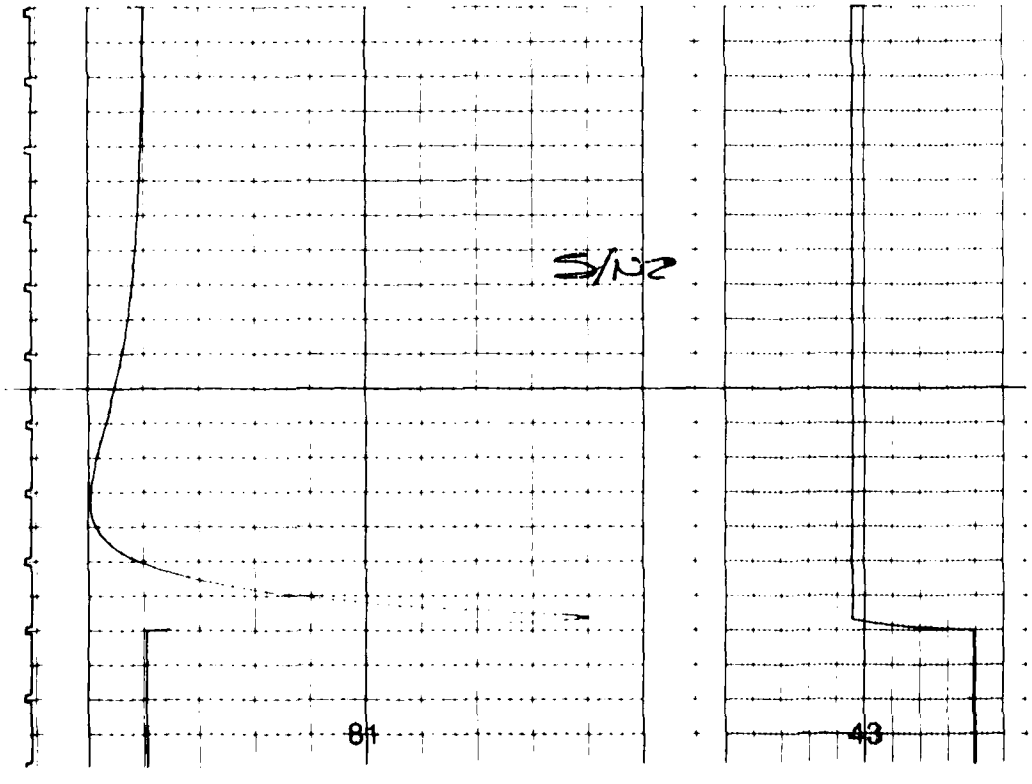

Figure 42. S/N 2 Step Response 3000°/sec

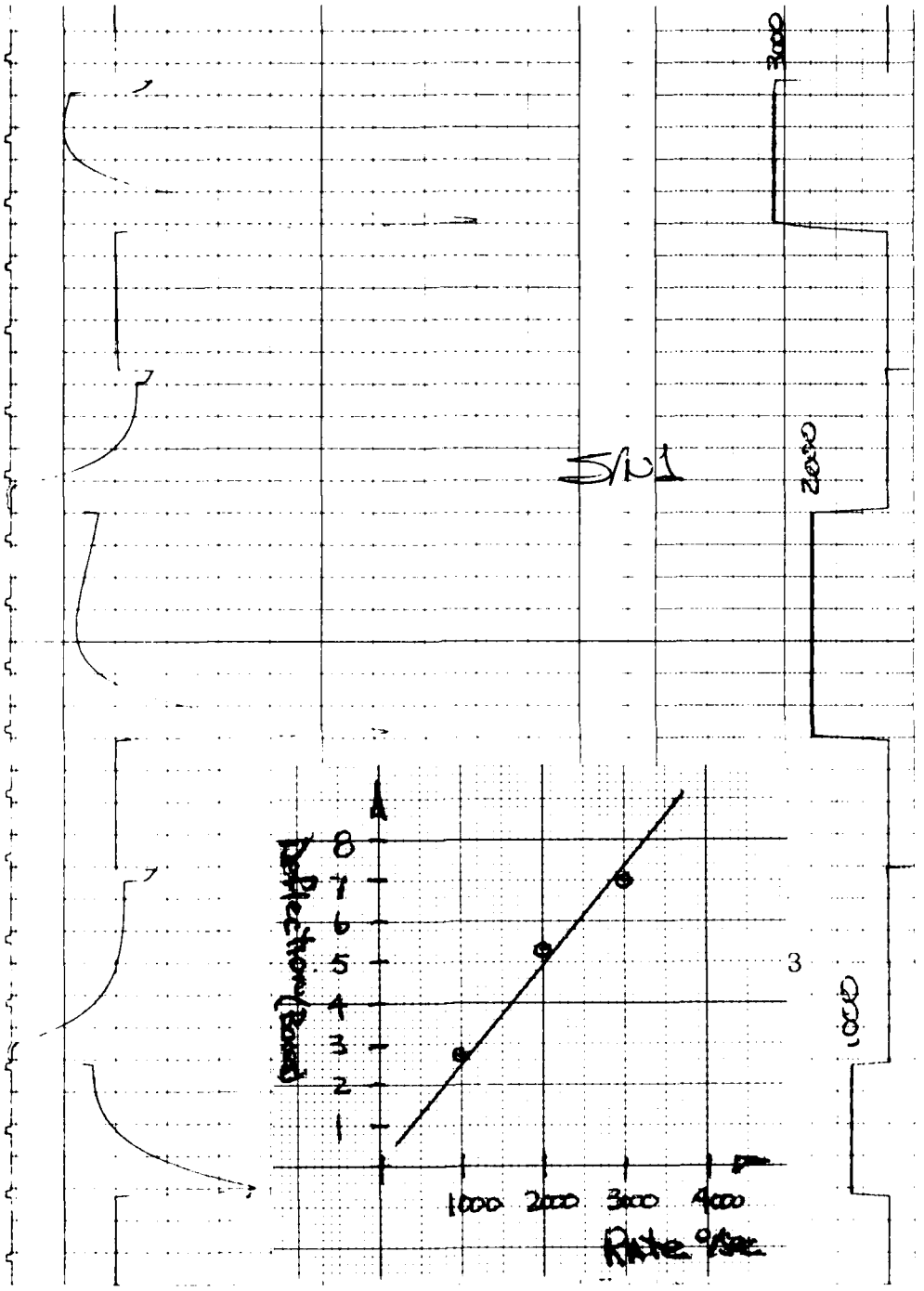

Figure 43. S/N 1 Response to Various Step Inputs

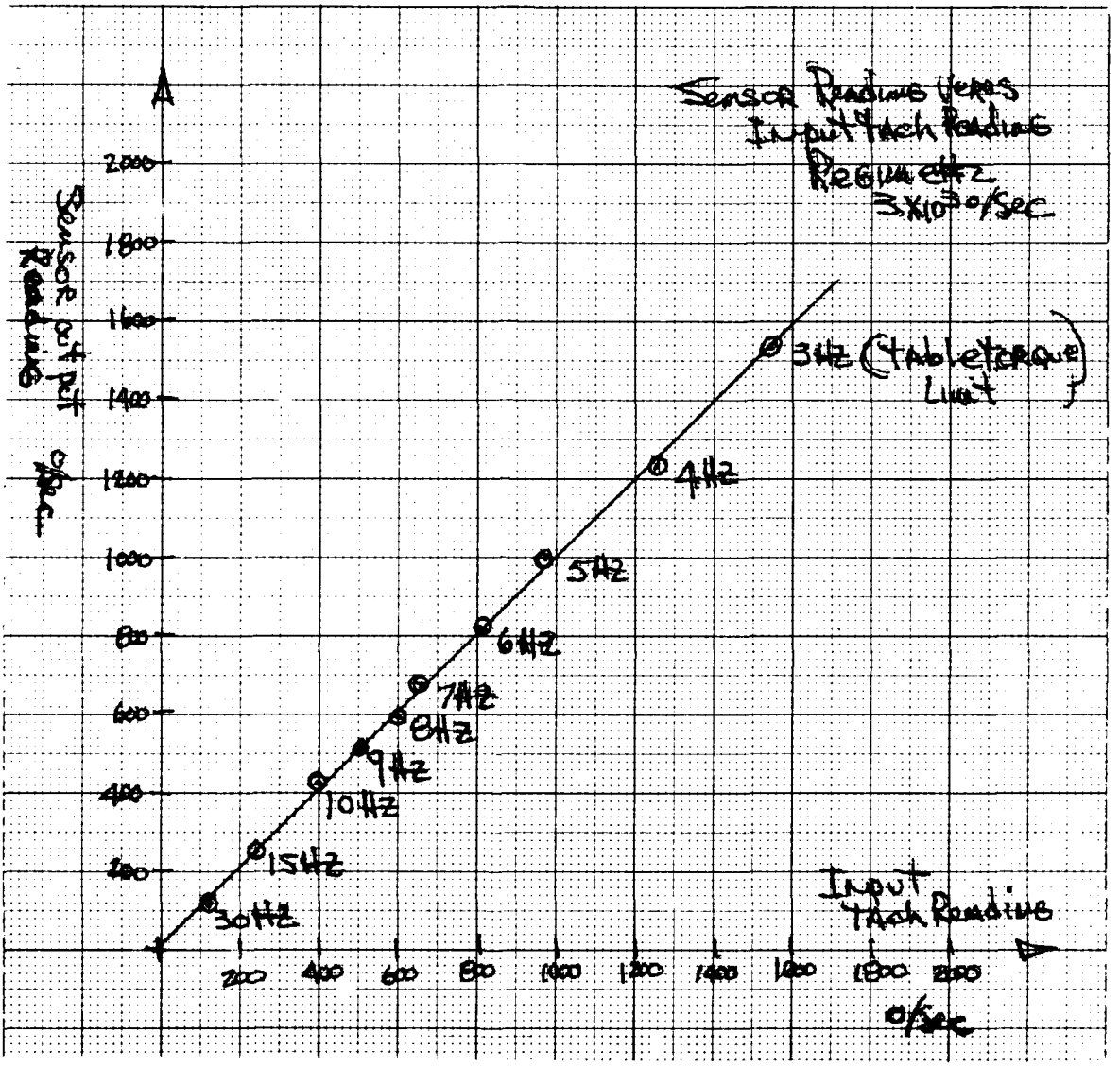

Figure 44. S/N 1 Plot Max Rate Data Regime #2

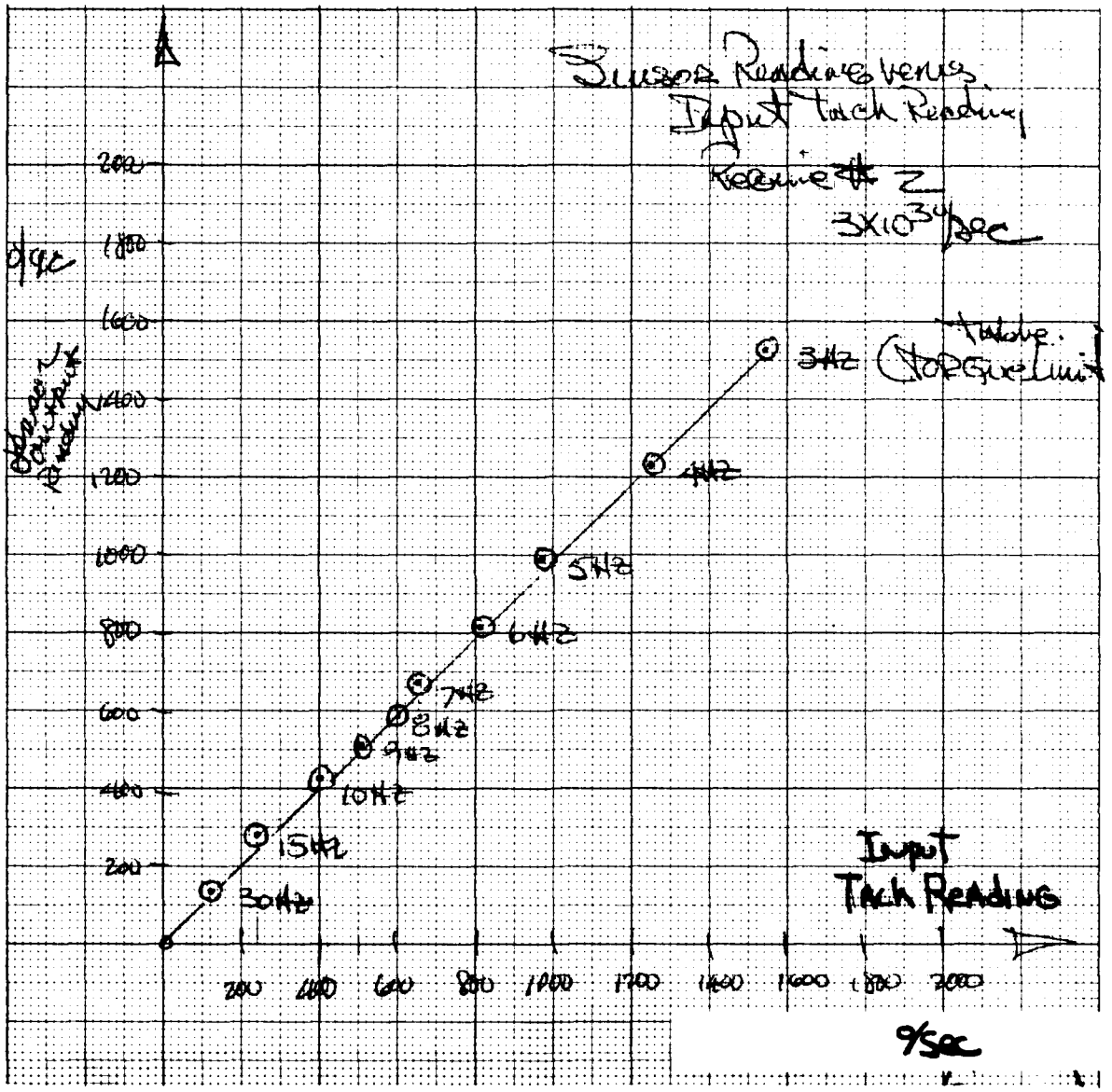

Figure 45. S/N 2 Plot Max Rate Data Regime #2

In addition, for S/N 1 the response to various step inputs were recorded and appears as Figure 43. In general a linear relationship as expected is shown in the insert.

High rate testing of the sensors was done at various frequencies at maximum table input rates. Figures 44 and 45 show a plot of input, measured by the rate table tachometer generator, and measured value by the KARS sensor S/N 1 and S/N 2 respectively. As can be seen rates on the order of 1500°/sec could be generated and KARS was capable of sensing this rate accurately.

Input axis misalignment was measured by mounting the sensor input axis at a right angle to the rate table spin axis. In this orientation the rate table input was applied to the cross axis of the sensor. Under these conditions the output from regime #1 (10°/sec) was monitored with a 10°/sec input. The results are that misalignments are 19.1 and 14.1 arc minutes for S/N 1 and S/N 2 respectively.

8.3 Environmental

The KARS deliverable production prototypes were evaluated in three principle areas as listed in Table 6.

Table 6

Environmental Test Areas

Number	Description
1	Temperature
2	Vibration
3	Shock

The results are covered in this section. To establish environmental effects, scale factor tests in the 10°/sec regime #1 output were taken before and after exposure.

No testing was done in the magnetic interference area since the flux density in the pickoff is at least 3000 gauss. The presence or absence of the earths magnetic field of 1/2 gauss will have a trival effect on the sensor. The KARS will meet any realistic magnetic requirements.

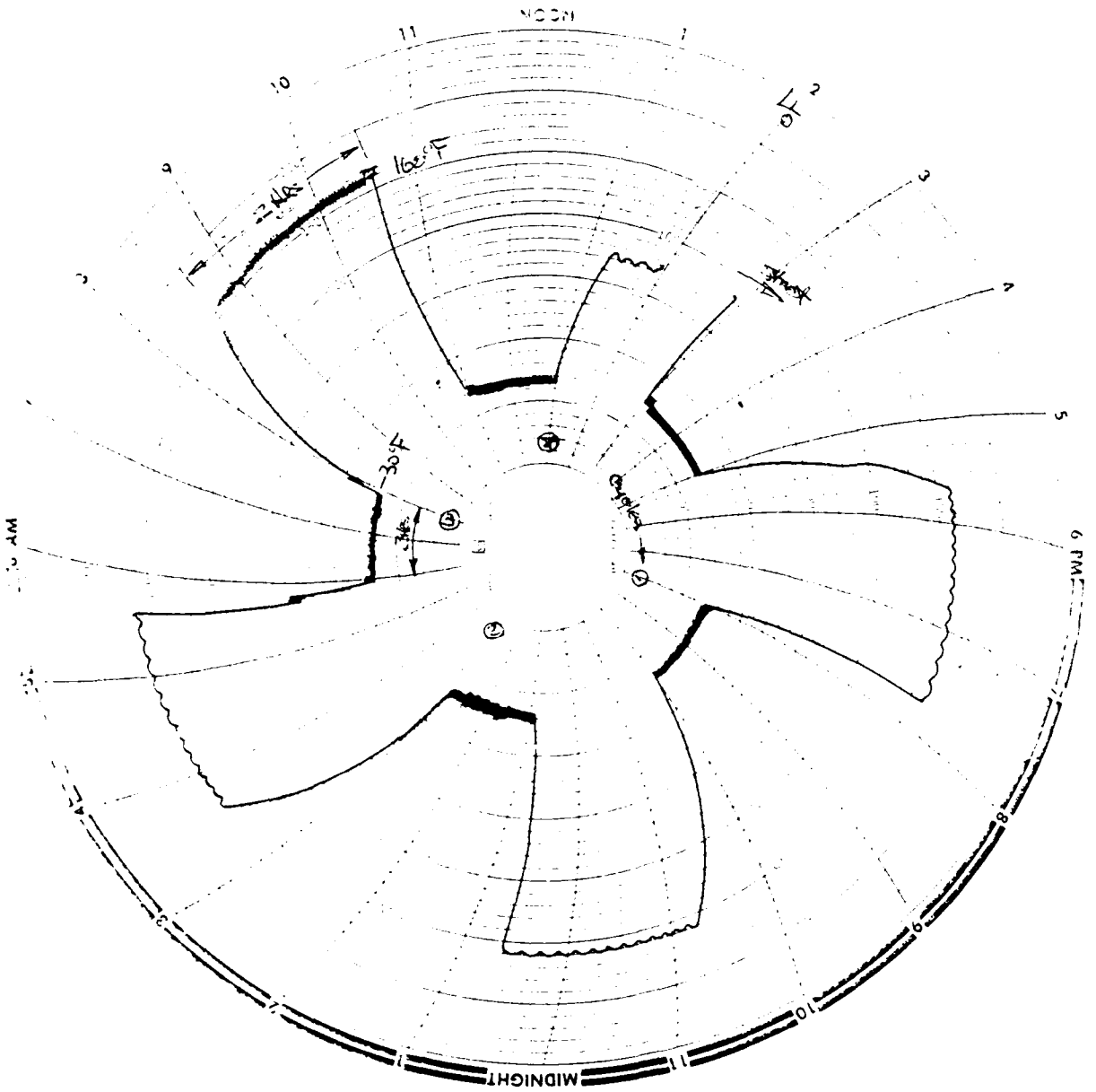

Figure 46. Environmental Temperature Cycle KARS

Temperature

Temperature testing was performed by placing the KARS in a standard environmental test oven and subjecting them to temperature extremes of -35°C to 71°C. A typical temperature time plot is shown as Figure 46. It can be seen that the soak time at the two extremes was 2 hrs., oven rate was used as the thermal shock between extremes and the cycle repeated four times. The temperature represented on this chart are the ambient conditions, a temperature probe on the KARS surface showed good agreement with a slight lag to these readings Scale factor check shows a 0.6% change after temperature exposure.

Vibration

The units were subjected to MIL Standard 810C Method 514 (Figure 514.2-6 curve AB) for a 9 minute logarithmic cycle. Figure 47 is a copy of the specified curve and this input was applied to both the input and cross axis of the units. Figure 48A is the input axis direction and Figure 48B shows the units mounted on a standard fixture cube for cross axis inputs.

Figure 49 shows a typical response curve in g's of the control accelerometer used in the servo loop of the vibration table. The unit can be clearly identified in Figure 48A as the center object on vibration head with an electrical lead connected to it. Scale factor check after vibration exposure showed no change.

Mechanical Shock

A method of evaluating the sensor during the required 10,000 g peak shock in the form of 3.2 millisec half sine could not be located in The Singer Organization. There is an Avco Shock Test Machine Model SM-005 with a Shock Amplifier Kit suitable for high accelerations (10,000 g) but only short (0.12 millisec) duration pulses. The shock amplifier kit was assembled and tested and 10,000 g's at 0.12 millisec was obtainable. The units were subjected to this input in both input and across axis directions as go-no go tests.

Figure 50 shows the pulse shape where the vertical scale is 20 volts/cm and horizontal scale is 0.1 millisec/cm. The monitoring accelerometer scale factor (83.3 V/g) curve is shown as Figure 51. Scale factor testing shows a 1% change. Figure 52 shows the units mounted on the shock machine in the cross axis and input axis direction.

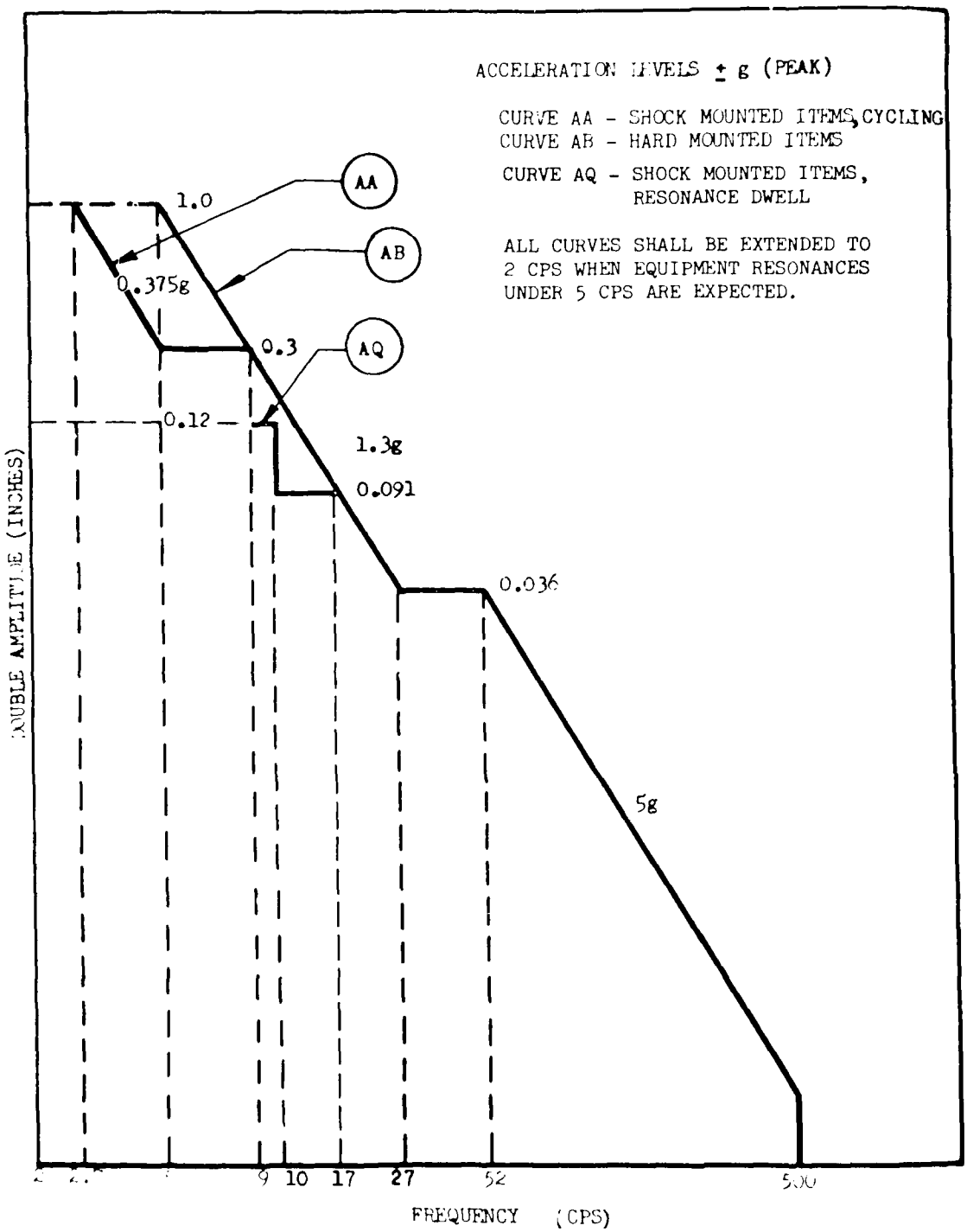

Figure 47. Mil Standard 810C Figure 514.2-6

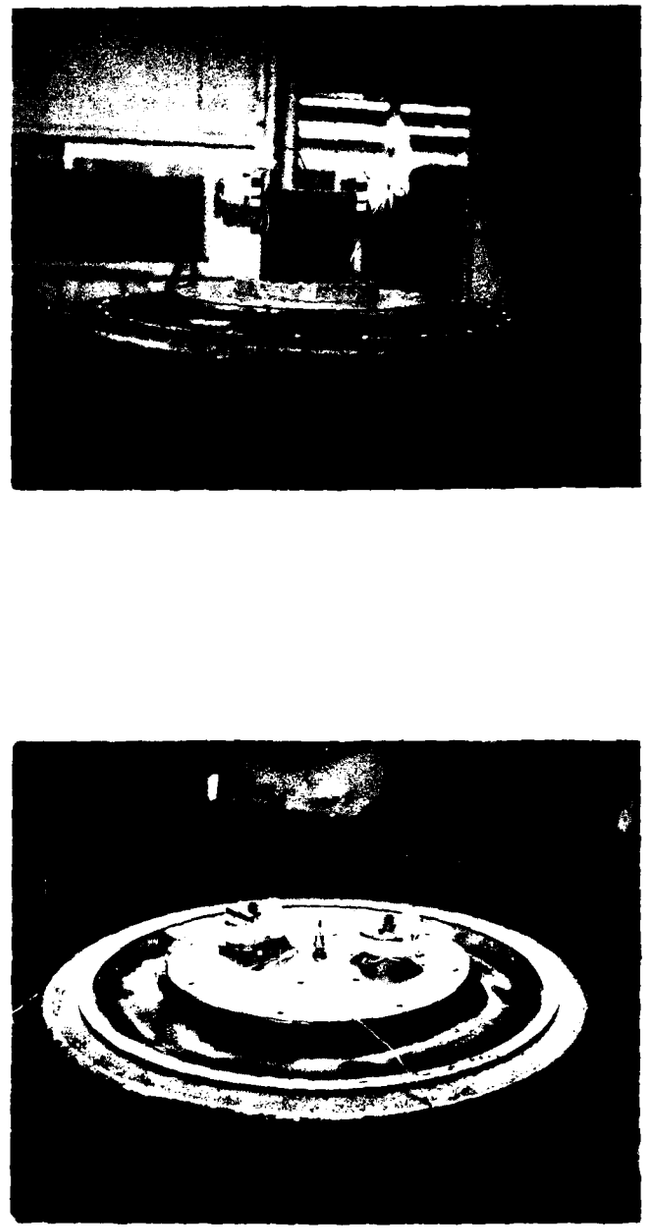

Figure 48. Vibration Test Fixtures KARS

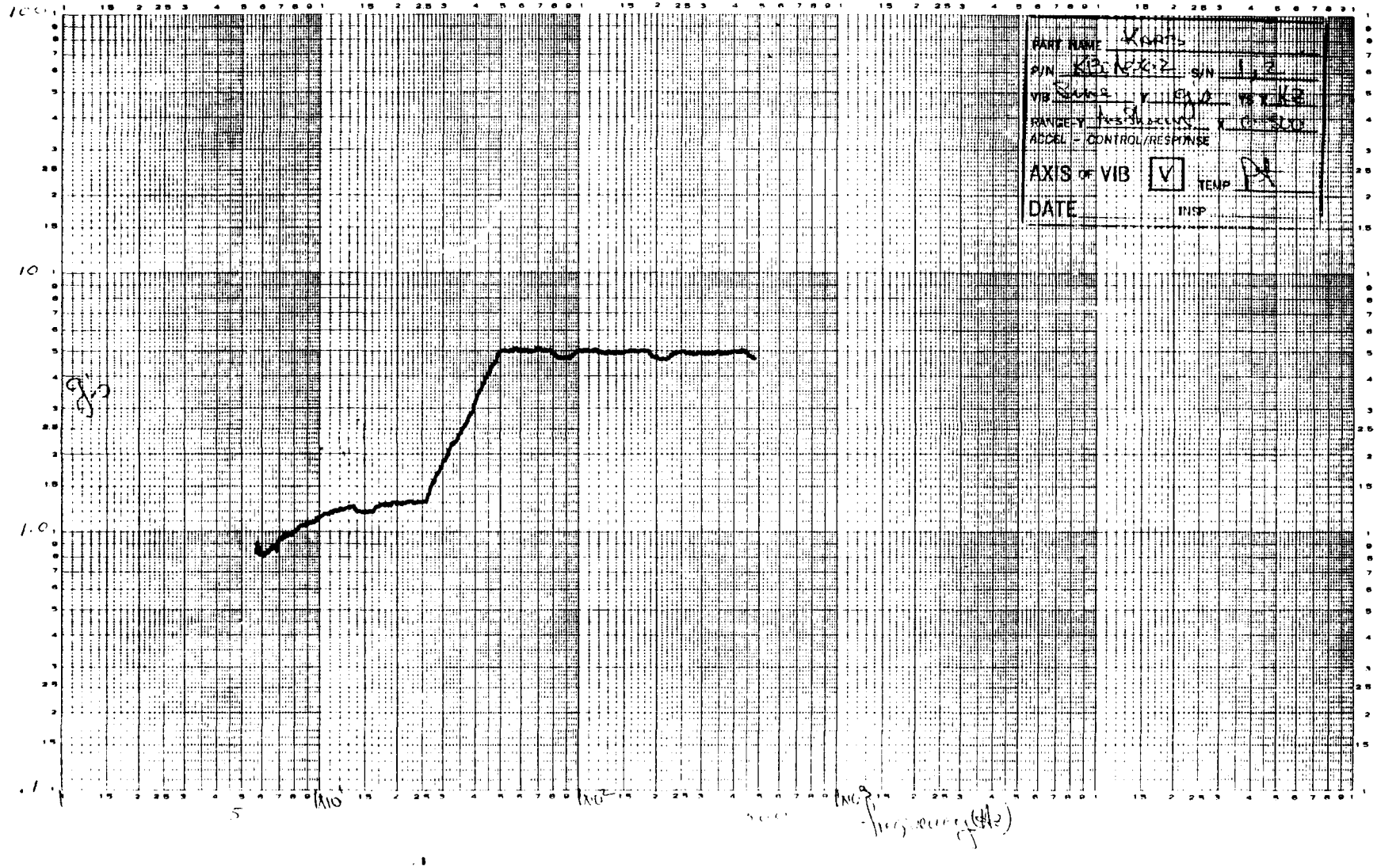

Figure 49. Vibration Test Acceleration Input

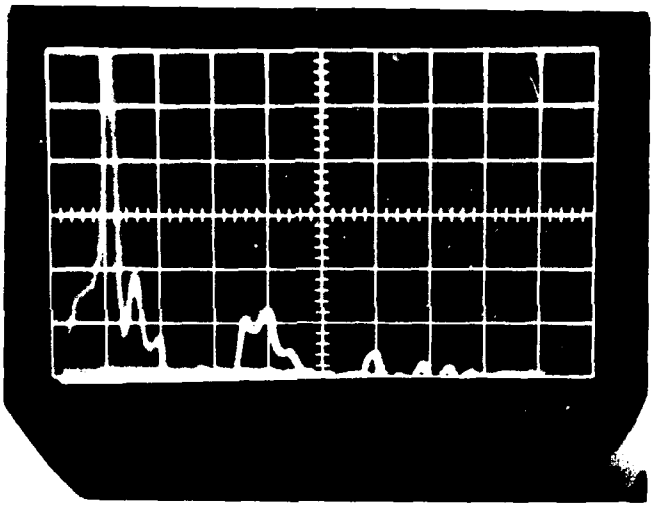

Figure 50. Shock Pulse Input KARS

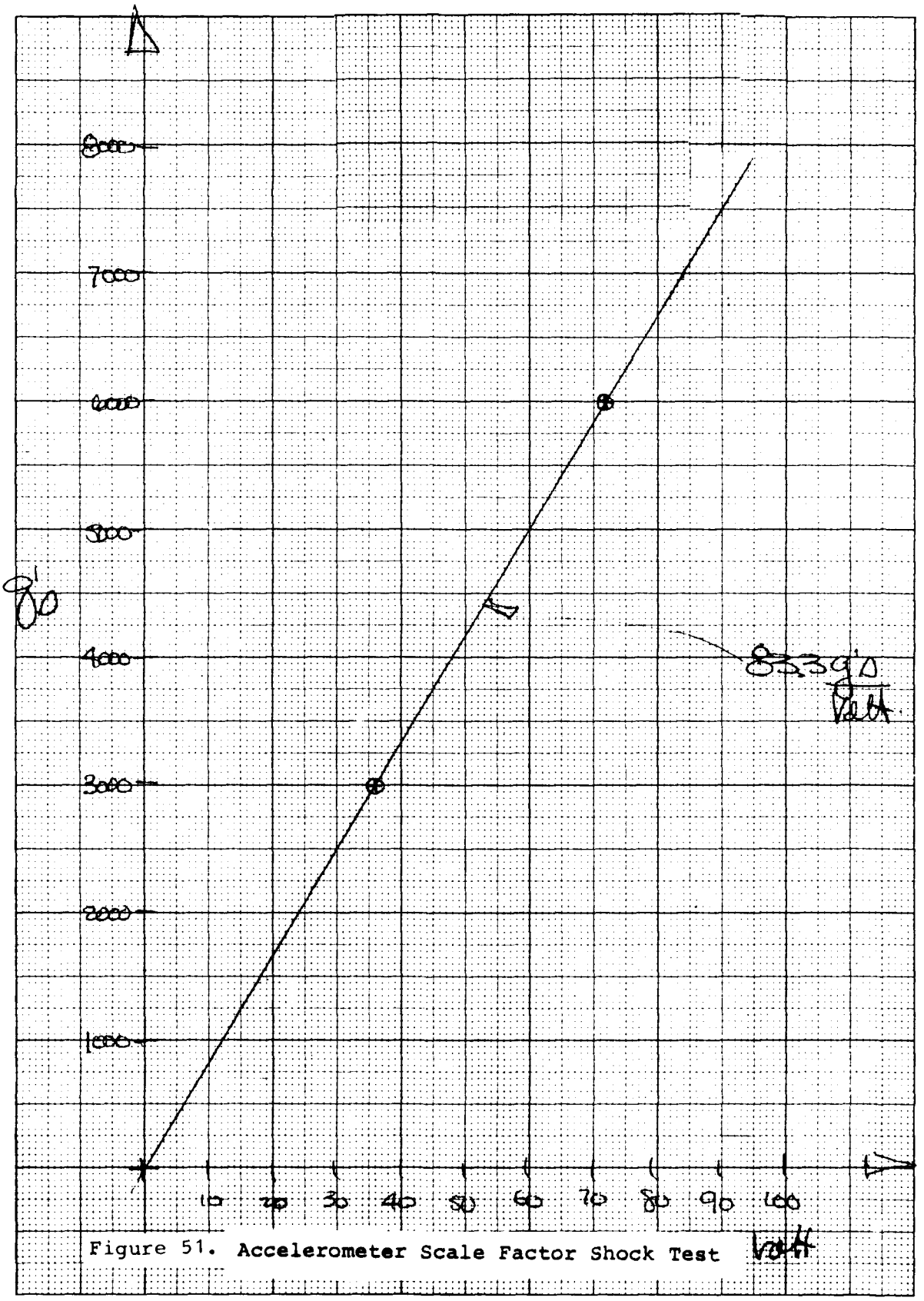

Figure 51. Accelerometer Scale Factor Shock Test

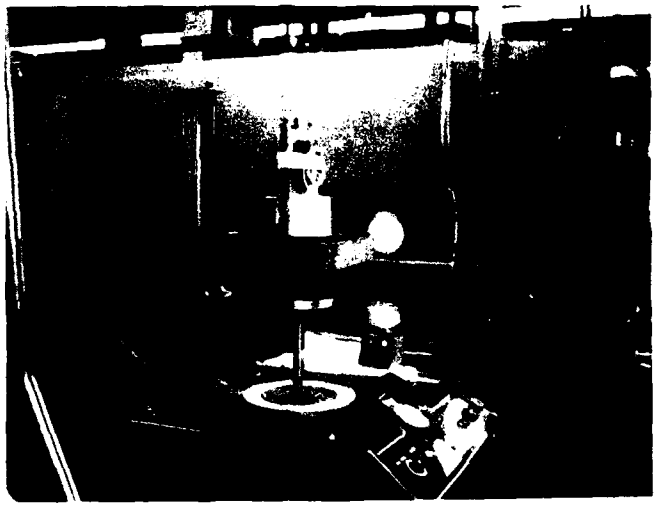

CROSS-AXIS INPUT

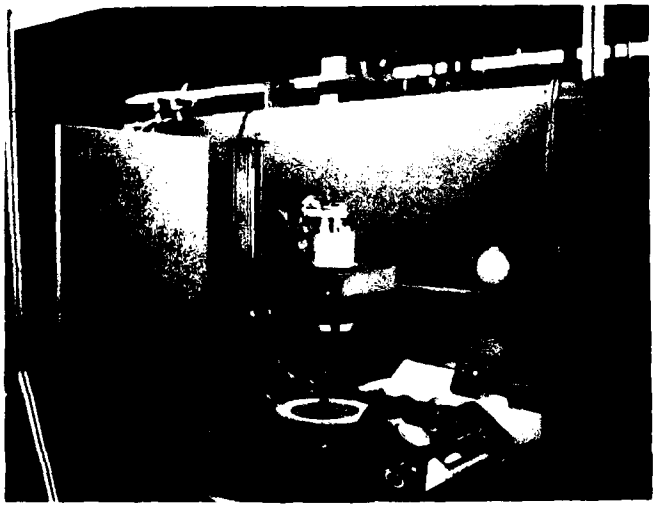

INPUT AXIS INPUT

Figure 52. Shock Machine Testing

SECTION IV

CONCLUSIONS

Two prototype production KARS were designed and built for the Defense Nuclear Agency. These units were tested and met the design goals specified by DNA. An interesting result was that the 30,000°/sec regime had a threshold of 20°/sec which is well below the 600°/sec required. In the 3000°/sec regime the threshold was 5°/sec where the requirement was 60°/sec. Even though there was no linearity requirement, a rough look at the numbers show a 2% linearity number. In conclusion, the KARS is a rugged design capable of measuring accurately high rates. The key test will be field test where the 10,000 g's at 3.2 millisec half sine wave is experienced.

Appendix A

Development Spec
For
Angular Rate Sensor

1. SCOPE

1.1 General. This specification establishes the performance, design, development and test requirements of the Angular Rate Sensor, herein referred to as the End Item.

2. APPLICABLE DOCUMENTS

2.1 The following documents, of the exact issue specified, form a part of this specification to the extend specified herein.

STANDARDS

Military

MIL-STD-810C 10 March 1975	Environmental Test Methods

OTHER PUBLICATIONS

AIA

AIA EETC Report 30 June 1965	Aerospace Industries Association Standard Accelerometer Terminology EETC Report

2.2 The following documents, of the latest issue in effect, form a part of this specification to the extend specified herein.

DRAWINGS

Kearfott Division

K130A062	Sensor, Angular Rate
Y216A315	Schematic Diagram Wiring

3. REQUIREMENTS

3.1 Item Definition. The End Item is a damped angular accelerometer, and comprises a conductive liquid annulus (mercury) positioned in the gap of a permanent magnet. The conductive liquid is held in a disk shaped insulative housing. Upon application of an angular input to the housing, the liquid annulus is coerced into motion by viscous forces. The relative motion of the liquid to the case is sensed by measurement of the potential generated in the liquid as it cuts the lines of force of the permanent magnet. The output potential is amplified to a suitable level by a preamplifier filter assembly.

3.1.1 Orientation. The End Item input axis shall be as defined in Figure A-1.

3.1.2 Mounting Plane. The End Item mounting plane shall be as identified in K130A062.

3.2 General Requirements.

3.2.1 Definitions. The following document defines terminology used in this specification: Aerospace Industries Assocation, Standard Accelerometer Terminology, EETC Report.

3.3 Performance. The performance specified for all parameters of the End Item are stated as a design goal. An actual performance value, not meeting the requirements stated, shall not be considered in conflict with contractual requirements. The device shall be expected to be useable in three distinctly different regimes known as Regime 1, 2 and 3. The difference between the three regimes manifests itself in the sensor as changes in the characteristics of the electronics package. All three regimes appear as outputs and can be monitored simultaneously.

3.3.1 Maximum Input Rate. The End Item shall perform over a maximum input rate of 10°/s for Regime 1, 3000°/s for Regime 2 and 30,000°/s for Regime 3.

3.3.2 Resolution. The End Item shall perform with a minimum resolution of 2% of full scale.

3.3.3 Bandwidth. The End Item shall operate over a bandwidth of 500 Hz for Regime 1, 2000 Hz for Regime 2 and 5000 Hz for Regime 3.

3.3.4 Gain/Scale Factor. The End Item shall have a nominal scale factor of 0.5 volts/°/s for Regime 1, 0.00167 volts/°/s for Regime 2 and 0.000167 V/°/s for Regime 3.

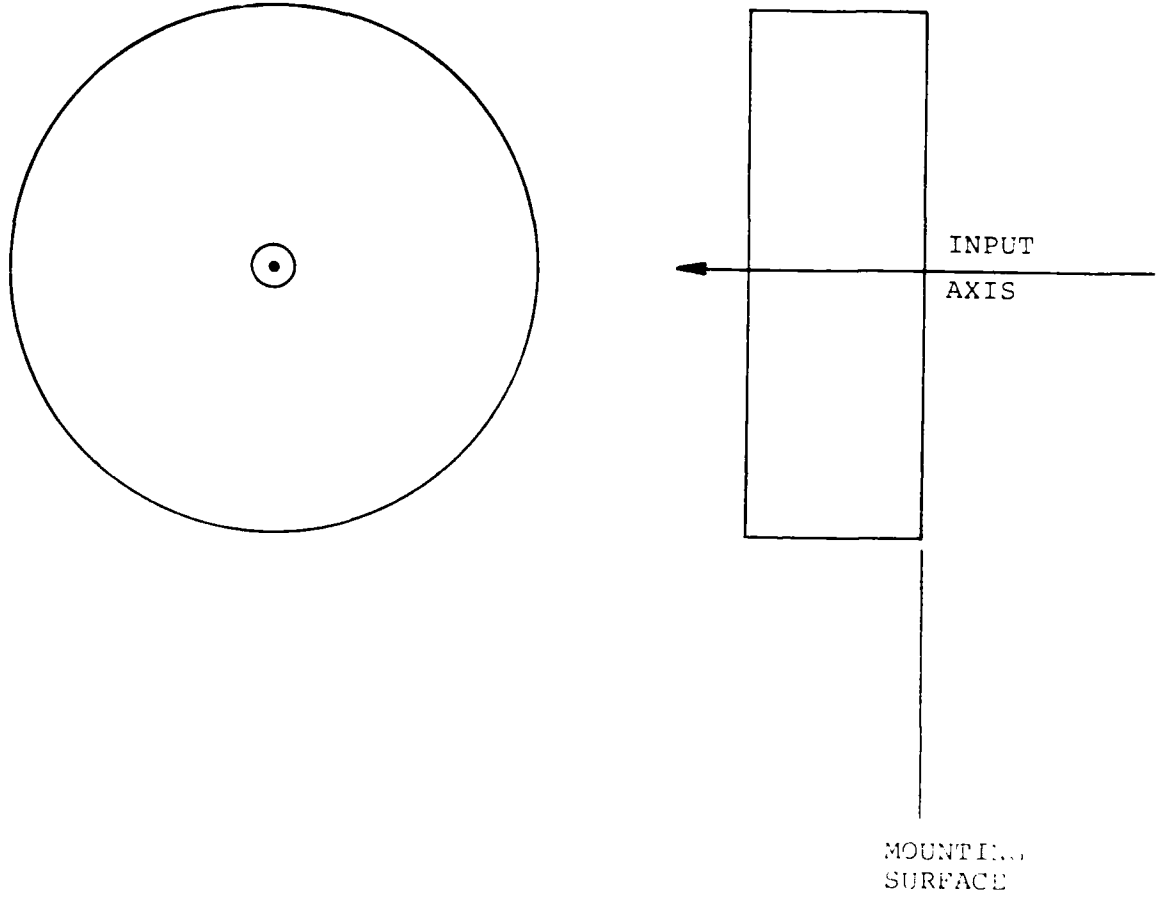

Figure A-1. Input Axis Definition

3.3.5 Corner Frequency. The End Item shall have a corner frequency less than 1 Hz.

3.3.6 Rate/Acceleration Contamination. The End Item will have a small component, at very low frequencies, which is proportional to angular acceleration instead of rate. The transfer function for the unit is defined as follows.

$$Co = \frac{K\ \ddot{\theta}}{1+\tau S}$$

Co = Output voltage before electrical gain

K/τ = Gain factor

3.4 Input/Output Requirements.

3.4.1 Supply Voltage. The End Item shall require a supply voltage of ±15 ±1/2 Volt. Noise ripple shall be less than 0.05 Vp-p.

3.4.2 Output Signal Level. The End Item shall have an output level of 5 volts for maximum input.

3.5 Mechanical Requirements.

3.5.1 Exterior Surfaces. All exterior surfaces shall withstand the environment herein specified and the handling expected in the normal course of operation, testing, and maintenance without deterioration which causes non conformance to this specification.

3.5.2 Dimensions. The outline, mounting dimensions and location of the center of gravity shall conform to K130A062.

3.5.3 Angular Rate Sensor Axis. The input axis and its positive direction shall be defined by external markings and by reference mounting surface as indicated by Figure A-1.

3.5.4 Weight. The weight shall be 2.7 pounds maximum.

3.6 Environmental Requirements. The environmental conditions listed in this section are those to which the End Item may be subjected during storage, transportation, and handling or operation, or both. The End Item shall be designed to survive these environments and to successfully complete the environmental tests specified in Section 4.

3.6.1 Non Operative Environment. The following conditions, occuring separately or in combination may be encountered during transportation and handling, or storage, or both. The End Item shall conform to all requirements of 3.3 after exposure or any reasonable combinations of the specified service conditions.

3.6.1.1 Temperature and Thermal Radiation. Ambient temperature may vary from a minimum of -35°C to a maximum of +71°C under unsheltered ground conditions. Areas exposed to direct sunlight shall be consodered as unsheltered conditions.

3.6.1.2 Thermal Shock. Thermal shock shall be from -35°C to 71°C. The heating and cooling rates of the ambient environment shall be approximately 20°C/s.

3.6.1.3 Vibration. Vibration shall be in accordance with Mil Standard 810 Method 514, Figure 514.2-6 curve AB for a 9 minute logarithmic cycle.

3.6.2 Operative Environment. The following conditions, occuring separately, or in combination may be encountered during operation. The End Item shall conform to all the requirements of 3.3 during, unless otherwise specified, and after exposure to any reasonable combination of the specified service conditions.

3.6.2.1 Mechanical Shock. The End Item shall be capable of withstanding the shock environment of 10,000 g peak in a 3.2 millisecond half sine.

3.6.2.2 Temperature. The End Item shall be capable of operating over a temperature range of -29°C to +71°C.

3.6.2.3 Magnetic Fields. The End Item shall be capable of withstanding magnetic fields of ±TBD gauss without any degradation of performance.

4. QUALITY ASSURANCE

4.1 General. All tests governed by this specification shall be conducted in accordance with test procedures prepared by the contractor.

4.2 Acceptance Tests. Each End Item shall be subjected to an Acceptance test consisting of the following individual tests.

a. Examination of Product

b. Scale factor

c. Input axis misalignment

APPENDIX B

LIST OF TEST EQUIPMENT

Genisco Rate Table
Model 1100-5
S/N 2

Interstate Electronics Corporation
Function Generator
Model F51A
S/N 1

Power Design Inc.
Power Supply
Model TW5005

John Fluke Mfg. Co.
AC/DC Differential Voltmeter
Model 873A, 887A
S/N 12, S/N 2

Tektronix, Inc.
Scope
Model 545A
S/N 63
Plug In For Above
Type 1A7A

Hewlett Packard
Scope
Model 1205B
S/N 12

Disa Inc.
RMS Meter
Model 55D35

Solartron EMR
Frequency Response Analyzer
Model 1410-01
S/N 9

Nicolet Scientific Corporation
Fast Fourier Transform Analyzer
Model 440A
S/N 1
with
Tektronix Digital Plotting Option
Model 4662
S/N 2

GOULD BRUSH
STRIP CHART RECORDER
MODEL MAEK 240
S/N 1

AVCO
STOCK TEST MACHINE
MODEL SM-005-3
S/N 1

APPENDIX C

TEST LOGS KARS S/N 1, 2

	PARAMETER		S/N 1	S/N 2
1	Scale Factor Regime #1	(V/°/sec)	0.485	0.537
2	Scale Factor Regime #2	(V/°/sec)	0.00154	0.00173
3	Scale Factor Regime #3	(V/°/sec)	0.000158	0.000168
4	Bandwidth Regime #1	(Hz)	513	480
5	Bandwidth Regime #2	(Hz)	2000	2030
6	Bandwidth Regime #3	(Hz)	5920	5800
7	Low Frequency Corner Regime #1	(Hz)	0.75	0.59
8	Low Frequency Corner Regime #2 #3	(Hz)	0.57	0.60
9	Noise Regime #1	(V)	0.0515	0.0571
10	Noise Regime #2	(V)	0.00099	0.00064
11	Noise Regime #3	(V)	0.00036	0.00036
12	Axis Misalignment	(min)	19.1	14.1

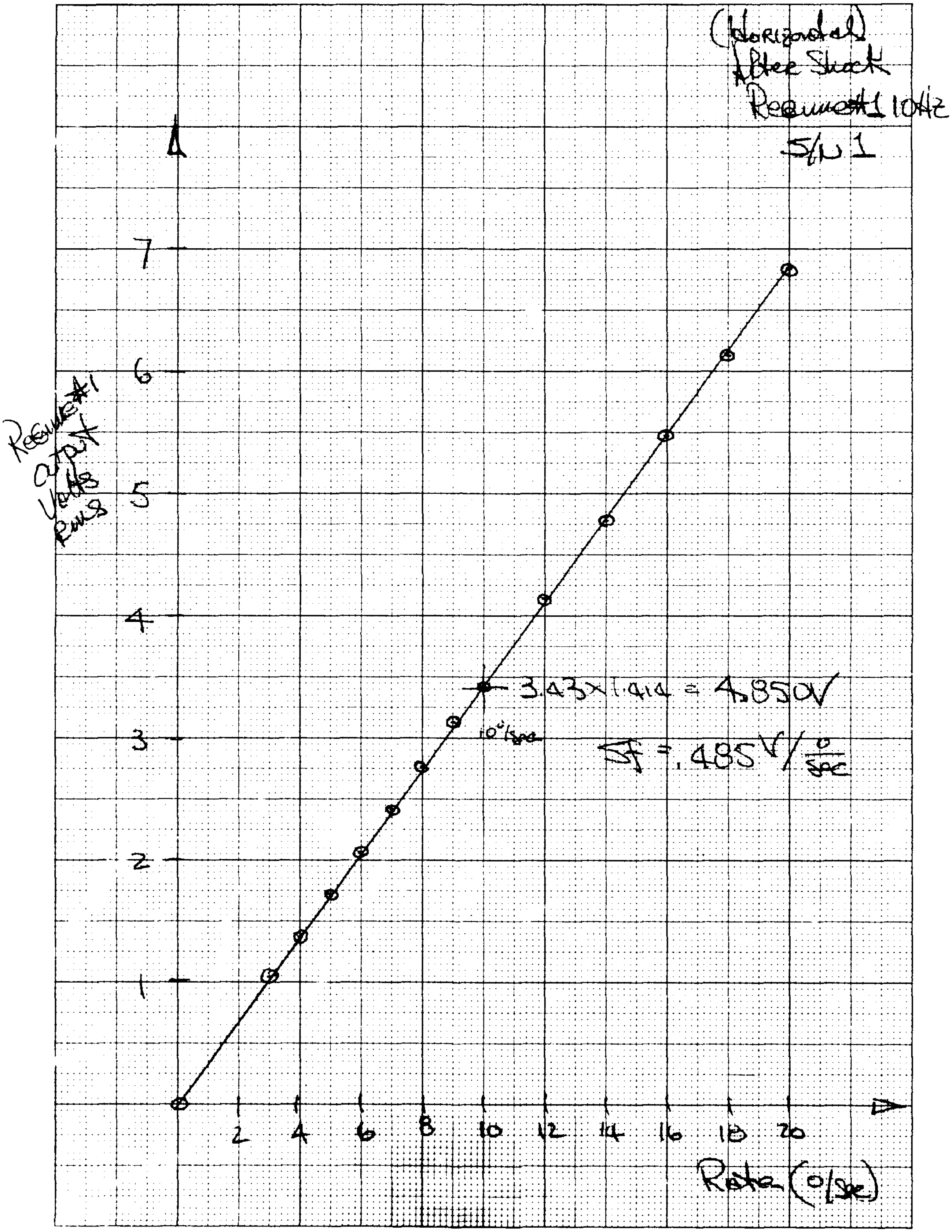
(Horizontal)
After Shock
10Hz
S/N 1
7
6
5
4
3
2
1
2
4
6
8
10
12
14
16
18
20
Rate (°/sec)
3.43×1.414 = 4.850V
10°/sec
SF = .485 V/°/sec

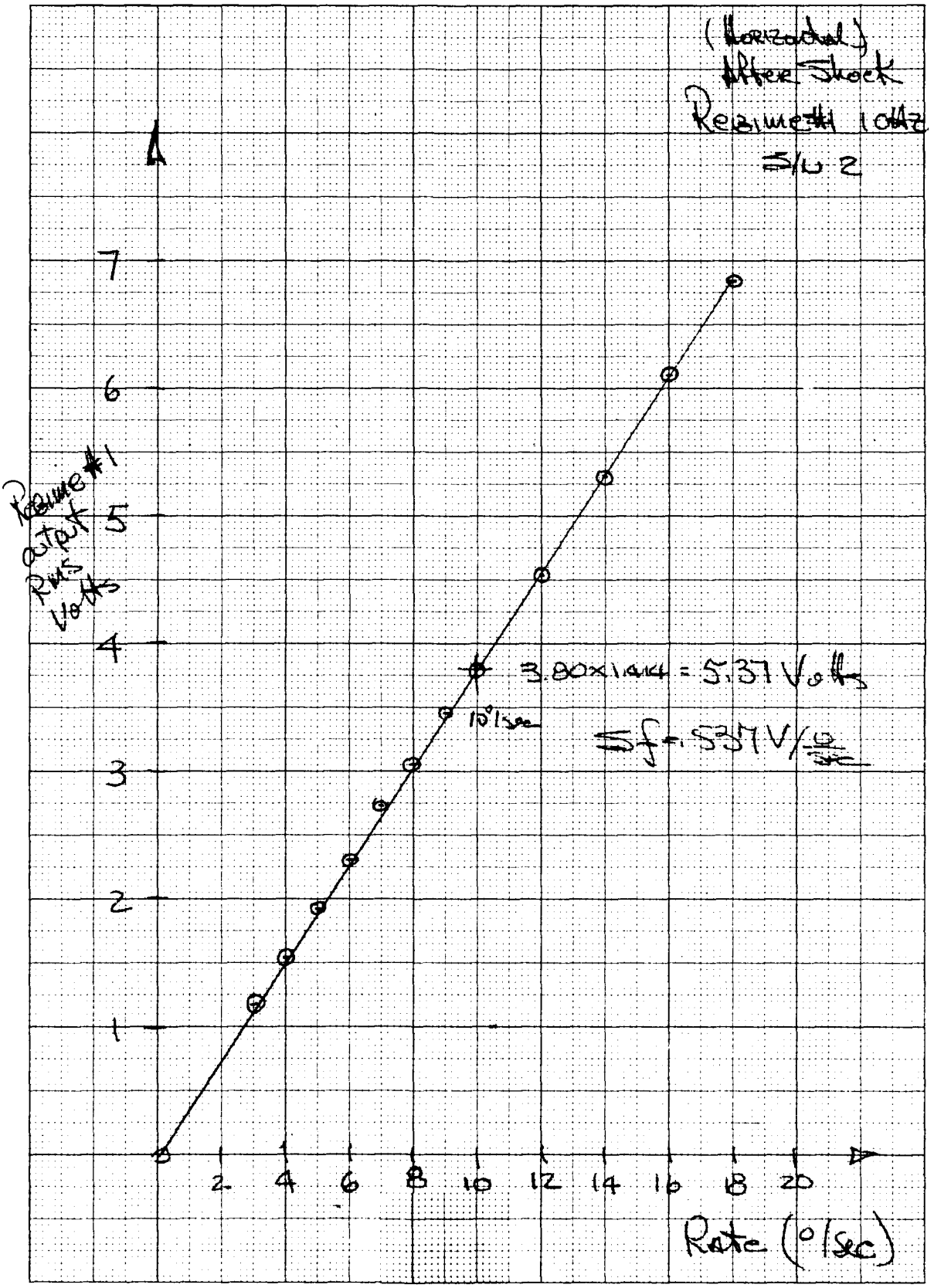
(Horizontal)
After Shock
Resonant 10Hz
S/N 2
Resonant #1 output RMS Volts
7
6
5
4
3
2
1
3.80 x 1.414 = 5.37 Volts
10°/sec
Sf = 5.37 V/10°/sec
2
4
6
8
10
12
14
16
18
20
Rate (°/sec)

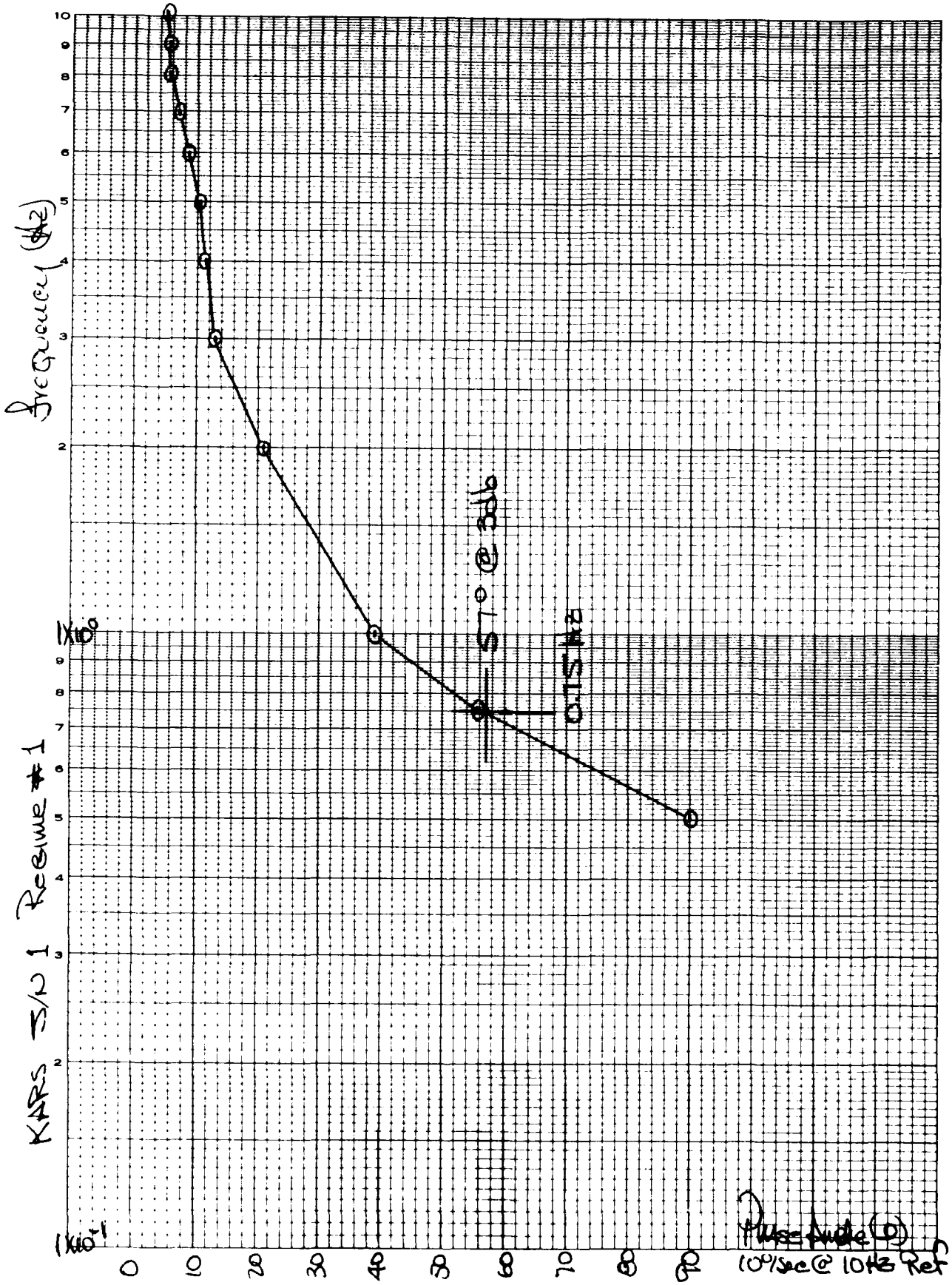
Frequency (Hz)
KARS F/A 1 Regime #1
1X10⁰
1X10⁻¹
0.1 Hz @ -57° @ 30db
Pitch Rate (Q)
10°/sec @ 10Hz Ref
0
10
20
30
40
50
60
70
80
90

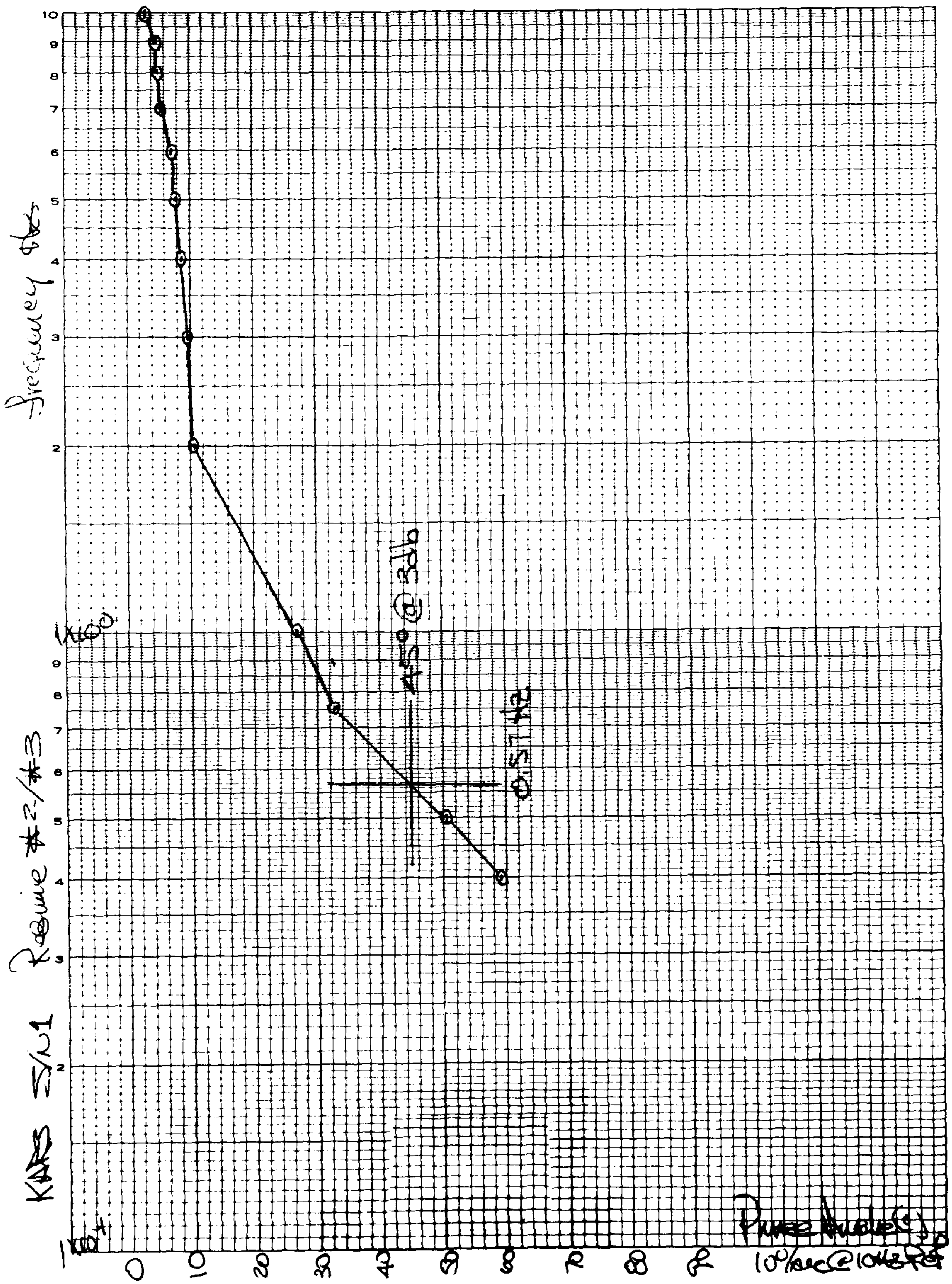

-45° @ 3db
0.57 Hz
Frequency Hz
Phase Angle (°)
0
10
20
30
40
50
60

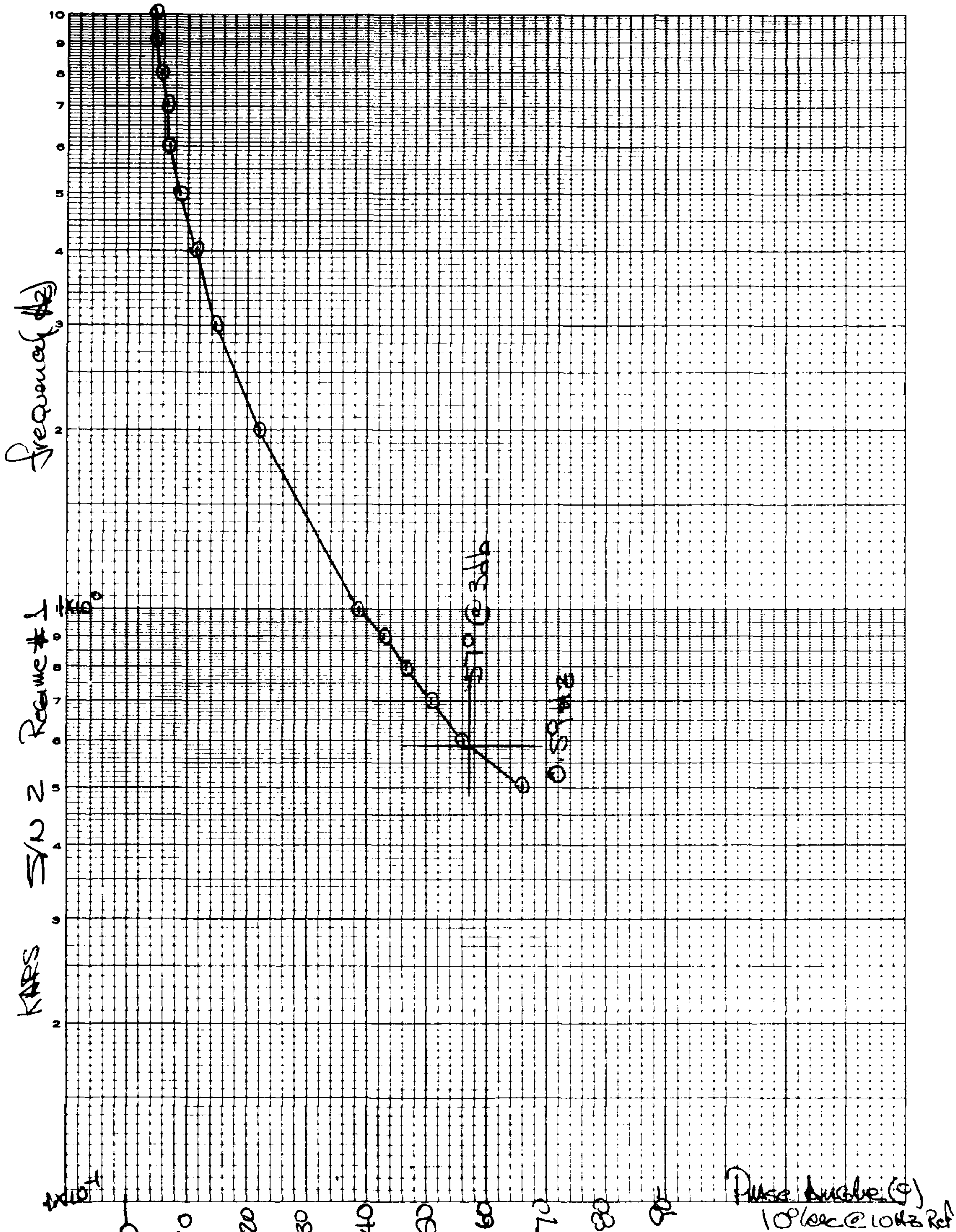
Frequency (Hz)
KARS S/N 2 Regime #1
51° @ 3db
0.59 Hz
Phase Angle (°)
10°/sec @ 10Hz Ref
0
10
20
30
40
50
60
70
80
90

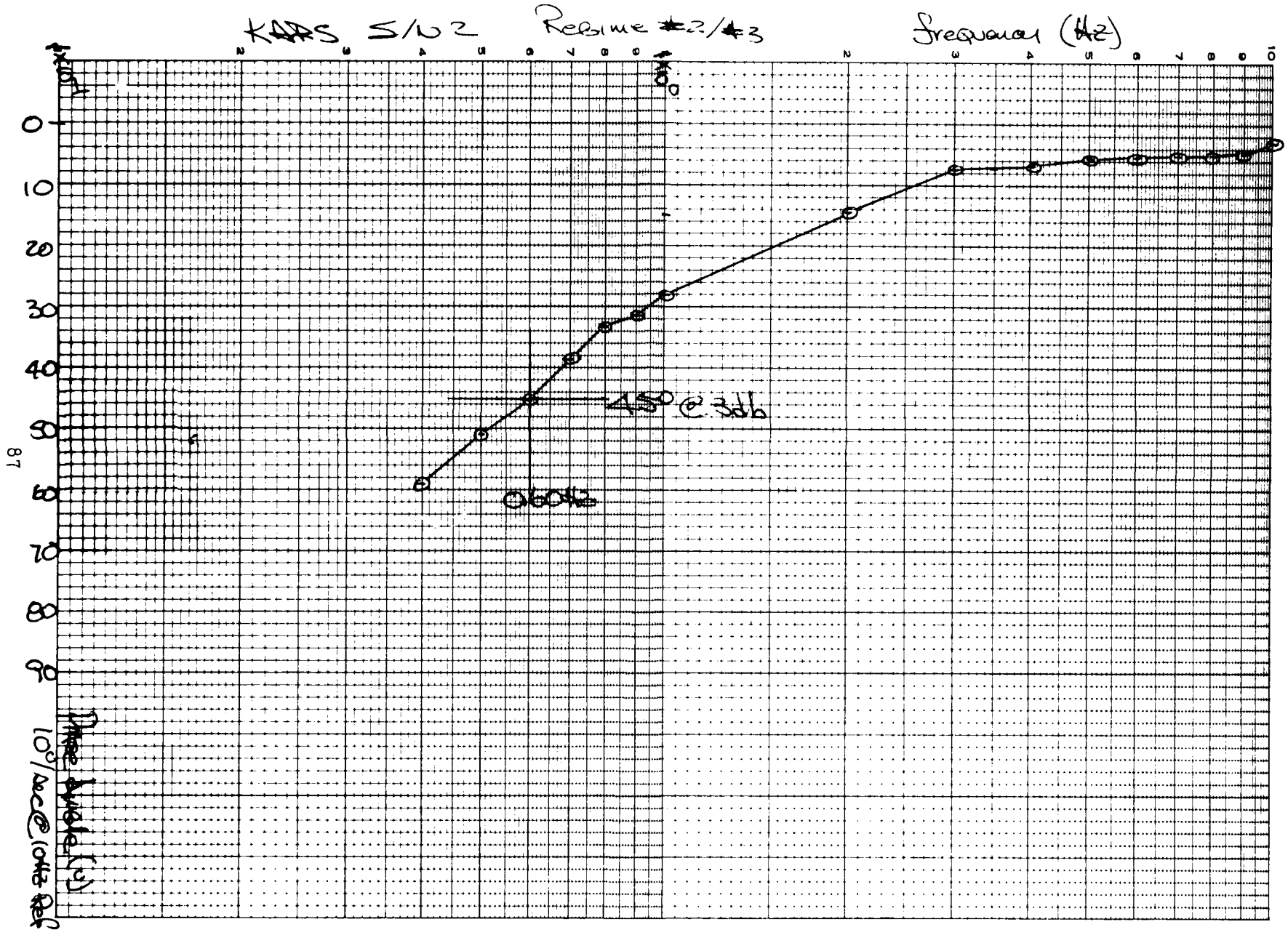
KARS 5/62 Regime #2/#3
Frequency (Hz)
Phase Angle (-)
0
10
20
30
40
50
60
70
80
90
-45° @ 3db
0.6Hz
10°/sec @ 10Hz Ref

DISTRIBUTION LIST

DEPARTMENT OF DEFENSE

Assistant to the Secretary of Defense
Atomic Energy
ATTN: Executive Assistant

Defense Advanced Rsch. Proj. Agency
ATTN: TIO

Defense Nuclear Agency
ATTN: SPTD
2 cy ATTN: SPSS
4 cy ATTN: TITL

Defense Technical Information Center
12 cy ATTN: DD

Field Command
Defense Nuclear Agency
ATTN: FCPR
ATTN: FCT
ATTN: FCTMOF

Field Command
Defense Nuclear Agency
Livermore Division
ATTN: FCPRL

NATO School (SHAPE)
ATTN: U.S. Documents Officer

Undersecretary of Defense for Rsch. & Engrg.
ATTN: Strategic & Space Systems (OS)

DEPARTMENT OF THE ARMY

Harry Diamond Laboratories
Department of the Army
ATTN: DELHD-I-TL
ATTN: DELHD-N-P

U.S. Army Ballistic Research Labs.
ATTN: DRDAR-BLV
ATTN: DRDAR-BLE, J. Keefer
ATTN: DRDAR-TSB-S

U.S. Army Cold Region Res. Engr. Lab.
ATTN: CRREL-EM

U.S. Army Engr. Waterways Exper. Station
ATTN: J. Ingram
ATTN: Library
ATTN: WESSA, W. Flathau
ATTN: F. Hanes
ATTN: WESSE, L. Ingram

U.S. Army Materiel Dev. & Readiness Cmd.
ATTN: DRXAM-TL

U.S. Army Nuclear & Chemical Agency
ATTN: Library

DEPARTMENT OF THE NAVY

David Taylor Naval Ship R&D Ctr.
ATTN: Code L42-3
ATTN: Code 1720

DEPARTMENT OF THE NAVY (Continued)

Naval Construction Battalion Center
ATTN: Code L51, R. O'Dello
ATTN: L08A

Naval Facilities Engineering Command
ATTN: Code 09M22C

Naval Ship Engineering Center
ATTN: Code 09G3

Naval Surface Weapons Center
ATTN: Code F31

Office of Naval Research
ATTN: Code 715

DEPARTMENT OF THE AIR FORCE

Air Force Institute of Technology
ATTN: Library

Air Force Weapons Laboratory
Air Force Systems Command
ATTN: NTE, M. Plamondon
ATTN: DEX, J. Renick
ATTN: SUL
ATTN: DEX

Assistant Chief of Staff
Intelligence
Department of the Air Force
ATTN: INT

DEPARTMENT OF ENERGY

Department of Energy
Albuquerque Operations Office
ATTN: CTID

Department of Energy
Nevada Operations Office
ATTN: Mail & Records for Technical Library

DEPARTMENT OF ENERGY CONTRACTORS

Lawrence Livermore National Laboratory
ATTN: Technical Information Dept. Library

Sandia National Laboratories
Livermore Laboratory
ATTN: Library & Security Classification Div.

Sandia National Laboratories
ATTN: L. Vortman
ATTN: 3141
ATTN: A. Chabai

OTHER GOVERNMENT AGENCIES

Central Intelligence Agency
ATTN: OSI/NED, J. Ingley

Department of the Interior
U.S. Geological Survey
ATTN: D. Roddy

OTHER GOVERNMENT AGENCIES (Continued)

Federal Emergency Management Agency
ATTN: Asst. Dir. for Rsch., J. Buchanon

DEPARTMENT OF DEFENSE CONTRACTORS

Acurex Corp.
ATTN: K. Triebes

Aerospace Corp.
ATTN: P. Mathur
ATTN: Technical Information Services

Agbabian Associates
ATTN: M. Agbabian

Artec Associates, Inc.
ATTN: D. Baum

BDM Corp.
ATTN: T. Neighbors
ATTN: Corporate Library

Boeing Co.
ATTN: Aerospace Library
ATTN: B. Lempriere

California Research & Technology, Inc.
ATTN: K. Kreyenhagen

Civil Systems, Inc.
ATTN: J. Bratton

Develco, Inc.
ATTN: L. Rorden

Effects Technology, Inc.
ATTN: R. Wengler

EG&G Washington Analytical Services Center, Inc.
ATTN: Library

Electromechanical Sys. of New Mexico, Inc.
ATTN: R. Shunk

Eric H. Wang
Civil Engineering Rsch. Fac.
ATTN: N. Baum

General Electric Company—TEMPO
ATTN: DASIAC
ATTN: J. Shoutens

Geocenters, Inc.
ATTN: L. Isaacson

H-Tech Labs, Inc.
ATTN: B. Hartenbaum

IIT Research Institute
ATTN: Documents Library

JAYCOR
ATTN: H. Linnerud

DEPARTMENT OF DEFENSE CONTRACTORS (Continued)

Kaman Sciences Corp.
ATTN: D. Sachs
ATTN: Library

Merritt CASES, Inc.
ATTN: Library
ATTN: J. Merritt

Nathan M. Newmark Consult. Eng. Svcs.
ATTN: W. Hall

Physics Applications, Inc.
ATTN: C. Vincent

Physics International Co.
ATTN: F. Sauer
ATTN: Technical Library

R & D Associates
ATTN: C. MacDonald
ATTN: J. Lewis
ATTN: Technical Information Center
ATTN: P. Haas

Science Applications, Inc.
ATTN: Technical Library

Science Applications, Inc.
ATTN: J. Dishon

Science Applications, Inc.
ATTN: K. Sites

Southwest Research Institute
ATTN: W. Baker

SRI International
ATTN: P. De Carli
ATTN: G. Abrahamson

Systems, Science & Software, Inc.
ATTN: D. Grine
ATTN: Library

Terra Tek, Inc.
ATTN: S. Green

TRW Defense & Space Sys. Group
ATTN: Technical Information Center

TRW Defense & Space Sys. Group
ATTN: E. Wong
2 cy ATTN: P. Dai

Weidlinger Assoc., Consulting Engineers
ATTN: M. Baron

Weidlinger Assoc., Consulting Engineers
ATTN: J. Isenberg

The Singer Company
25 cy ATTN: L. Smith

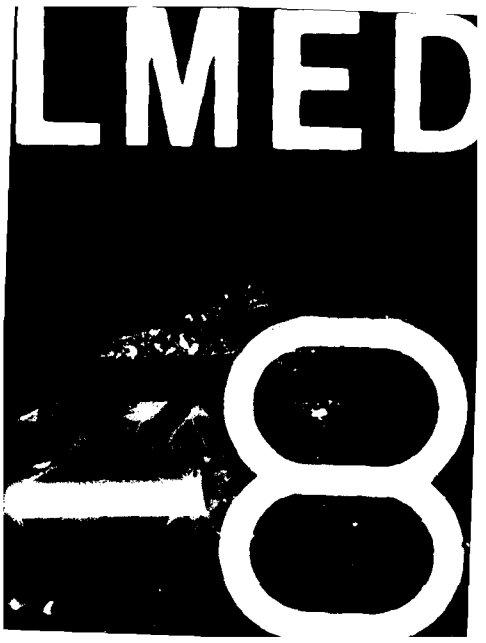
LMED
8